Handbook of MRI Technique

Second Edition

Catherine Westbrook

Training and Education, HealthSouth (UK) plc

b

Blackwell
Science

CONTENTS

PREFACE

The first edition of *Handbook of MRI Technique* was a resounding success. The rapidly increasing number of radiographers and technologists entering the modality, coupled with the development of education and training courses worldwide, has resulted in an increased demand for MRI books of any shape and size. The education of radiographers, technologists and radiologists often lags behind the rapid technological advances in MR. In addition, a lack of educational facilities and funding, as well as the complex nature of the subject, has resulted in many practitioners experiencing difficulty in learning MRI techniques.

MRI in Practice (also published by Blackwell Science) provides radiographers and radiologists with a user-friendly approach to MRI theory and how it may be applied in practice. *Handbook of MRI Technique* was originally intended to guide the uninitiated through scanning techniques and to help more experienced technologists improve image quality. It would seem that the first edition more than met these objectives and proved that, despite the fact we all work with different systems and in different environments, information on techniques and image optimization is still required on a global scale.

Due to this success, it has been my intention to continue with the objectives of the first edition but to add more information and update the reader on recent technical advances. I also felt that, in order to better reflect the different circumstances under which we work, the second edition should have contributions from experienced technologists in other countries who work on a variety of systems. Technologists and radiographers from the USA and Australia have made large and important contributions to the book and, as a result, I believe the second edition is even more comprehensive than the first. The following authors have assisted me in updating these sections: Bill Faulkner – Head, Neck and Spine; Carolyn Kaut – Chest, Abdomen and Pelvis; Greg Brown – Upper and Lower Limb; Mike Kean – Paediatrics. In addition all the authors helped me to reorganize some topics in Part 1.

The second edition of *Handbook of MRI Technique* is still split into two parts. Part 1 summarizes the main aspects of theory that relate to scanning and also includes practical tips on gating and equipment use, patient care and safety, and information on contrast media. Several useful tables are added for ease of reference and the pulse sequence section has been updated to include newer sequences. Part 2 includes a step-by-step guide to examining each anatomical area. It covers most of the techniques commonly used in MRI as well as paediatric imaging. As in the first edition, this section is not meant to be totally comprehensive but rather a working guide to the most widespread applications of MRI. Under each examination, categories such as indications, patient positioning, equipment, artefacts and tips on optimizing image quality are included. Guidance on technique and contrast

FOREWORD

Although the first images based on magnetic resonance imaging techniques were produced more than 20 years ago, the growth of the clinical and research magnetic resonance industry has shown no signs of slowing down. Each year seems to bring some new hardware and software advance that pushes the envelope even further, helping to redefine once again the state of the art in diagnostic medical imaging today. The past decade-plus has seen the industry advance well beyond the initial partial saturation spin echo imaging sequences. Partial flip angle gradient echo imaging sequences, various fat saturation techniques, inversion recovery imaging (including especially short and long TI, or FLAIR, variants), fast imaging techniques including fast/turbo spin echo and echo planar imaging and their variants, various types of magnetic resonance angiography, MR spectroscopy, diffusion and perfusion weighted imaging, magnetization transfer imaging, and functional MR imaging, are just a few of the myriad new sequences and capabilities that have been added to the diagnostic armamentarium of the clinical diagnostic MR practitioner. A more than US$ 1 billion annual industry has emerged virtually overnight around the development and integration of MRI contrast agents for clinical applications that virtually span the gamut of human disease. The development of entire industries of radiofrequency and magnet coil designers and developers have accompanied marked advances in software and hardware over the years. Yet the industry continues to grow and develop, with new advances and novel imaging techniques that seem to appear and find their way into routine clinical practice on a regular basis.

For someone just starting out today, the objective of becoming proficient in the art and science of magnetic resonance imaging and its clinical (and research) applications is daunting indeed. There is so much more to know and master today than there was just a few years ago. The reader can only take solace in knowing that it is less than will be required in order to master this field in a few short years from now. Catherine Westbrook has done a remarkable job in attempting to ease this transition from novice to accomplished, and from experienced to expert. While no text can cover everything one needs to know to capably perform as an MR technologist, it performs admirably in the comprehensive nature with which it approaches the field, as seen from the eyes of an MR technologist. Clearly this text is not attempting to teach 'the' correct way to approach MR imaging and patient care. What it does do, however, and does well at that, is provide rapid access to reasonable approaches to scanning clinical patients for virtually any anatomic and pathologic region of interest. Each section is accompanied by a set of references that are pertinent, extensive and current, virtually all having been published within the past three years. This encourages the reader think for themselves as they acquire more knowledge about the topic being discussed. Catherine Westbrook and

her co-authors, a veritable Who's Who of MR technologist leadership today, are to be commended for their approach to the patient as a whole, refusing to focus solely on the MR technology or sequence parameters alone. The Problem Solving Exercise section does a wonderful job of forcing the reader to approach MR imaging via this total-patient orientation in order to successfully acquire what may otherwise have been a difficult study.

The MR technologist has the unique position of being able to make or break a busy clinical MR site. The more knowledgeable the technologist, the more able he or she will be to rapidly, efficiently and accurately scan patients for the specific diagnostic problems with which they present. I am most confident that this text will prove to be a powerful asset in one's transition from the role of MR technician to one of the select few who have proudly earned the title of MR Technologist.

Emanuel Kanal MD, FACR
Director, Clinical and Educational Magnetic Resonance
Associate Professor, Neuroradiology
University of Pittsburgh Medical Center

usage is also provided, as well as suggestions of articles to further the reader's knowledge. Due to the variety of imaging systems and differences in radiological preferences, information on protocols is mainly limited to pulse sequence, scan plane and slice prescription. The advice given on protocols is intended only to direct either technologists who are scanning alone, or radiologists who are unfamiliar with the examination and do not have a clear idea on how to proceed. In addition, a basic anatomy section has been added at the beginning of each examination area and at the end of Part 2 the reader will find a section of problem-solving exercises and a reading and resource list. Throughout Part 2 there is also an extensive number of images demonstrating slice prescription protocols, appropriate sequence selections and common pathologies.

Handbook of MRI Technique endeavours to provide a much needed guide to the operation of MR systems and to enhance the education of MR users. It should be especially beneficial to those technologists studying for board certification or post-graduate and MSc courses, as well as to radiographers and radiologists who wish to further their knowledge of MRI techniques. The contributing authors and I hope that it continues to achieve these goals.

Catherine Westbrook

HOW TO USE THIS BOOK

Introduction

This book has been written with the intention of providing a step-by-step explanation of the most common examinations currently carried out using magnetic resonance imaging (MRI). It is divided into two parts.

Part 1 contains reviews or summaries of those theoretical and practical concepts that are frequently discussed in Part 2. These are:

- Parameters and trade-offs
- Pulse sequences
- Flow phenomena and artefacts
- Gating and respiratory compensation techniques
- Patient care and safety
- Contrast agents

These summaries are not intended to be comprehensive but contain only a brief description of definitions and uses. For a more detailed discussion of these and other concepts, the reader is referred to the several MRI physics books now available. *MRI in Practice* by C. Westbrook and C. Kaut (Blackwell Science, 1998, second edition) describes them in more depth. In addition a reading and resource list is provided at the end of the book.

Part 2 is divided into the following examination areas:

- Head and neck
- Spine
- Chest
- Abdomen
- Pelvis
- Upper limb
- Lower limb
- Paediatric imaging
- Problem-solving exercises

Each anatomical region is subdivided into separate examinations. For example, the section entitled *Head and neck* includes explanations on imaging the brain, temporal lobes, pituitary fossa, etc. Under each examination the following categories are described:

- Basic anatomy

- Common indications
- Equipment
- Patient positioning
- Suggested protocol
- Image optimization
- Further reading

Basic anatomy

Simple anatomical diagrams are provided for most examination areas to assist the reader. A reading list of anatomy texts is provided at the end of the book for those wanting more comprehensive information.

Common indications

These are the most usual reasons for scanning each area, although occasionally some rarer indications are included.

Equipment

This contains a list of the equipment required for each examination and includes coil type, gating leads, bellows and immobilization devices. The correct use of gating and respiratory compensation is discussed in Part 1 (see *Gating and respiratory compensation techniques*). The coil types described are the most common currently available. These are:

- ***Volume coils*** that both transmit and receive radio-frequency (RF) pulses and are specifically called transceivers. Most of these coils are quadrature coils which means that they use two pairs of coils to transmit and receive signal, so improving the signal to noise ratio (SNR). They have the advantages of encompassing large areas of anatomy and yielding a uniform signal across the whole field of view (FOV). In Part 2, the *head*, *body*, *extremity*, and *volume coils* specifically constructed for certain anatomical areas (e.g. the neck) are presumed to be of this type of coil.

- ***Phased array coils*** consist of multiple coils and receivers. The signal from the receiver of each coil is combined to form one image. This image has the advantages of both a small coil (improved SNR), and those of the larger volume coils (increased coverage). Therefore phased array coils can either be used to examine large areas, such as the entire length of the spinal cord, or to improve signal uniformity and intensity in small areas such as the breast. In Part 2 these types of coils have been suggested for *spine*, *breast*, *torso*, *pelvic* and *temporomandibular imaging*, although their use in other areas is rapidly expanding.

- **Surface/local coils** are traditionally used to improve the SNR when imaging structures near to the skin surface. They are often specially designed to fit a certain area and, in general, they only receive signal. RF is usually transmitted by the body coil when using this type of coil. Surface coils increase SNR compared to volume coils. This is because they are placed close to the region under examination, thereby increasing the signal amplitude generated in the coil, and noise is only received in the vicinity of the coil. However, surface coils only receive signal up to the edges of the coil and to a depth equal to the radius of the coil. To visualize structures deep within the patient, either a volume or phased array coil or a local coil inserted into an orifice must be utilized (e.g. a rectal coil). Occasionally the use of two surface coils linked together is suggested. This enables increased and uniform signal return compared to one coil. In Part 2 all specifically designed *surface coils*, *Helmholtz pairs* and *local coils* are presumed to be surface coils.

The choice of coil for any examination is one of the most important factors that determine the resultant SNR of the image. When using any type of coil remember to:

- Check that the cables are intact and undamaged.
- Check that the coil is plugged in properly and that the correct connector box is used.
- Ensure that the receiving side of the coil faces the patient. This is usually labelled on the coil itself. **Note:** Both sides of the coil receive signal but coils are designed so that one side receives optimum signal. This is especially true of shaped coils that fit a certain anatomical area. If the wrong side of the coil faces the patient, signal is lost and image quality suffers.
- Place the coil as close as possible to the area under examination. The coil should not directly touch the patient's skin as it may become warm during the examination and cause discomfort. A small foam pad or tissue paper placed between the skin surface and the coil is usually sufficient insulation.
- Always ensure that the receiving surface of the coil is parallel to the Z axis of the magnet. This guarantees that the transverse component of magnetization is perpendicular to the coil and that maximum signal is induced. Placing the coil at an angle to this axis, or parallel to the X or Y axis, results in a loss of signal (Fig. 1).

Patient positioning

This contains a description of the correct patient position, placement of the patient within the coil and proper immobilization techniques. Centring and landmarking are described relative to the laser light system as follows:

- The **longitudinal alignment light** refers to the light running **parallel** to the bore of the magnet in the **Z axis**.

isocentre as it often requires the patient to shift their body across to one side of the bore. Positioning foam pads or RF-shielding material between the patient and the walls of the bore is often required.

Examining areas of the body away from magnetic isocentre has its difficulties especially in older, more restrictive systems. So beware of offset situations!

Suggested protocol

This is intended as a guideline only. Almost every centre uses different protocols depending on the type of system and radiological preference. However, this section can be helpful for those technologists/radiographers scanning without a radiologist, or where the examination is so rare that perhaps neither the radiologist nor the technologist/radiographer knows how to proceed. The protocols given are mainly limited to scan plane, weighting, suggested pulse sequence choices and slice positioning. **It must be stressed that all the protocols listed are only a reflection of the authors' practice and research, and are in no way to be considered the law!** If all your established protocols are satisfactory, this section is included for interest only. If, however, you are unfamiliar with a certain examination, the suggested protocol should be useful.

Occasionally in this section coordinates for slice prescription are given in **bold** type in millimetres (mm) where explicit prescription can be utilized (mainly for localizers). Graphic prescription coordinates cannot be given as they depend on the exact position of the patient within the magnet and the ROI. The explicit coordinates are always given as follows:

- Left to Right   **L** to **R**
- Inferior to Superior   **I** to **S**
- Posterior to Anterior **P** to **A**

In the suggested protocols a certain format is adopted when some parameters remain constant and others change. For example, in the protocol for a coronal spin echo (SE), proton density (PD)/T2 sequence of the brain the text reads:

Coronal SE/FSE PD/T2

As for Axial PD/T2,
except   prescribe slices from the cerebellum to the frontal lobe.

This indicates that the pulse sequence, timing parameters, slice thickness, and matrix are the same as the axial except the slices are prescribed through a different area. This format is intended to avoid repetition. In most examinations there is a section reserved for additional sequences. These are extra sequences that we do not regard as routine but may be included in the examination. Of course, some practitioners may regard what we call 'additional' as 'routine', and vice versa.
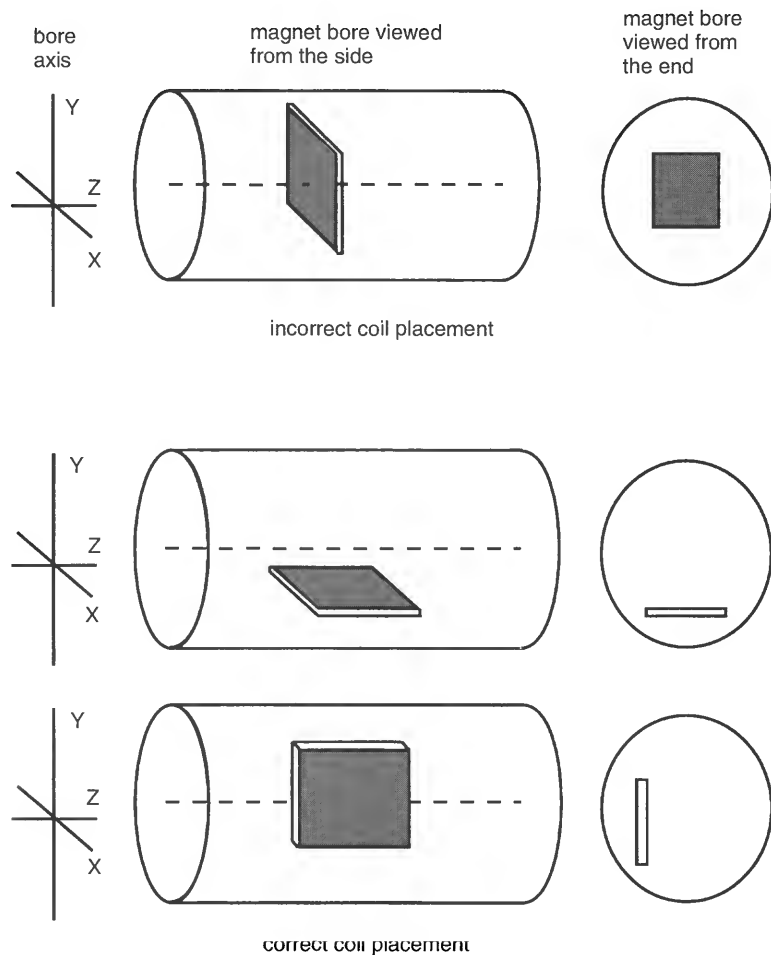
bore
axis

magnet bore viewed
from the side

magnet bore
viewed from
the end

incorrect coil placement

correct coil placement

Fig. 1. Correct placement of a flat surface coil in the bore of the magnet. The surface of the coil (shaded) area must be parallel to the Z axis to receive signal. The coil is therefore positioned so that transverse magnetization created in the X and Y axes is perpendicular to the coil.

- The **horizontal alignment light** refers to the light that runs from **left to right** of the bore of the magnet in the **X axis**.

- The **vertical alignment light** refers to the light than runs from the **top to the bottom** of the magnet in the **Y axis**. (Fig. 2)

It is assumed in Part 2 that the following areas are examined with the patient placed **head first** in the magnet:

- Head and neck (all areas)
- Cervical, thoracic and whole spine
- Chest (all areas)
- Abdomen (for areas superior to the iliac crests)
- Shoulders and upper limb (except where specified)

longitudinal alignment light

horizontal
alignment
light

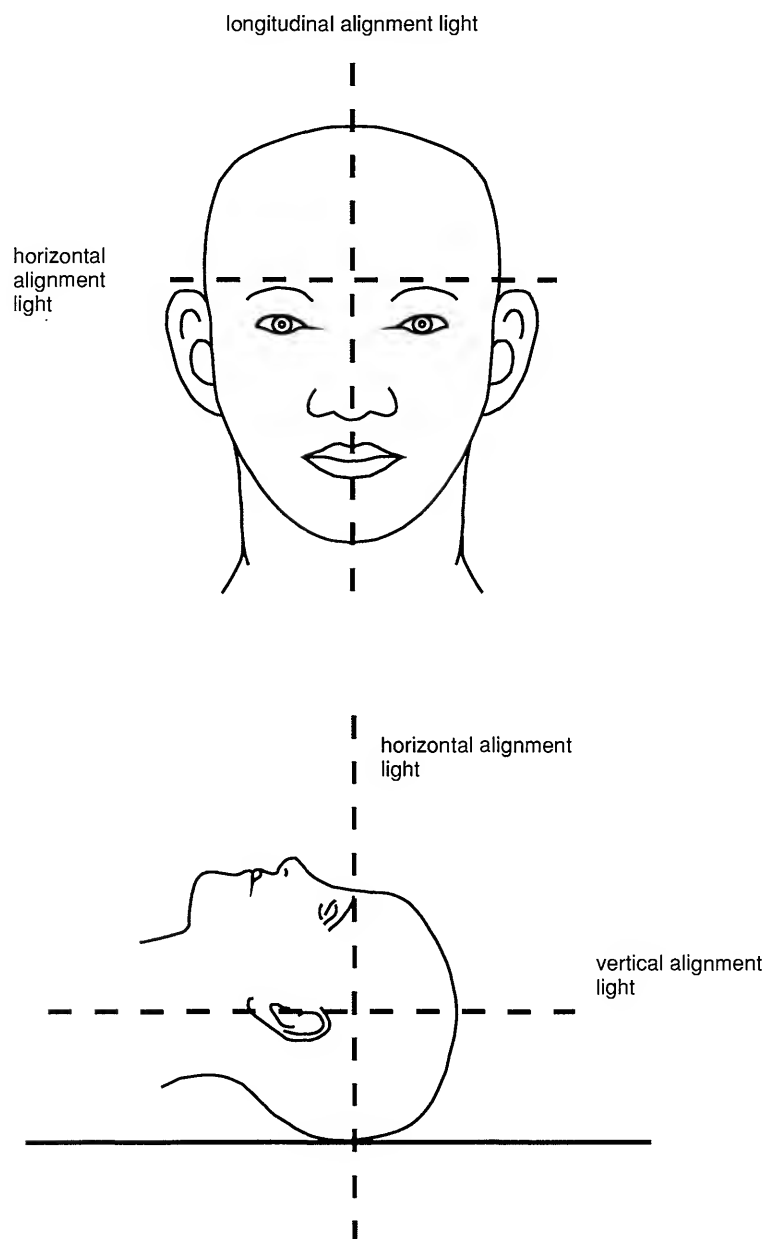horizontal alignment
light

vertical alignment
light

Fig. 2.   Positioning of the alignment lights.

The remaining anatomical regions are examined with the patient placed **feet first** in the magnet. These are:

- Pelvis
- Hips
- Lower limbs

Offset imaging

Imaging structures that are not in the midline leads to reduced image quality because the magnetic field homogeneity at the edge of the bore is rarely as good as at the centre. Therefore, it is advantageous to try to place the area under examination at magnetic isocentre. However, this may not always be possible. A good example is imaging a single hip on a patient who, due to the dimensions of the bore, cannot move over enough to place the centre of the hip at isocentre. The same problem may be encountered when imaging the humerus, elbow, forearm, wrist, knee, or a single lower limb. In these instances shimming the magnetic field after patient positioning is important to obtain the best image quality, particularly for gradient echo (GRE) sequences and fat suppression. The capacity to shim an offset FOV is an extra advantage that should be used if available.

Difficulties experienced with correctly positioning offcentre FOVs have been overcome with the development of flexible gradient control systems and improvements in scan prescription software. Most scanners now allow interactive offset of the imaging FOV in any direction. However, if your system is not equipped with this, an offset FOV can be accurately positioned by measuring the offset from the middle of the region of interest (ROI) to the longitudinal alignment light using a plastic ruler. Offset measurements can then be selected on the system.

Offsetting the FOV ensures that the area under examination is in the middle of the image. Usually the offset is relative to the longitudinal alignment light, as most offsetting occurs when trying to examine the arm or a single leg which is situated laterally in the bore of the magnet. However, sometimes the ROI may be offset from isocentre relative to either the horizontal or vertical alignment lights, or both. Be aware that multiple offsets can restrict subsequent scan prescriptions on some older systems. When working with these restrictions, try to place the area under examination at isocentre along all three axes of the magnet. If the FOV is offset in one axis, then ensure that the ROI is at isocentre in the other two axes. For example, if the wrist is being examined with the arm at the side, raise the wrist and coil using pads until the vertical alignment light lies through the centre of the wrist in the vertical axis. Then ensure that the horizontal alignment light lies through the middle of the wrist joint. In this way, although there is an offset of the wrist to either the right or the left of the longitudinal alignment light, the wrist is centred to the horizontal and vertical alignment lights.

The main problem associated with offset imaging on old systems is that they may only allow an offset in the frequency encoding axis. Therefore, to obtain an offset, the frequency and phase axes may have to be swapped to place the frequency encoding axis in the direction of the offset. This strategy is most commonly required in coronal and axial imaging. For example, in coronal imaging of a single hip, frequency encoding normally assumes the longest axis of the anatomy, and phase the shortest. Therefore frequency is placed superior (S) to inferior (I), and right (R) to left (L). However, to ensure an offset to the right by 250 mm, for example, frequency must be placed R to L and an offset of R 250 mm selected
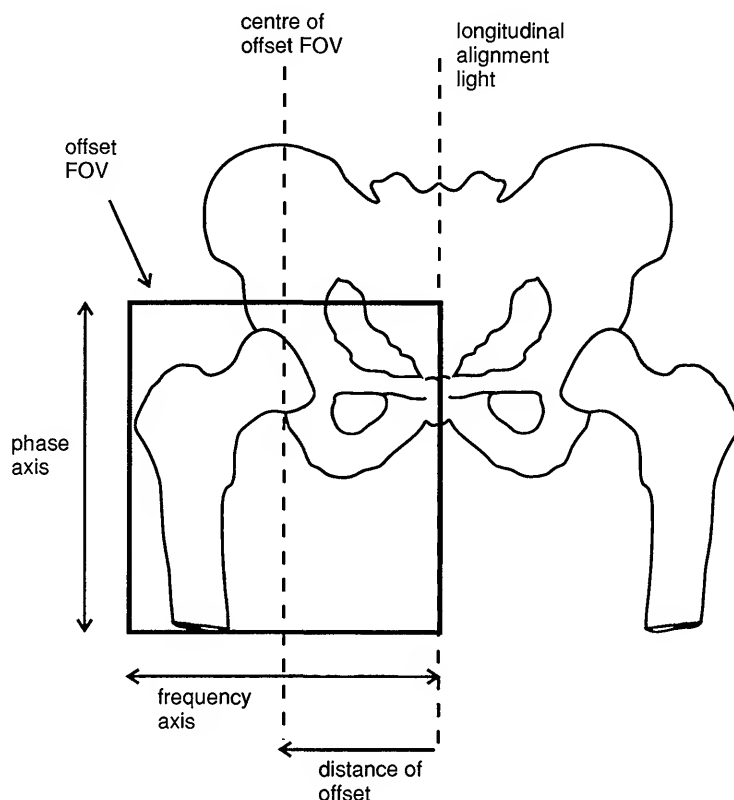
Fig. 3.   The rationale for offset imaging in the hips.

(Fig. 3). The phase axis therefore lies S to I and oversampling is necessary to eliminate aliasing from anatomy above and below the FOV (see *Flow phenomena and artefacts* in Part 1). Failure to appreciate this leads to an image where the hip under investigation is not in the centre of the FOV, or missed altogether, and/or where aliasing ruins the examination.

When there is some doubt about offset imaging it is advisable to run a short repetition time (TR) sequence with a single slice and lowest possible resolution matrix which has the same FOV, encoding directions and oversampling as the imaging sequence you are planning. The time taken to set up and run this short sequence is negligible when compared to repeating a longer sequence that was ruined by artefact. In addition, some old systems do not allow the operator to control the direction of phase and frequency when oblique slices are selected. Under these circumstances, the system determines the direction of both the frequency and phase encoding axes and aliasing is common. It is therefore very important to ensure that the area under examination is at isocentre in at least two axes, and oversampling used if oblique imaging is carried out.

An additional concern with offset imaging is that, depending on the design of the bore covers and body coil, shading artefact can occur if the patient is touching the sides of the magnet. This mainly occurs when trying to position the ROI at

Localizers

Most new systems now support three-plane localization. However, single-plane localizers have also been included for readers using older systems. Sometimes localizers are used as a diagnostic sequence. An example of this is when imaging the chest, abdomen and pelvis where a coronal incoherent (spoiled) GRE T1 sequence is used as a localizer for placement of subsequent slices, but also acts as a diagnostic sequence, in that the factors selected give good SNR and resolution. As long as the patient has been positioned and centred correctly, localizers can often be dispensed with and the examination time shortened.

In spinal imaging, both coronal and sagittal localizers have been described. Coronal localizers have the advantage of enabling very accurate graphic prescription of the subsequent sagittal series, but distinguishing vertebral levels is often difficult. In addition, the distance of the spine from the coil varies depending on the patient's size, and therefore the explicit prescription coordinates of the coronal slices may also vary. Sagittal localizers dispense with these problems as, as long as the patient is correctly positioned, they can be explicitly prescribed on either side of the longitudinal alignment light/midline. It is also much easier to ascertain vertebral levels when using sagittal localizers. However, problems can arise if the patient is incorrectly positioned, as the midline of the patient does not then correspond to the middle slice in the stack of localizing images. If sagittal localizers are used and the patient is not in the midline, it is necessary to estimate the amount of offset of the patient relative to the longitudinal alignment light. This is easily done by finding the localizer image that best demonstrates midline anatomy, and noting the coordinates of this slice. The subsequent sagittal images are then offset by this amount so that the middle slice now shows the midline anatomy.

Example   Three sagittal localizers are acquired in positions L 7 mm, L 0 mm and R 7 mm. If the patient is positioned to the left of the longitudinal alignment light so that the slice at L 7 mm demonstrates midline anatomy, the sagittal T1 and T2 series are explicitly prescribed from L 29 mm to R 15 mm instead of L 22 mm to R 22 mm, in order to ensure that they are correctly centred.

Image optimization

This section is subdivided into:

- Technical issues
- Artefact problems
- Patient considerations
- Contrast usage

Technical issues

This includes a discussion of the relationship of SNR, spatial resolution and scan time pertaining to each examination. Suggestions on how to optimize these factors

are described (see *Parameters and trade-offs* in Part 1). The correct use of pulse sequences and various imaging options are also discussed (see also *Pulse sequences* in Part 1).

Artefact problems

This contains a description of the common artefacts encountered and ways in which they can be eliminated or reduced (see also *Flow phenomena and artefacts* in Part 1).

Patient considerations

This encompasses the condition of the patient, including symptoms and claustrophobia. Suggestions to overcome these are given (see also *Patient care and safety* in Part 1).

Contrast usage

The reasons for administering contrast in each particular area are discussed. Again, contrast usage varies widely according to radiological preferences. This section is a guideline only (see also *Contrast agents* in Part 1).

Further reading

At the end of each examination the reader will find some suggested articles that are intended to give a greater understanding of imaging techniques. These articles have been selected because they are relatively recent and have a technical bias.

Problem-solving exercises

At the end of Part 2 there are exercises designed to enable the reader to modify the techniques described to a particular clinical situation. Many people find problem solving a very effective learning method. Solving a difficult patient scenario requires the technologist/radiographer to draw on their knowledge of theory and routine technical applications and modify patient positioning, equipment, pulse sequences, parameters and imaging options. After all, radiographers are professional problem solvers! When examining these problem-solving exercises it may help to follow this ten point plan for good radiographic practice:

- Review all cases carefully and select appropriate protocols.
- Have flexible protocols that can reflect the needs of each individual clinical case.
- Regularly review your procedures and benchmark them against current best practice.
- Have clear diagnostic goals including the minimum accepted sequences necessary to obtain a useful diagnostic/clinical outcome.

- Regularly review your protocols and procedures.
- Understand the capabilities of your system.
- Recognize your limitations and if necessary refer to another site rather than risking an incomplete or diagnostically unacceptable procedure.
- Educate all levels of staff to new procedures and/or system capabilities.
- Be safety paranoid to ensure your unit does not fall victim to the dreaded MRI incident.
- Most importantly, enjoy your patients and give them the highest standard of care possible.

Terms and abbreviations used in Part 2

Wherever possible generic terms have been used to describe pulse sequences and imaging options. Explanations of these can be found in the various sections of Part 1. To avoid ambiguity the specific following terms have been used:

Chemical/spectral pre-saturation: fat suppression techniques such as fat saturation (FAT SAT), spectrally selective inversion recovery (SPIR).
Gradient moment nulling (GMN): gradient moment rephasing (GMR) and flow compensation (FC).
Oversampling: no phase wrap, anti-aliasing and anti-foldover.
Rectangular/asymmetric FOV: rectangular FOV.
Respiratory compensation (RC): phase reordering and respiratory triggering techniques.

Abbreviations are used throughout the book for simplification purposes. A summary of these can be found in the following section *Abbreviations*. In addition a comparison of acronyms used by certain manufacturers to describe pulse sequences and imaging options is given later in Table 3 under *Pulse sequences* in Part 1.

Summary

To use this book

- Find the anatomical region required and then locate the specific examination.
- Study the categories under each section. It is possible that all the categories are relevant if the examination is being performed for the first time. However, there may be occasions when only one item is appropriate. For example, there could be a specific artefact that is regularly observed in chest examinations, or image quality is not up to standard on lumbar spines. Under these circumstances read the subsection entitled *Image optimization*.
- If the terms used, or concepts discussed, in Part 2 are unfamiliar, then turn to Part 1 and read the summaries described there.

ABBREVIATIONS

A summary of common abbreviations used in the field of MRI and throughout this book is given below.

A	Anterior
AC	Number of acquisitions
ADEM	Acute disseminating encephelomyelitis
ASIS	Anterior superior iliac spine
AVM	Arterio-venous malformation
AVN	Avascular necrosis
BOLD	Blood oxygenation level dependent
CDH	Congenitally dislocated hips
CE FAST	Contrast enhanced FAST
CNR	Contrast to noise ratio
CNS	Central nervous system
CSE	Conventional spin echo
CSF	Cerebrospinal fluid
CT	Computer tomography
CVA	Cerebral vascular accident
DE prep	Driven equilibrium magnetization preparation
DWI	Diffusion weighted imaging
ECG	Echocardiogram
EPI	Echo planar imaging
E short	Short repetition technique based on echo
ETL	Echo train length
FAST	Fourier acquired steady state
FAT SAT	Fat saturation
FC	Flow compensation
FDA	Food and Drugs Administration
FFE	Fast field echo
FID	Free induction decay signal
FISP	Fast imaging with steady precession
FLAG	Flow adjusted gradients
FLAIR	Fluid attenuated inversion recovery
FLASH	Fast low angled shot
fMRI	Functional MRI
FOV	Field of view
FREEZE	Respiratory selection of phase encoding steps
FSE	Fast spin echo
F short	Short repetition technique based on free induction decay

GFE	Gradient field echo
GFEC	Gradient field echo with contrast
GMN	Gradient moment nulling
GMR	Gradient moment rephasing
GR	Gradient rephasing
GRASS	Gradient recalled acquisition in the steady state
GRE	Gradient echo
GRE-EPI	Gradient echo EPI
HASTE	Half acquisition single shot turbo SE
I	Inferior
IAM	Internal auditory meatus(i)
IM	Intramuscular
IR	Inversion recovery
IR-FSE	Inversion recovery FSE
IR prep	Inversion recovery magnetization preparation
IV	Intravenous
IVC	Inferior vena cava
L	Left
MAST	Motion artefact suppression
MEMP	Multi-echo multiplanar
MPGR	Multiplanar GRASS
MPIR	Multiplanar inversion recovery
MP RAGE	Magnetization prepared rapid gradient echo
MR	Magnetic resonance
MRA	Magnetic resonance angiography
MRCP	Magnetic resonance cholangiopancreatography
MRI	Magnetic resonance imaging
MS	Multiple sclerosis
MT	Magnetization transfer
NEX	Number of excitations
NSA	Number of signal averages
P	Posterior
PC	Phase contrast
PC-MRA	Phase contrast MRA
PD	Proton density
Pe	Peripheral
PEAR	Phase encoding artefact reduction
PRIZE	Respiratory selection of phase encoding steps
PSIF	Reverse FISP
R	Right
RAM FAST	Rapid acquisition matrix FAST
RC	Respiratory compensation
REST	Regional saturation technique
RF	Radio frequency
RF spoiled FAST	Radio frequency spoiled FAST
ROI	Region of interest

RR	R to R interval
S	Superior
SAR	Specific absorption rate
SAT	Saturation
SE	Spin echo
SE-EPI	Spin echo EPI
Short	Short repetition techniques
SMART	Shimadzu motion artefact reduction technique
SMASH	Short minimum angled shot
SNR	Signal to noise ratio
SPAMM	Spatial modulation of magnetization
SPGR	Spoiled GRASS
SPIR	Spectrally selective inversion recovery
SS	Single shot
SS-EPI	Single shot EPI
SSFP	Steady state free precession
SS-FSE	Single shot FSE
STAGE	Small tip angle gradient echo
STERF	Steady state technique with refocused FID
STILL	Flow motion compensation
STIR	Short TI inversion recovery
TE	Echo time
TFE	Turbo field echo
TI	Inversion time
TIA	Transient ischaemic attack
TLE	Temporal lobe epilepsy
TMJ	Temporomandibular joint
TOF	Time of flight
TOF-MRA	Time of flight MRA
TR	Repetition time
TSE	Turbo spin echo
VEMP	Variable echo multiplanar
VENC	Velocity encoding

PART 1

PARAMETERS AND TRADE-OFFS

Introduction

This section refers mainly to the *Technical issues* subheading discussed under the *Image optimization* heading considered for each examination in Part 2. The main considerations of image quality are:

- Signal to noise ratio (SNR)
- Contrast to noise ratio (CNR)
- Spatial resolution
- Scan time

Each factor is controlled by certain parameters, and each 'trades off' against the other (see later in Table 2). This section summarizes the parameters available and the trade-offs involved. Suggested parameters are outlined in Table 1 which can be found here and at the beginning of each anatomical region in Part 2. The parameters given should be universally acceptable on most systems. However, weighting parameters in particular are field-strength dependent and therefore some modification may be required if you are operating at extremely low or high field strengths.

Signal to noise ratio (SNR)

The signal to noise ratio (SNR) is defined as the ratio of the amplitude of signal received by the coil to the amplitude of the noise. The signal is the voltage induced in the receiver coil, and the noise is a constant value depending on the area under examination and the background electrical noise of the system. SNR may be increased by using:

- Spin echo (SE) and fast spin echo (FSE) pulse sequences
- A long repetition time (TR) and a short echo time (TE)
- A flip angle of 90°
- A well-tuned and correctly sized coil
- A coarse matrix
- A large FOV
- Thick slices
- The narrowest receive bandwidth available
- As many excitations and signal averages (NEX/NSA) as possible

Table 1.   Summary of parameters. The figures given are general and should be adjusted according to the system used.

Spin echo (SE)				Coherent GRE		
0.2 T to 0.5 T	short TE	min–30 ms			long TE	15 ms+
	long TE	70 ms+			short TR	<50 ms
	short TR	250–500 ms			low flip	5°–20°
	long TR	2000 ms+			medium flip	20°–40°
1 T to 1.5 T	short TE	min–20 ms			high flip	60°+
	long TE	70 ms+		**Incoherent GRE**		
	short TR	300–600 ms			short TE	min–5 ms
	long TR	2000 ms+			short TR	<50 ms
					medium flip	20°–40°
					high flip	60°+

Fast spin echo (FSE)				Inversion recovery (IR)		
	short TE	min–20 ms			short TE	min–20 ms
	long TE	90 ms+			long TE	60 ms+
	short TR	400–600 ms			short TR	1800 ms
	long TR	4000 ms+			long TR	6000 ms+
	short ETL	2–6			short TI	100–175 ms
	long ETL	16+			medium TI	200–600 ms
					long TI	1700–2200 ms

Slice thickness				Slice numbers		
2D	thin	2.5–4 mm		Volumes	small	<32
	medium	5–6 mm			medium	64
	thick	8 mm+			large	128+
3D	thin	<1 mm		**Matrix**		
	thick	>3 mm			coarse	256 × 128
					medium	256 × 192
					fine	256 × 256
					very fine	512 × 256

FOV				PC-MRA		
	small	<18 cm		2D and 3D	TE	min
	medium	20–26 cm			TR	25–33 ms
	large	30 cm+			flip	30°
					VENC venous	20–40 cm/s
					VENC arterial	60 cm/s

NEX/NSA				TOF-MRA		
	short	1 or less		2D	TE	min
	medium	2–3			TR	28–45 ms
	multiple	4+			flip	40°–60°
				3D	TE	min
					TR	25–50 ms
					flip	20°–30°

In Part 2, the following terms and approximate parameters are suggested when discussing the number of signal averages (NEX/NSA) (see also Table 1):

- Short NEX/NSA is 1 or less (partial averaging)
- Medium NEX/NSA is 2/3
- Long or multiple NEX/NSA is 4 or more

Contrast to noise ratio (CNR)

The contrast to noise ratio (CNR) is defined as the difference in the SNR between two adjacent areas. It is controlled by the same factors that affect the SNR. All examinations should include images that demonstrate a good CNR between pathology and surrounding normal anatomy. In this way pathology is well visualized. The CNR between pathology and other structures can be increased by the following:

- Administration of contrast agents.
- Utilization of T2 weighted sequences.
- Selection of magnetization transfer (MT) sequences.
- Suppression of normal tissues via chemical/spectral pre-saturation, or sequences that null signal from certain tissues (short TI inversion recovery (STIR), fluid alternated inversion recovery (FLAIR), magnetization-prepared sequences).

Spatial resolution

The spatial resolution is the ability to distinguish between two points as separate and distinct. It is controlled by the voxel size. Spatial resolution may be increased by selecting:

- Thin slices
- Fine matrices
- A small FOV
- Rectangular/asymmetric FOV

The above criteria assume a square FOV so that if an uneven matrix is used, the pixels are rectangular and therefore resolution is lost. Some systems utilize square pixels so that the phase matrix determines the size of the FOV along the phase encoding axis. In this way resolution is maintained because the pixels are always square. The disadvantage of this system is that the size of the FOV may be inadequate to cover the required anatomy in the phase direction, and SNR is often reduced due to the use of smaller, square pixels. Therefore these systems usually have the option to utilize a square FOV in circumstances where either coverage is required or the SNR is low. In the interests of simplicity, a **square FOV** is assumed in Part 2, whereby the phase matrix size determines the resolution of the image, not the size of the FOV.

In Part 2 the following terms and approximate parameters are suggested when discussing spatial resolution (see also Table 1):

- A coarse matrix is 256×128
- A medium matrix is 256×192
- A fine matrix is 256×256
- A very fine matrix is 512×256 or more.

- A small FOV is usually less than 18 cm
- A large FOV is more than 30 cm
- On the whole, the FOV should fit the ROI

- A thin slice/gap is 2.5 mm/1 mm to 4 mm/1.5 mm
- A medium slice/gap is 5 mm/2.5 mm to 6 mm/2.5 mm
- A large slice/gap is 8 mm/2 mm+

Scan time

The scan time is the time required to complete the acquisition of data. The scan time can be decreased by using:

- A short TR
- A coarse matrix
- The lowest NEX/NSA possible

In addition to the SNR, CNR, spatial resolution and scan time, the following imaging options are also described under the *Technical issues* subheading mentioned before.

Rectangular/asymmetric FOV

The use of rectangular/asymmetric FOV is often discussed in Part 2. It enables the acquisition of fine matrices but in scan times associated with coarse matrices. It is most useful when anatomy fits into the shape of a rectangle, e.g. sagittal spine. The long axis of the rectangle usually corresponds to the frequency encoding axis and the shorter axis to phase encoding. This is important as certain phase artefacts, such as ghosting and aliasing, occur along the short axis of the rectangle. The dimension of the phase axis is usually expressed as a proportion or percentage of the frequency axis, e.g. $\frac{3}{4}$ or 75%. On some systems, rectangular/asymmetric FOV and oversampling are not compatible. If this is so, signal-producing anatomy existing beyond the FOV along the shorter phase axis is wrapped into the image. This is reduced by increasing the FOV, using spatial pre-saturation bands to nullify unwanted signal or, if this function is available, by expanding the short axis dimension to incorporate all signal-producing anatomy (see *Flow phenomena and artefacts*).

Volume imaging

Volume imaging or 3D acquisition collects data from an imaging volume or slab and then applies an extra phase encoding along the slice select axis. In this way, very thin slices with no gap are obtained, and the data set may be viewed in any plane. Steady state sequences and FSE are commonly used (see *Pulse sequences*), as they result in shorter scan times. To maintain resolution in all viewing planes, the voxels should be isotropic, i.e. they have the same dimensions in all three planes. This is achieved by selecting an even matrix and a slice thickness equal to, or less than, the pixel size. For example, if a matrix size of 256 × 256 is chosen and the FOV is 25 cm, a slice thickness of 1 mm achieves the required resolution. With a larger FOV a slightly thicker slice can be used.

The penalty of isotropic voxels, however, is a reduction in SNR due to the use of smaller voxels. This is compensated for to some degree by the fact that, as there are no gaps, a greater volume of tissue is excited and therefore overall signal return is greater. Nevertheless when volume imaging is employed, the need for resolution in all planes must be weighed against some loss of SNR. As the slices are not individually excited as in conventional acquisitions, but are located by an extra phase encoding gradient, aliasing along the slice select axis occurs. This originates from anatomy that lies within the coil (and therefore produces signal), and exists outside the volume along the slice encoding axis. It manifests itself by the first and last few slices of the imaging volume wrapping into each other and potentially obscuring important anatomy. To avoid this always over-prescribe the volume slab so that the ROI, and some anatomy on either side of it, are included. In this way any slice wrap does not interfere with the ROI (see *Flow phenomena and artefacts*). Volume imaging is commonly used in the brain and to examine joint anatomy, especially when very thin slices are required. In Part 2 the following terms and approximate parameters are suggested when discussing volume imaging (see also Table 1):

- A thin slice is less than 1 mm
- A thick slice is more than 3 mm

- A small number of slice locations is approximately <32
- A medium number of slice locations is approximately 64
- A large number of slice locations is approximately 128

The following combination of parameters *usually* yields the optimum SNR and scan time in volume imaging, although this depends on the coil type, the proton density of the area under examination, the slice thickness, and the field strength.

- 32 locations use 2 or more NEX/NSA
- 64 locations use 1 NEX/NSA
- 128 locations use less than 1 NEX/NSA

Table 2. Parameters and their trade-offs.

Parameter	Advantages	Disadvantages
TR increased	Increased SNR Increased number of slices per acquisition	Increased scan time Decreased T1 weighting
TR decreased	Decreased scan time Increased T1 weighting	Decreased SNR Decreased number of slices per acquistion
TE increased	Increased T2 weighting	Decreased SNR
TE decreased	Increased SNR	Decreased T2 weighting
NEX increased	Increased SNR of all tissues Reduced flow artefact due to signal averaging	Direct proportional increase in scan time
NEX decreased	Direct proportional decrease in scan time	Decreased SNR in all tissues Increased flow artefact due to less signal averaging
Slice thickness increased	Increased SNR in all tissues Increased coverage of anatomy	Decreased spatial resolution and partial voluming in slice select direction
Slice thickness decreased	Increased spatial resolution and reduced partial voluming in slice select direction	Decreased SNR in all tissues Decreased coverage of anatomy
FOV increased	Increased SNR Increased coverage of anatomy Decreased likelihood of aliasing	Decreased spatial resolution
FOV decreased	Decreased SNR in all tissues Decreased coverage of anatomy Increased likelihood of aliasing	Increased spatial resolution
Matrix increased	Increased spatial resolution	Decreased SNR if pixel size decreases. If pixel size remains same SNR will increase because more encodings are performed Increased scan time
Matrix decreased	Increased SNR in all tissues if pixel size increases. If pixel size remains the same SNR decreases as fewer phase encodings are performed Decreased scan time	Decreased resolution
Receive bandwidth increased	Decreased SNR	Decrease of minimum TE Decrease in chemical shift
Receive bandwidth decreased	Increased SNR	Increase in minimum TE Increase in chemical shift

Decision strategies

To optimize image quality the data should have a high SNR, good resolution and be acquired in a short scan time. This is usually impossible, however, as the factors that must be increased to improve SNR may have to be decreased to gain spatial resolution. An example of this is matrix selection. A coarse matrix is required to obtain large voxels and therefore a high SNR. However, a fine matrix with small voxels and low SNR is not only necessary to maintain good spatial resolution, but also increases the scan time as more phase encodings are performed. The operator must decide which factor (either SNR, resolution or scan time) is the most important and optimize this. One or both of the other two may have to be sacrificed accordingly.

When discussing these issues in Part 2 the importance of good SNR over the other factors is emphasized, as in our view there is little point in having an image with good resolution if the SNR is poor. The selection of an appropriately sized and tuned coil is also important, together with the proton density of the area under examination. For example, when examining the chest which has a low SNR, the parameters selected must optimize the SNR as much as possible, and resolution and scan time are sacrificed. The importance of limiting the scan time for patient toleration is also discussed in Part 2. If the scan time is lengthy, all patients will eventually become uncomfortable and move. The resultant motion artefact degrades any image regardless of its SNR or resolution characteristics. Therefore it is important to minimize scan times to acceptable levels. If patients are in pain or uncooperative, this strategy is even more important.

Conclusion

The variety of parameters used in MRI is often bewildering, but their importance is undisputed, especially in determining image quality. A good working knowledge of these parameters and how they interrelate is necessary to ensure an optimum examination. Table 2 summarizes these trade-offs. The choice of pulse sequence is also important in determining image contrast, and these are outlined in the next section.

PULSE SEQUENCES

Introduction

This section refers mainly to the *Suggested protocol* heading considered for each examination in Part 2, although pulse sequences are sometimes mentioned under the *Technical issues* subheading of *Image optimization*. A summary of the mechanisms and uses of the most commonly used pulse sequences are described. All pulse sequences are described using their generic name. Table 3 provides a comparison of the acronyms used by different manufacturers to describe their pulse sequences and imaging options. Omission of a certain term does not necessarily mean that the manufacturer does not support an option. It simply indicates that it was not possible to determine the acronym. The parameters given in Table 1 should be universally acceptable on most systems. However, weighting parameters in particular are field-strength dependent and therefore some modification may be required if you are operating at extremely low or high field strengths.

Spin Echo (SE)

A spin echo (SE) pulse sequence (also known as conventional spin echo (CSE)) usually uses a 90° excitation pulse followed by a 180° rephasing pulse to produce a spin echo. Some newer SE sequences use a variable flip angle, but traditionally the excitation pulse has a magnitude of 90°. This amplitude of the flip angle is consistently assumed in the protocols. SE sequences can be used to generate one or several spin echoes. One echo is usually used for T1 weighting while two echoes are used for proton density (PD) and T2 weighting. SE pulse sequences are the most commonly implemented sequences as they produce optimum SNR and CNR.

For **T1 weighting** in SE use:
    short TE   min–20 ms
    short TR   250–600 ms

For **PD/T2 weighting** in SE use:
    short TE   20 ms (first echo PD)
    long TE   70 ms+ (second echo T2)
    long TR   2000 ms+

Fast spin echo (FSE)

Fast spin echo (FSE) uses a 90° flip angle followed by several 180° rephasing pulses to produce several spin echoes in a given TR. Each echo is phase encoded with a

Table 3. Comparison of manufacturer acronyms (see *How to use this book* for abbreviations).

Pulse sequence/ imaging option	General Electric	Philips	Siemens	Picker	Elscint	Hitachi	Shimadzu
Spin echo	Spin echo MEMP VEMP	Spin echo	Spin echo	Spin echo	Spin echo	Spin echo	Spin echo
Fast spin echo	FSE	TSE	TSE	FSE		FSE	
Coherent gradient echo	GRASS	FFE	FISP	FAST	F short	GFEC	SSFP
Incoherent gradient echo (RF spoiled)	SPGR	T1 FFE		RF spoiled FAST			STAGE T1W
Incoherent gradient echo (gradient spoiled)	MPGR		FLASH		Short	GRE	STAGE
Steady state free precession	SSFP	T2 FFE	PSIF	CE FAST	E short	GFEC contrast	STERF
Inversion recovery (IR)	MPIR	IR	IR	IR	IR	IR	IR
Ultra-fast sequences	FAST GRASS (IR/DE prep) FAST SPGR	TFE	Turbo FLASH 3D MP RAGE	RAM FAST			SMASH
Short TI inversion recovery	STIR	SPIR	STIR	STIR	STIR	STIR	STIR
Pre-saturation	SAT	REST	SAT	Pre-SAT	Spatial pre-SAT	SAT	SAT
Gradient moment nulling	FC	FLAG	GMR	MAST	STILL	GR	SMART
Respiratory compensation	RC	PEAR	Respiratory triggering	Respiratory gating PRIZE	FREEZE	Phase reordering	
Signal averaging	NEX	NSA	AC	NSA		NSA	
Partial averaging	Fractional NEX	Half scan	Half Fourier	Phase conjugate symmetry	Single-side encoding	Half Fourier	
Partial echo	Fractional echo	Partial echo		Read conjugate symmetry	Single-side view		
Oversampling	No phase wrap	Fold over suppression	Oversampling	Oversampling	Anti-aliasing	Anti-wrap	
Rectangular/ asymmetric FOV	Rectangular FOV	Rectangular FOV	Half Fourier imaging	Undersampling	Rectangular FOV	Rectangular FOV	

different amplitude of gradient slope, so that data from each echo are collected and stored in a different line of K space. In this way more than one line of K space is filled per TR, and the scan time is reduced accordingly. The echo train length (ETL) refers to the number of 180° rephasing pulses that correspond to the number of lines of K space filled per TR. The longer the ETL, the shorter the scan time as more lines of K space are filled per TR.

FSE can be used to produce either one or two echoes as in SE. On many systems

the echo train may be split so that data are collected from the first half of the echo train to acquire the first echo, and from the latter half to acquire the second echo. This strategy is commonly used to produce PD and T2 images that demonstrate similar weighting to SE. However, T2 images can be acquired without a PD image. A T2 image alone, rather than a dual echo, is often acquired in Part 2. It is of course perfectly justified to use a dual echo sequence if this is required. FSE sequences have been further modified to include 3D acquisitions and single-shot techniques. Single shot FSE (SS-FSE), which is also termed HASTE (half acquisition single shot turbo echo), combines long ETLs which fill all of K space in one shot with half Fourier acquisition techniques that acquire only half of K space and then transpose data into the other half. This technique allows very rapid acquisitions which enables multiple slice breath-hold and real-time imaging.

Some contrast characteristics of FSE differ from conventional SE. Fat remains bright on T2 weighted images and fat suppression techniques may be needed to compensate for this. The multiple 180° RF pulses used in FSE sequences cause lengthening of the T2 decay time of fat so that the signal intensity of fat on T2 weighted FSE images is higher than in SE. This sometimes makes the detection of marrow abnormalities difficult. Therefore when imaging the vertebral bodies for metastatic disease, a STIR sequence should be utilized. Muscle can appear darker than usual especially on the T2 weighted images. This is again due to the multiple 180° pulses causing a MT effect.

In addition, certain artefacts may be prominent in FSE sequences. Image blurring is often a problem in long ETL sequences. This occurs because each line of K space contains data from echoes with a different TE. In long ETL sequences, the very late echoes have a low signal amplitude and, as the outer lines of K space are filled with data from these echoes, there are insufficient data to provide adequate resolution. Image blurring is most commonly seen at the edges of tissues with different T2 decay times. It may be reduced by decreasing the size of the FOV in the phase direction (depending on how the manufacturer implements a rapid FSE sequence) or by selecting a broad receive bandwidth. However, while the latter does improve overall image quality by reducing blurring, it also reduces the SNR. Lastly, FSE is not always compatible with options such as phase reordered respiratory compensation (RC) and therefore conventional SE or breath-hold sequences are often the sequence of choice when respiratory artefact is likely to be troublesome.

For **T1 weighting** in FSE use:

short TE	min–20 ms
short TR	400–600 ms
short ETL	2–6

For **T2 weighting** in FSE use:

long TE	90 ms+
long TR	4000 ms+
long ETL	16+

For **PD/T2 weighting** in FSE use:

short TE	min–20 ms (first echo PD)
long TE	90 ms+ (second echo T2)
long TR	4000 ms+
medium ETL	8–12 (split 4 and 4 or 6 and 6)

Inversion recovery (IR/IR-FSE)

Inversion recovery (IR) pulse sequences begin with a 180° pulse that inverts the net magnetization vector into full saturation. When the inverting pulse is removed, the magnetization begins to recover and return towards B_0. After a specific time TI (inversion time), a 90° excitation pulse is applied which transfers the proportion of magnetization that has recovered to B_0 into the transverse plane. This transverse magnetization is then rephased by a 180° rephasing pulse to produce an echo. In IR-FSE several 180° rephasing pulses are applied as in FSE, so that more than one line of K space can be filled per TR, so reducing the scan times.

Conventional IR is most commonly used to produce heavily T1 weighted images. However, it and IR-FSE may also be implemented to eliminate the signal from certain tissues by applying the 90° excitation pulse when the magnetization in that tissue has recovered into the transverse plane and therefore has no longitudinal component. In this way the signal from the tissue is nulled by the excitation pulse. There are two main uses of this technique. Short TI inversion recovery (STIR) uses a short TI that corresponds to the null point of fat so that the excitation pulse specifically nulls the signal from fat. In Part 2 STIR is used as a fat suppression technique in conjunction with a FSE sequence to produce T2 weighting by using long TEs and ETLs. Fluid attenuated inversion recovery (FLAIR) utilizes a long TI corresponding to the null point of cerebrospinal fluid (CSF) so that the excitation pulse specifically nulls the signal from CSF. In Part 2 FLAIR is used in conjunction with a T2 weighted FSE sequence. It is especially useful to increase the conspicuity of periventricular lesions.

For **T1 weighting** in IR use:

short TE	min–20 ms
long TR	2200 ms+ (to allow full recovery of all magnetization before the next inverting pulse is applied)
medium TI	200–600 ms (depending on the field strength)

For **STIR** use:

TE	60 ms
TR	6000 ms+
ETL	16+
short TI	100–175 ms

For **FLAIR** use:

TE	60 ms
TR	6000–10 000 ms
ETL	16+
long TI	1700–2200 ms

In all IR sequences the TI is field-strength dependent. In FLAIR sequences combined with long ETL FSE, if the TR is not long enough to allow full recovery of +z magnetization after the last echo in the train has been collected, a shorter TI than usual may be required to adequately null the CSF signal. This is because if only partial +z magnetization has recovered at the end of the TR period, this is converted into only partial -z magnetization after inversion and therefore the magnetization in CSF does not take as long to reach its null point.

Coherent gradient echo (GRE) (T2*)

Coherent gradient echo (GRE) pulse sequences use a variable flip angle followed by gradient rephasing to produce a gradient echo. This sequence utilizes the steady state so that the transverse component of magnetization is allowed to build up over successive repetition times. This is achieved by a reversal of the phase encoding gradient prior to each repetition that rephases this transverse magnetization. In this way the coherence of the transverse magnetization is maintained, so that mainly signal from tissues with a high water content and a long T2 is present in the image. They are often said to demonstrate an angiographic, myelographic or arthrographic effect as blood, CSF and joint fluid are bright. As the TR is short, these sequences are mainly used for breath-holding or in a volume acquisition. The TR can be lengthened, however, to achieve multi-slice acquisitions demonstrating excellent contrast. This strategy is common in spinal and joint imaging.

Faster versions of this sequence are now available enabling multiple slice breath-hold, dynamic and real-time imaging. Scan times are reduced by a combination of partial RF pulses, partial Fourier acquisitions and centric K space filling. Due to the inherent lack of contrast in this sequence, magnetization preparation pulses are sometimes used which either null the signal from certain tissues, thereby increasing the CNR between them and the surrounding structures, or increase overall T2 contrast.

For **T2* coherent GRE** use:

short TR	<50 ms (300–600 ms in multi-slice acquisitions)
long TE	15 ms+
medium flip angles	30°–45°

Incoherent (spoiled) gradient echo (GRE) (T1/PD)

Incoherent (spoiled) GRE sequences also use a variable flip angle and gradient rephasing resulting in a gradient echo. They are commonly used in the steady state so that residual magnetization builds up in the transverse plane. However, these sequences spoil this magnetization with phase shifted RF pulses which do not allow the residual transverse magnetization to be received. T2* weighting does not, therefore, dominate image contrast to as great an extent as coherent GRE pulse sequences, and the images are mainly T1/PD weighted. Due to the short TR, these sequences can be used for breath-holding, dynamic imaging, and in cine and volume acquisitions. As they are mainly T1/PD weighted, they are very effective in conjunction with contrast enhancement and to demonstrate anatomy.

As with coherent GRE there is a faster version of this sequence enabling multiple slice breath-hold, dynamic imaging after contrast and real-time imaging. Scan times are reduced by a combination of partial RF pulses, partial Fourier acquisitions and centric K space filling. Due to the inherent lack of contrast in this sequence,

magnetization preparation pulses are sometimes used which either null the signal from certain tissues, thereby increasing the CNR between them and surrounding structures, or increase the overall T2 contrast.

For **T1/PD incoherent (spoiled) GRE** use:

short TR	<50 ms
short TE	min–5 ms
medium flip angle	30°–45°

Note: Some systems utilize GRE sequences in conjunction with gradient spoiling (instead of rephasing), and with either a long or short TR. The use of a longer TR allows for improved image quality in a multi-slice acquisition, although under these circumstances, the steady state is not employed (as the TR is now longer than the T1 and T2 times of the tissues). Although gradient spoiling also dephases the residual transverse magnetization, it allows more $T2^*$ weighting to appear in the image than RF spoiled sequences. To avoid confusion in Part 2, coherent GRE sequences have been used only to acquire $T2^*$ weighted images. Incoherent (spoiled) GRE pulse sequences have been used to acquire T1 and PD weighted images.

Echo planar imaging (EPI)

Echo planar imaging (EPI) sequences fill all of K space in one repetition by using very long echo trains. Echoes can be generated by multiple 180° pulses (termed spin echo EPI [SE-EPI]) or by gradients (termed gradient echo EPI [GE-EPI]). If all of K space is filled in one go, this is termed single shot EPI (SS-EPI). SS-EPI produces images much more rapidly than SS-FSE as it uses a train of gradient echoes rather than spin echoes and can therefore fill K space in a fraction of a second. However, SS-EPI sequences are very prone to artefacts such as chemical shift, distortion and blurring. These artefacts increase relative to the echo spacing and therefore the time of the echo train. For this reason EPI sequences are often used in multi-shot mode where a quarter or a half of K space is filled per TR period thereby reducing the time of the echo train. This can also be minimized by implementing any, or all, of the following:

- Increasing the FOV
- Increasing the receive bandwidth
- Reducing the frequency encoding matrix
- Reducing the phase FOV

EPI and the fast versions of both coherent and incoherent (spoiled) GRE sequences currently represent the fastest acquisition modes in MRI. Real-time, dynamic and functional studies are possible using this technique. Some of these are discussed in Part 2 and are therefore summarized here.

Real-time imaging

Very fast sequences, such as EPI, permit real-time imaging of moving structures. This is proving to be very useful in interventional procedures where a biopsy needle, laser probe or other instrument can be visualized in real-time. Biopsies, thermal ablations of tumours, angioplasties, endoscopies and limited-field surgical operations are the most promising applications of this technique (see also *Dynamic imaging* below).

Dynamic imaging

Dynamic imaging refers to the rapid acquisition of images either after contrast enhancement, or to observe movement. It may be utilized to visualize the motion of a joint (e.g. a knee), or a structure such as the cervical spine or pelvic floor. Single images may be obtained using GRE or EPI sequences in various degrees of motion. Alternatively multiple slices can be acquired to either cover more anatomy, or to visualize the structure in many positions during data acquisition. When used with EPI, acquisitions in the order of 20 images per second are possible and therefore these techniques are termed real-time. If used in conjunction with GRE sequences, however, data acquisition is much slower and therefore these techniques are termed quasi real-time. Depending on the temporal resolution of the structure under examination, quasi real-time techniques may not always provide an accurate representation of motion.

Used in conjunction with contrast enhancement, dynamic imaging visualizes the speed of uptake of contrast, which may be necessary to determine the nature of a lesion. This is termed *perfusion imaging*. It can be used in many areas including the brain, pancreas, liver and prostate. One of the most important applications of dynamic imaging is in the breast where contrast enhancement is useful to characterize a lesion. Some literature suggests that benign lesions take longer to enhance than malignant lesions, and scar tissue may not enhance at all. As gadolinium is given, a T1 sequence is required and due to the dynamic nature of the series, the acquisition times must be as short as possible. Incoherent (spoiled) GRE or FSE sequences are therefore ideal for this type of examination. The entire breast, rather than only a few slices through a lesion, can be demonstrated (some systems now have ultrafast volume acquisition available). This method is obviously important if multi-focal disease is suspected. Tissue characterization by measuring uptake of contrast is also a useful technique in the prostate.

Functional imaging (fMRI)

Functional imaging (fMRI) is a rapid technique that acquires images of the brain during activity or stimulus and at rest. The two sets of images are then subtracted demonstrating functional brain activity as a result of increased blood flow to the activated cortex. The mechanism responsible for contrast in functional imaging is termed BOLD (blood oxygenation level dependent) which exploits the differences in magnetic susceptibility between oxy- and deoxyhaemaglobin. This results in an

increased signal intensity in activated areas of the cortex which have lower levels of deoxyhaemaglobin than inactivated areas. The high signal is then overlaid onto anatomical images. Functional MRI is useful to evaluate brain activity in a whole range of disorders including epilepsy, stroke and behavioural problems.

Diffusion weighted imaging (DWI)

Diffusion weighted imaging (DWI) demonstrates areas with restricted diffusion of extracellular water such as infarcted tissue. In normal tissue, extracellular water diffuses randomly whereas in ischaemic tissue, cells swell and absorb water thereby reducing average diffusion. Diffusion weighted images are most effectively acquired by combining a rapid sequence such as EPI or GRE with two bipolar gradients. These gradient pulses are designed to cancel out the phase shift of stationary spins whilst moving spins experience a phase shift. Therefore signal attenuation occurs in normal tissue with random motion and high signal appears in tissues with restricted diffusion. The amount of attenuation depends on the amplitude of the gradients which is altered by selection of a b-value (expressed as s/mm^2). Gradient pulses can be applied along the X, Y and Z axis to determine the axis of restricted diffusion. The term isotropic diffusion is used to describe diffusion gradients applied in all three axis. DWI is mainly useful in the brain to differentiate salvageable and non-salvageable tissue after stroke. It may also be useful in the liver.

Magnetic resonance angiography (MRA)

The principle of magnetic resonance angiography (MRA) is to acquire images where the signal returned from flowing nuclei is high, and the signal from stationary nuclei is low. In this way contrast between vessels and background tissue is achieved. There are several techniques available to obtain this contrast. Black-blood imaging combines SE or FSE sequences with spatial pre-saturation pulses to produce images in which flowing vessels appear black. High signal seen in this type of sequence may indicate stenosis or occlusion of the vessel (see *Flow phenomena and artefacts*). Bright-blood imaging combines GRE sequences with GMN to produce images where flowing vessels are bright. A signal void seen in this type of sequence may indicate either a stenosis or occlusion of the vessel (see *Flow phenomena and artefacts*).

There are additional techniques designed especially for angiography. Both allow for data acquisition in either sequential (2D) or volume (3D) mode. Each has its own advantages and disadvantages and therefore each is used for different purposes. The two types of MRA are summarized below. These are *time of flight* (TOF) and *phase contrast* (PC).

Time of flight (TOF)

This usually uses an incoherent (spoiled) GRE sequence in conjunction with TR and flip angle combinations that saturate background tissue, but allow moving spins to

enter the slice/volume fresh and therefore return a high signal. Spatial pre-saturation pulses placed between the origin of flow and the FOV saturate moving spins entering the FOV, thereby improving visualization of either arterial or venous circulation. These pulses are often concatenated in 2D acquisitions so that the spatial pre-saturation pulse is applied around each slice in the stack, as opposed to the whole set of slices. This strategy improves the efficiency of pre-saturation. Unwanted signal is sometimes generated by tissues that have very short T1 recovery times (such as fat), as they recover some of their longitudinal magnetization between each RF pulse and therefore produce signal. Spectral/chemical pre-saturation pulses, imaging with a TE that collects the echo when fat and water are out of phase with each other, and utilizing magnetization transfer (MT) contrast, commonly reduce this problem.

In volume imaging, flowing spins often become saturated by the RF pulses, thereby reducing their signal. This problem can be minimized by the implementation of ramped flip angles which initially use small flip angles, and then gradually increase them incrementally during data acquisition. In this way the saturation of flowing nuclei is delayed, therefore maintaining vessel signal. In 2D acquisitions, however, TOF-MRA provides good vessel contrast as nuclei are not usually present in the slice long enough to become saturated. Common applications are to demonstrate venous and arterial flow in the head, neck and peripheral vessels.

For **2D TOF-MRA** use:

TR	28–45 ms
Flip angle	40°–60°
TE	minimum

For **3D TOF-MRA** use:

TR	25–50 ms
Flip angle	20°–30°
TE	minimum

Phase contrast (PC)

This usually uses a coherent GRE sequence acquired both with, and without, a bipolar gradient pulse. The phase acquired by flowing spins as a result of the application of the bipolar gradient is used to produce images based on subtraction. Sensitivity to flow velocity is controlled by a parameter called velocity encoding or VENC, which can be applied in one, or all three orthogonal planes. PC-MRA provides excellent background suppression and avoids intra-slice/slab flow saturation. However, the scan times associated with PC-MRA are often very long as the scan time is dependent not only on the TR, matrix size and NEX/NSA, but also on the number of flow encoded axes. Common applications are to demonstrate arterial flow in the head and major veins.

For **2D** and **3D PC MRA** use:

TR	25–33 ms
Flip angle	20°
TE	minimum
VENC	20–40 cm/s for venous flow, increase up to 60 cm/s for arterial flow

Magnetization transfer (MT) contrast

Magnetization transfer (MT) is a technique that is commonly used to suppress background tissue thereby enhancing the conspicuity of vessels and certain disease processes. Its function is based on the relaxation differences between water protons in different environments. Water protons broadly fall into two categories: those that are free, and those that are bound to surrounding immobile macromolecules. MT involves the exchange of magnetization between the free and bound water protons. Pre-saturation off-resonant pulses applied just before the RF excitation pulse saturate the bound protons and promote an exchange of some of this saturated magnetization onto the free protons. This pulse is designed to excite hydrogen protons in macromolecules such as proteins. These relatively large molecules have a very short T2 and usually do not contribute to the MR image. With the MT pulse, however, some of these spins transfer their magnetization to the more mobile water spins. This results in a reduced signal return from the free protons. For example, grey and white matter loses 30–40% of its signal when an MT pulse sequence is utilized. The common uses of MT are to increase the conspicuity

Table 4. Summary of the contrast characteristics of pathology and normal anatomy.

	T1	T2
High signal	Fat Haemangioma Intra-osseous lipoma Radiation change Degenerative fatty deposition Methaemoglobin Cysts with proteinaceous fluid Paramagnetic contrast agents Slow-flowing blood	CSF Synovial fluid Haemangioma Infection Inflammation Oedema Some tumours Haemorrhage Slow-flowing blood Cysts
Low signal	Cortical bone AVN Infarction Infection Tumours Sclerosis Cysts Calcification	Cortical bone Bone islands Deoxyhaemoglobin Haemosiderin Calcification T2 paramagnetic agents
No signal	T1 and T2	
	Air Fast flowing blood Ligaments Tendons Cortical bone Scar tissue Calcification	

of certain disease processes such as multiple sclerosis, haemorrhage and AIDS, and to improve vessel contrast in TOF-MRA images by suppressing background tissue.

Conclusion

The choice of pulse sequence is usually the first decision made by either the radiologist or radiographer/technologist as it determines the weighting and contrast characteristics of the image. Table 4 summarizes the contrast characteristics of pathology and normal anatomy. Careful consideration of the image quality and the required scan time parameters is also necessary to achieve the optimum examination. The flow and artefact phenomena common to the area under examination must also be taken into account, as some compensation techniques may compromise the pulse sequence chosen. These phenomena are discussed in the next section.

FLOW PHENOMENA AND ARTEFACTS

Introduction

This section refers mainly to the *Artefact problems* subheading discussed under the *Image optimization* heading considered for each examination in Part 2. The most common flow phenomena and artefacts are summarized in Table 5.

Flow phenomena

Time of flight (TOF)

Time of flight (TOF) phenomenon occurs because nuclei that move through the slice may receive only one of the RF pulses applied. In GRE sequences the gradient rephasing is not slice selective, so nuclei produce signal as long as they have been excited at some point and are rephased by the gradient. In a SE sequence, a nucleus may receive the excitation pulse but then exit the slice before the 180° rephasing pulse can be applied. Conversely, it may not be present in the slice when the excitation pulse is applied, and then enter the slice to receive only the 180° pulse. Under these circumstances the nucleus does not produce a signal. In SE sequences, TOF effects cause either a signal loss or signal enhancement from flowing nuclei, and they are compensated for by using pre-saturation pulses placed between the origin of the flow and the FOV.

Entry slice phenomenon

This phenomenon depends on the excitation history of nuclei flowing within a vessel, and is largely controlled by the direction of flow relative to slice excitation. Nuclei that flow in the same direction as slice excitation receive several RF excitation pulses and quickly become saturated. Nuclei that flow in the opposite direction to the slice excitation do not experience repeated RF excitation pulses, as they are always entering the selected slice 'fresh'. They are, therefore, not saturated as quickly as nuclei flowing in the same direction as slice excitation. These phenomena result in a difference in signal between arteries and veins where flow is perpendicular to the slice plane, and is most prominent in the first and last slices of the imaging stack. Entry slice phenomenon is compensated for by using pre-saturation pulses placed between the origin of the flow and the FOV.

Intra-voxel dephasing

This is caused by the presence of gradients that either accelerate or decelerate flowing nuclei as they move from areas of differing field strength along the gradient. As a result of this acceleration or deceleration, the flowing nuclei either gain or lose phase relative to their stationary counterparts. This phase difference between stationary and flowing nuclei in the same voxel causes dephasing and a signal loss. Intra-voxel dephasing is compensated for by using gradient moment nulling (GMN).

Flow artefact remedies

The two main remedies of flow-related artefacts are spatial pre-saturation pulses and GMN. Spatial pre-saturation nullifies signal from nuclei that produce unwanted signal or artefact by applying a 90° RF pulse to selected tissue before the pulse sequence begins. Therefore, the magnetic moments of these nuclei are inverted to 180° by the excitation pulse and return no signal. Pre-saturation pulses may also be delivered at the specific precessional frequency of either fat or water to nullify signal from these types of tissue. This technique, which is called chemical/spectral pre-saturation, either utilizes a 90° saturation pulse as described above, or the pulse has a greater magnitude and inverts the magnetization in the tissue as in inversion recovery pulse sequences (see *Pulse sequences*). Chemical pre-saturation can be used to distinguish between fat and enhancing pathology in T1 weighted sequences and in FSE T2 weighted sequences where fat and pathology are often isointense.

   GMN utilizes extra gradients to rephase the magnetic moments of flowing nuclei so that they have a similar phase to their stationary counterparts. Both GMN and spatial pre-saturation decrease flow artefact seen on an image, but are also valuable in reducing phase mismapping and motion artefact. However, there are penalties associated with their use. Their advantages and disadvantages are summarized below.

Spatial pre-saturation:
- Produces low signal from flowing nuclei.
- Reduces motion and aliasing if bands are placed over signal-producing anatomy.
- Increases the specific absorption rate (SAR) and may reduce the slice number available per TR.
- Mainly reduces time of flight and entry slice phenomena.

GMN:
- Produces high signal from flowing nuclei.
- Increases the minimum TE and may reduce the slice number available.
- Mainly reduces intra-voxel dephasing.

Artefacts

Phase mismapping

Phase mismapping or ghosting is caused by anatomy moving between each application of the phase encoding gradient, and by motion along the phase encoding gradient during the acquisition of data. Pulsatile motion of vessels, movement of the chest wall during respiration and cardiac motion are the most common sources of this artefact (see later in Fig. 6). Phase mismapping is reduced by one or more of the following:

- Swapping the phase axis so that the artefact does not interfere with the area under examination (see later in Figs 29 and 85).
- Placement of spatial pre-saturation pulses between the origin of the artefact and the FOV.
- Using respiratory compensation (RC) (see *Gating and respiratory compensation techniques*).
- Using echocardiogram (ECG) gating or peripheral (Pe) gating (see *Gating and respiratory compensation techniques*).
- Selecting GMN.

Aliasing

Aliasing occurs when anatomy that lies within the boundaries of the receiver coil (and therefore produces signal) exists outside the FOV. If the data from the signal received are undersampled by the system, there is a duplication of frequency and phase values so that anatomy that exists outside the FOV is allocated a pixel position within the FOV. This anatomy is therefore 'wrapped' into the image (see later in Fig. 86). Aliasing can occur along both the frequency encoding axis (frequency wrap) and the phase encoding axis (phase wrap). Frequency wrap is largely eliminated with the use of digital filters that filter out signal originating outside the FOV. Phase wrap is reduced by:

- Increasing the FOV to the boundaries of the coil.
- Oversampling in the phase direction.
- Placing spatial pre-saturation pulses over signal-producing anatomy (see later in Fig. 87).

Chemical shift

Chemical shift artefact is caused by the dissimilar chemical environments of fat and water. This results in a precessional frequency difference between the magnetic moments of fat and water and is called chemical shift. Its magnitude depends on the magnetic field strength of the system and significantly increases at higher field strengths. Chemical shift artefact causes a displacement of signal between fat and water along the frequency axis. It is reduced by:

- Scanning with a low field-strength magnet.
- Removing either the fat or water signal by the use of STIR/chemical/ spectral pre-saturation, the Dixon technique (see *Chemical misregistration* below).
- Broadening the receive bandwidth.

Chemical misregistration

Chemical misregistration is also caused by the difference in precessional frequency between fat and water. However, this occurs because as fat and water are precessing at different frequencies, they are in phase with each other at certain times and out of phase at others. When the signals from both fat and water are out of phase, they cancel each other out so that signal loss results (see later in Fig. 148). This artefact mainly occurs along the phase axis and causes a dark ring around structures that contain both fat and water. It is most prevalent in GRE sequences and it can be used positively to reduce the signal from fat (Dixon technique). To reduce chemical misregistration:

- Use SE or FSE pulse sequences.
- Use a TE that matches the periodicity of fat and water so that the echo is generated when fat and water are in phase. The periodicity depends on the field strength (approximately 4.2 ms at 1.5 Tesla and 7 ms at 0.5 Tesla). The **Dixon technique** involves selecting a TE at half the periodicity so that fat and water are out of phase. In this way the signal from fat is reduced. This technique is mainly effective in areas where water and fat co-exist in a voxel.

Truncation

This is caused by undersampling of data at the interface of high and low signal. It occurs along the phase axis and produces a dark band running through a high signal area. It is most commonly seen in the cervical cord, where it is specifically known as Gibbs artefact. Truncation is mainly reduced by increasing the number of phase encoding steps.

Magnetic susceptibility

Magnetic susceptibility artefact occurs because all tissues magnetize to a different degree depending on their magnetic characteristics. This produces a difference in their individual precessional frequencies and phase. The phase discrepancy causes dephasing at the boundaries of structures with a very different magnetic susceptibility, and signal loss results. It is commonly seen on GRE sequences when the patient has a metal prosthesis *in situ* (see later in Fig. 234), but is also visualized at the interface of the petrous bone and the brain on coronal incoherent (spoiled) GRE images. Magnetic susceptibility can be used advanta-geously when investigating haemorrhage or blood products, as the presence of this

artefact suggests that bleeding has recently occurred. Magnetic susceptibility is reduced by:

- Using SE or FSE pulse sequences.
- Removing all metal items from the patient before the examination.

Patient motion

Involuntary movement such as respiratory or cardiac motion is compensated for by using the measures discussed earlier in this section under *Phase mismapping* and later in *Gating and respiratory compensation techniques*. Tips to reduce voluntary motion are discussed under *Patient care and safety*.

Table 5. Artefacts and their remedies.

Artefact	Remedy	Penalty of remedy
Truncation	Increase phase encodings Increase NEX/NSA	Increases scan time Increases scan time
Phase mismapping	Respiratory compensation Swap phase and frequency Gating Pre-saturation Gradient moment nulling	May lose slices May need oversampling TR variable May lose slices Increases minimum TE
Chemical shift	Reduce bandwidth Reduce FOV Use chemical saturation	Increases TE Reduces SNR Reduces SNR
Chemical misregistration	Set TE at multiple of periodicity	None
Aliasing	Oversampling (frequency) Oversampling (phase) Enlarge FOV	None None Reduces resolution
Zipper	Call engineer	Irate engineer!
Magnetic susceptibility	Use spin echo Remove metal where possible	Not flow sensitive
Shading	Load coil properly	None
Motion	Use antispasmodic agent Immobilize patient Counselling All remedies for mismapping Sedation	Costly, invasive None None See above Invasive, requires monitoring
Cross talk	None	None
Cross excitation	Interleaving of slice acquisition Squaring off of RF pulses	Doubles the scan time Reduces SNR

Conclusion

The main artefacts encountered in MRI are described here. In addition, phase artefact caused by pulsation of great vessels, CSF flow and cardiac and respiratory motion are compensated for by using appropriate software and these are discussed in the next section. Table 5 summarizes artefacts and how they may be remedied.

GATING AND RESPIRATORY COMPENSATION TECHNIQUES

Introduction

This section refers to the mechanisms and correct placement of gating leads and respiratory bellows. The basic concepts of these techniques are summarized below.

Cardiac gating (ECG gating)

Cardiac gating uses the electrical signal detected by leads placed onto the patient's chest to trigger each RF excitation pulse. In this way, each image is always acquired at the same phase of the cardiac cycle, so that phase mismapping from cardiac motion is reduced. The correct placement of the leads is very important to optimize image quality.

Lead placement

There are usually four leads that are colour coded for easy use. Some systems may only use three leads. In addition, not all systems use the same colour coding but the principle of their placement is the same. Leads can be placed either anteriorly on the chest, or posteriorly on the patient's back. Anterior placement is usually simpler as the landmarks are easier to find. In addition if the leads are placed posteriorly, the patient lies on them during the examination, which may be uncomfortable. The anterior lead placement is described here but if the trace on the ECG monitor is poor, the leads can be placed posteriorly in a mirror image to the anterior leads. This may improve the trace. Lay the patient supine on the examination couch. The patient wears a front opening gown for easy access. The lead stickers are then firmly attached to the patient's skin. The leads are usually colour coded thus:

Black
White
Red (live)
Green (ground or earth)

The white and the red leads are placed across the heart, as the voltage difference between the two produces the ECG trace. The green lead is positioned as close to, but not touching, the red lead as this acts as a ground. The black lead also acts as ground. Some systems may not have colour coding, but directions on lead
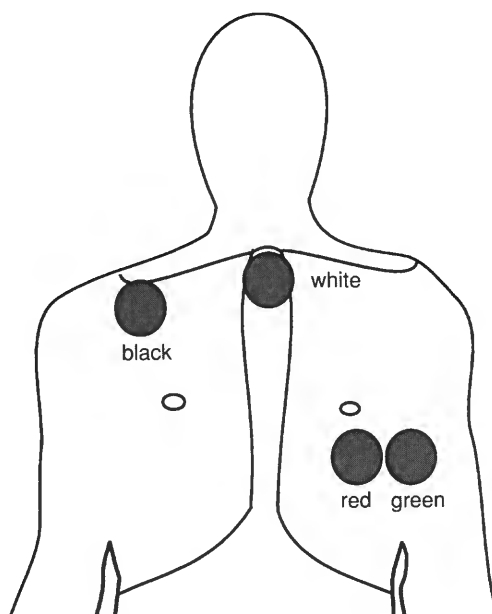
Fig. 4. The correct placement of gating leads.

placement are usually given by the manufacturer. Leads can be placed in a variety of ways as long as the above criteria are met. Described below is the simplest method of lead attachment (Fig. 4):

Black lead	right upper chest below the clavicle
White lead	in the midline on the superior aspect of the sternum
Red lead	one intercostal space directly inferior to the left nipple
Green lead	lateral to the red lead as close as possible to, but not touching, it

The black lead may be omitted if it is not available on the system. Once the leads are attached and plugged into the system, check that the ECG trace is satisfactory. Traces vary according to rate, rhythm and cardiac output. These in turn depend on the activity of the heart that is often altered by certain disease processes. Arrhythmias and poor cardiac output (which may be why the patient is being examined) are common problems. The signs of a good trace are:

- A regular rate – the PQRST complexes are spaced evenly apart.
- The R wave is significantly larger than the T wave.
- The PQRST complex has good amplitude (Fig. 5).

If the trace is satisfactory, the patient is placed within the magnet bore. This action frequently alters the trace, and often does so to such an extent that the trace is no longer acceptable. The commonest problem is an elevation of the T wave so that
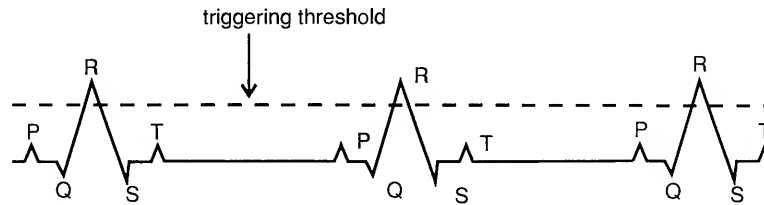
Fig. 5. A normal ECG trace and the correct placement of the triggering threshold relative to the R wave.

the system cannot distinguish it from the R wave. If this occurs, or if the original trace is unsatisfactory, several measures can be taken.

How to improve the trace

- Always ensure that the electrodes are firmly attached to the chest wall. In male patients, shave any chest hair in the region of the electrodes and clean the skin with alcohol. This removes grease that may prevent proper attachment. After the skin is dry, the electrodes are attached.
- Make sure that the leads are firmly attached to the stickers in the correct order.
- The leads may be swapped around or placed posteriorly to improve the trace. Initially, swap the black and the white leads or the red and the green leads. If this fails to improve the trace, try any other variation of lead placement.
- Place the patient inside the magnet feet first. Patients are usually positioned head first into the magnet for examinations of the chest, however placing them feet first is often beneficial, especially if the problem is an elevated T wave.
- Movement of the cable leads causes irregularities of the trace. Ensure that they are immobilized (see *Cable safety* below), and that the patient does not touch them during the examination. In addition coughing or sneezing can interrupt the trace, so ask the patient to try not to move during the acquisition of data.
- Change to peripheral gating or pseudo gating (dispensing with gating and setting a TR that is equal to the RR interval).

If after all these measures are taken the trace is still poor, the problem could be a faulty monitor or software problem. Gating is often unreliable and there are occasions when the operator has to make do with the trace displayed. In our experience awful traces can lead to excellent images, and vice versa (Fig. 6).

Cable safety

The cables that connect the leads to the system are conductors and are therefore capable of carrying considerable current. During the examination, the majority of the cables lie within the RF field and therefore high currents are induced within them. This current potentially results in the cables storing and transmitting heat to the patient. Although every cable is heavily insulated, a build-up of heat is possible,
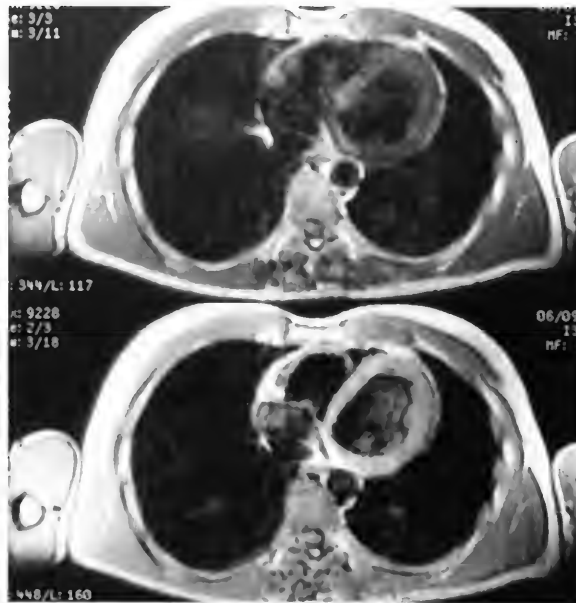
Fig. 6. Axial T1 weighted image without (above) and with (below) cardiac gating. Note the improved visualization of the walls of the heart on the gated image.

and this can cause minor burns if the cables are in direct contact with the skin. In addition if the insulation is damaged, high currents could be transmitted to the patient. To avoid this:

- Check the cable insulation for damage at regular intervals, not just when gating is required. If they are frayed or split do not, under any circumstances, use them.
- When positioning the cables, avoid looping and cross-over as their point of contact induces additional heat.
- Ensure that the cables do not touch the bore when the patient is inside the magnet. Run the cables down the middle of the patient. Looping them over the patient's foot prevents them from slipping to the side during the examination.
- Place foam pads between the cables and the patient's chest, and ensure that there is a layer of gown or blanket between the cables and the patient's skin.
- Tape the cables and pads to the side of the table. This ensures that they cannot slip out of place during the examination. In addition, this prevents movement of the cables that can interfere with the trace.

Peripheral gating (Pe gating)

Peripheral gating uses a photo sensor attached to either a finger or toe to detect the increase in volume in the capillary bed during systole. This affects the amount

of light returned to the sensor and a waveform is produced. The waveform does not have the characteristics of the ECG trace, but the peaks of the waves approximately correspond to the R wave (about 250 ms after the R wave). This waveform is displayed on the monitor.

A good trace has:

- Equally spaced peaks.
- Significant amplitude.

If the trace is unsatisfactory:

- Ensure that the photo sensor is firmly attached with the light source adjacent to the skin.
- Ensure the finger or toe is warm and well perfused. Placing it in warm water or rubbing it is often beneficial.
- Swap the sensor to the left hand as the left arm receives arterial blood directly from the aorta (rather than through the innominate artery) and sometimes has a larger pulse.

Gating parameters

For **T1 weighting** and ECG/Pe gating   use 1 R to R interval.
For **PD/T2 weighting** and ECG/Pe gating   use 2 or 3 R to R intervals.

Note: Other parameters used for gating depend on the system. However, the following usually suffice:

Trigger window   15% of the R to R interval.
Delay after trigger   minimum permissible to allow maximum slice number.

Slices are usually acquired evenly across the available imaging time, although cardiac motion is sometimes reduced if slice acquisition is delayed until diastole.

Cine imaging

Cine and coherent GRE sequences are beneficial to visualize heart function, blood flow and heart wall motion. For example, the restriction of flow through a coarctation or poorly functioning valve in the heart can be clearly visualized using cine. Good contrast between flowing blood and surrounding lung or cardiac tissue is important. Therefore the implementation of a coherent GRE sequence that enhances the signal intensity of blood is necessary. Select a flip angle and TR combination that maintains the steady state, and a longer TE to maximize $T2^*$. In

addition the application of GMN not only reduces flow artefact, but also increases the signal from flowing blood thereby improving CNR.

The efficiency of cine is mainly governed by the correct selection of the number of cardiac phases acquired for each slice during the TR. Data acquisition (data points) should coincide as closely as possible to these phases. If the system cannot match each phase with a data point, cine imaging is less efficient. Calculating the phase number required is best achieved by dividing the R to R interval by the effective TR of each slice.

GMN is essential to increase the signal in flowing vessels within the FOV and to reduce artefact. Spatial pre-saturation pulses also decrease the signal from flowing nuclei that come from outside the FOV. Unfortunately, cine images of this kind are often plagued with artefact. If compatible, RC effectively reduces respiratory ghosting. Alternatively, breath-holding single slice coherent GRE images eliminate respiratory motion. Susceptibility and misregistration artefacts are common due to gradient rephasing in GRE sequences. Reducing the TE decreases susceptibility problems, and selecting a TE when fat and water are in phase minimizes misregistration.

Respiratory compensation (RC)

Respiratory compensation (RC) reduces phase mismapping from the motion of the chest wall along the phase encoding gradient during the acquisition of data. This is achieved by placing expandable air-filled bellows around the patient's chest. The movement of air back and forth along the bellows during inspiration and expiration is converted to a waveform by a transducer. The system then orders the phase encoding gradients so that the steep slopes occur when maximum movement of the chest wall occurs, and reserves the shallow gradient slopes for minimum chest wall motion. In this way most of the signal is acquired when the chest wall is relatively still and therefore phase ghosting is reduced. Another form of respiratory motion compensation is called respiratory triggering. This works in much the same way as gating in that acquisition of data is gated to respiration. This technique is sometimes not as efficient as phase reordering but does have the advantage of being compatible with phase reordering sequences such as FSE.

Placement of the bellows

Ensure that there is no vacuum within the bellows as this inhibits the back and forth movement of air during respiration. This may entail disconnecting the bellows in between examinations and ensuring that they are kept on the ground until they are reattached. This guarantees that no air pockets collect in the bellows or connecting tubing. Some systems, however, require that you do not disconnect the bellows. Please refer to the manufacturer's specifications. To ensure correct placement of the bellows:
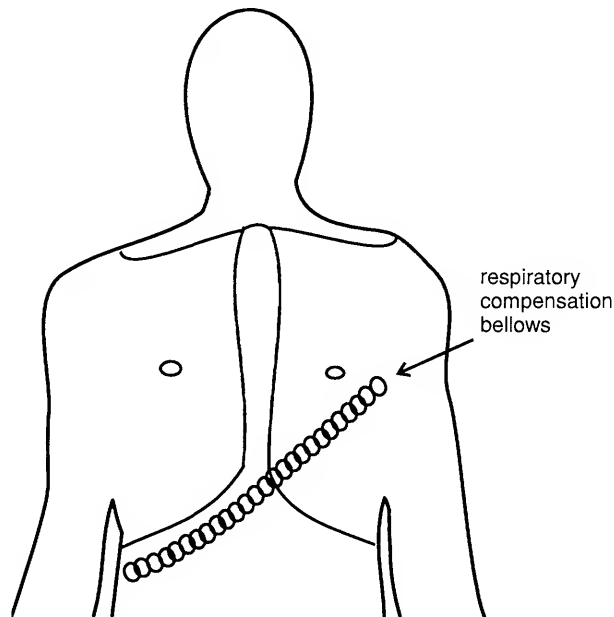
Fig. 7. Correct positioning of the respiratory bellows to 'catch' both thoracic and abdominal respiration.

- Place the bellows so that the corrugating portion lies over the anterior chest wall.
- Place the bellows diagonally across the chest and upper abdomen. This ensures that the bellows 'catch' both thoracic and abdominal movements during respiration (Fig. 7).
- Attach the bellows firmly. The bellows must be tight enough so that movement of the corrugated portion can be seen clearly during quiet respiration. However, if the bellows are too tight, the patient may become uncomfortable.
- Ensure that the bellows are firmly plugged into the transducer.

If the images show large amounts of respiratory mismapping, or the system informs you that compensation is not working adequately:

- Check that the bellows have not become loose or unattached.
- Ask the patient to breathe quietly. Uneven breaths can confuse the system.
- If the patient is small or a child, the bellows may not fit snugly and therefore their action can be compromised. Foam pads placed between the bellows and the patient are usually beneficial.

Conclusion

Gating and respiratory compensation is commonly utilized to examine the chest and abdomen, although gating also has uses in imaging the brain, spinal cord and

in cine. The correct use of these techniques can have a profound influence on image quality. If you are unfamiliar with the use of gating, it is often worth practising its implementation on volunteers so that all staff are prepared for its use on sick patients.

CONTRAST AGENTS

Introduction

Contrast enhancement is extremely valuable in many disease processes including tumours, inflammation and infection. Although these pathologies contain a high water content and are often visualized in T2 weighted images, sometimes there is insufficient contrast between the lesion and surrounding tissue. In addition, T1 weighted images demonstrate a higher SNR and are therefore advantageous, but water and pathology are commonly isointense in these sequences. Therefore it is sometimes necessary to selectively enhance pathology by administering contrast agents. This can be done either indirectly via the intravenous (IV), oral or rectal routes or directly into a structure such as a joint. There are two types of contrast agents: those that produce positive contrast and those that result in negative contrast.

Positive contrast agents

The most common positive contrast agent used in MRI is gadolinium (Gd). Gadolinium is a paramagnetic substance that has a relatively large magnetic moment. When introduced into the body, its presence causes increased fluctuations in the magnetic fields of water protons so that they tumble near to the Larmor frequency. As a result there is a transfer of energy to the surrounding lattice and both T1 and T2 relaxation times are reduced. Since T2 relaxation is much shorter than T1, a high concentration of agent is required to produce significant shortening of T2. However, much smaller doses are effective at shortening the T1 relaxation time of water protons thereby increasing their signal intensity on T1 weighted images. Gadolinium is therefore known as a *T1 enhancement agent*.

Gadolinium is a heavy metal and binds to certain elements in the body such as membranes and the osseous matrix. Therefore gadolinium cannot be excreted unless it is attached to a chelate. This chelate surrounds the gadolinium ion and enables its excretion, mainly through the kidneys. The most common chelate in use is diethylene triaminepentaacetic acid (DTPA) which binds to eight of the nine binding sites in the gadolinium ion and leaves the last free to facilitate the close approach to water molecules. Other examples of chelates used with gadolinium are gadopentetate dimeglumine, HP-DO3A, DTPA-BMA and DOTA.

Gadolinium may be given intravenously (IV), orally or rectally or injected directly into a joint. The recommended IV dose of Gd-DTPA and Gd-DTPA-BMA is 0.1 mmol/kg and 0.3 mmol/kg for Gd-HP-DO3A. Oral gadolinium provides positive contrast of the gastrointestinal tract to label the bowel thereby increasing the

visualization of abdominal organs such as the pancreas. Oral gadolinium has a neutral taste and is easily mixed with water prior to ingestion. Problems may arise from the bowel 'whiting out', although this can be minimized by careful adjustment of the dose and optimum timing of the scan sequence post-ingestion. Gadolinium may also be injected directly into a cavity such as a joint. Magnetic resonance arthrography is an important technique, especially in the hip, shoulder and ankle.

Other positive agents for bowel imaging include plain water and blueberry juice. These may prove to be as effective as gadolinium in the gastrointestinal tract and may enable imaging of bowel and rectal disorders in the future.

Negative contrast agents

Superparamagnetic agents such as iron oxides and manganese are termed *T2 enhancement agents*. This is because their presence causes a shortening of T2 decay times and reduced signal intensity. They are taken up by the reticulo-endothelial system and transported to the Kupffer cells of the liver parenchyma. Like gadolinium, superparamagnetic agents are dangerous in their pure form. However, unlike gadolinium, chemical barriers are not used. Instead the iron oxide particles are coated with either hydrophilic polymer or arabinagalactin to provide a physical barrier.

These agents dramatically shorten the T2 relaxation times of normal liver so that it appears dark and lesions appear bright on T2 weighted images. They are, therefore, specifically used for liver imaging and are given IV. A recommended dose is 0.56 mg of iron per kg of body weight. This is diluted in 100 ml of 50% dextrose and given over a 30 min period at a rate of 2–4 mm/min through a 5 micron filter.

The other negative agent used is air, which is used for bowel imaging to delineate the large bowel in pelvic examinations.

Current applications of contrast agents

Gadolinium has proved invaluable in imaging the central nervous system (CNS) because of its ability to pass through breakdowns in the blood–brain barrier. It is therefore required in the diagnosis of tumours, infection, infarction, inflammation and post-traumatic lesions. In the body, since the liver, spleen and kidneys are vascular organs, contrast enhances them almost immediately after injection. For this reason, rapid imaging is recommended. Dynamic enhancement in conjunction with rapid imaging sequences is required to evaluate abdominal and peripheral, arterial and venous flow. The use of an MR compatible injector and navigator echoes allows accurate timing of the sequence so that data acquisition begins when contrast first passes through the area under investigation (see *Dynamic imaging* under *Pulse sequences*). The right antecubital vein is the optimum site for a bolus injection. A catheter no smaller than a 23 gauge should be used.

Conclusion

The development of contrast agents has rapidly advanced and their use will increase the diagnostic capabilities of MRI in the future. It is therefore important that MR users keep abreast of these developments so that their optimum and safe use is assured.

Further reading

Anelli P.L., Calabi L., de Haen C. *et al.* (1997) Hepatocyte-directed MR contrast agents. Can we take advantage of bile acids? *Acta Radiologica*, **412**(Supplement), 125–33.

Burton S.S., Liebig T., Frazier S.D. & Ros P.R. (1997) High-density oral barium sulfate in abdominal MRI: efficacy and tolerance in a clinical setting. *Magnetic Resonance Imaging*, **15**(2), 147–53.

Cavagna F.M., Dapra M., Castelli P.M., Maggioni F. & Kirchin M.A. (1997) Trends and developments in MRI contrast agent research. *European Radiology*, **7**(Supplement 5), 222–4.

Chu W.J., Simor T. & Elgavish G.A. (1997) In vivo characterization of Gd(BME-DTTA), a myocardial MRI contrast agent: tissue distribution of its MRI intensity enhancement, and its effect on heart function. *NMR Biomedicine*, **10**(2), 87–92.

Colosimo C., Manfredi R. & Tartaglione T. (1997) Contrast enhancement issues in the MR evaluation of the central nervous system. *European Radiology*, **7**(Supplement 5), 231–7.

Hahn P.F. & Saini S. (1998) Liver-specific MR imaging contrast agents. *Radiological Clinics of North America*, **36**(2), 287–97.

Hatrick A.G., Jarosz J.M. & Irvine A.T. (1997) Gadopentate dimeglumine as an alternative contrast agent for use in interventional procedures. *Clinical Radiology*, **52**(12), 948–52.

Huot P., Dousset V., Hatier F., Degreze P., Carlier P. & Caille J.M. (1997) Improvement of post-gadolinium contrast with magnetization transfer. *European Radiology*, **7**(Supplement 5), 174–7.

Kettritz U., Warshauer D.M., Brown E.D., Schlund J.F., Eisenberg L.B. & Semelka R.C. (1996) Enhancement of the normal pancreas: comparison of manganese-DPDP and gadolinium chelate. *European Radiology*, **6**(1), 14–18.

Kopp A.F., Laniado M., Dammann F. *et al.* (1997) MR imaging of the liver with Resovist: safety, efficacy, and pharmacodynamic properties. *Radiology*, **204**(3), 749–56.

Kuperman V.Y., Karczmar G.S., Blomley M.J., Lewis M.Z., Lubich L.M. & Lipton M.J. (1996) Differentiating between T1 and T2* changes caused by gadopentetate dimeglumine in the kidney by using a double-echo dynamic MR imaging sequence. *Journal of Magnetic Resonance Imaging*, **6**(5), 764–8.

Mahfouz A.E., Hamm B. & Taupitz M. (1997) Contrast agents for MR imaging of the liver: a clinical overview. *European Radiology*, **7**(4), 507–13.

Mandeville J.B., Moore J., Chesler D.A., Garrido L., Weissleder R. & Weisskoff R.M. (1997) Dynamic liver imaging with iron oxide agents: effects of size and biodistribution on contrast. *Magnetic Resonance in Medicine*, **37**(6), 885–90.

Mascalchi M., Jin X.N., Agen C. *et al.* (1997) Ex-vivo MR imaging of liver intracellular contrast agents, *Magnetic Resonance Imaging*, **15**(4), 469–74.

Mitchell D.G., Stolpen A.H., Siegelman E.S., Bolinger L. & Outwater E.K. (1996) Fatty tissue on opposed-phase MR images: paradoxical suppression of signal intensity by paramagnetic contrast agents. *Radiology*, **198**(2), 351–7.

Miyati T., Banno T., Mase M. *et al.* (1997) Dual dynamic contrast-enhanced MR imaging. *Journal of Magnetic Resonance Imaging*, **7**(1), 230–35.

Murphy K.J., Brunberg J.A. & Cohan R.H. (1996) Adverse reactions to gadolinium contrast media: a review of 36 cases. *American Journal of Roentgenology*, **167**(4), 847–9.

Oswald P., Clement O., Chambon C., Schouman-Claeys E. & Frija G. (1997) Liver positive enhancement after injection of superparamagnetic nanoparticles: respective role of circulating and uptaken particles. *Magnetic Resonance Imaging*, **15**(9), 1025–31.

Pochon S., Hyacinthe R., Terrettaz J., Robert F., Schneider M. & Tournier H. (1997) Long circulating superparamagnetic particles with high T2 relaxivity. *Acta Radiologica*, **412**, 69–72.

Rofsky N.M. & Earls J.P. (1996) Mangafodipir trisodium injection (Mn-DPDP). A contrast agent for abdominal MR imaging. *Magnetic Resonance Imaging Clinics of North America*, **4**(1), 73–85.

Schima W., Petersein J., Hahn P.F., Harisinghani M., Halpern E. & Saini S. (1997) Contrast-enhanced MR imaging of the liver: comparison between Gd-BOPTA and Mangafodipir. *Journal of Magnetic Resonance Imaging*, **7**(1), 130–35.

Shamsi K., Balzer T., Saini S. *et al.* (1998) Superparamagnetic iron oxide particles (SHU555 A): evaluation of efficacy in three doses for hepatic MR imaging. *Radiology*, **206**(2), 365–71.

Tresley R.M., Stone L.A., Fields N., Maloni H., McFarland H. & Frank J.A. (1997) Clinical safety of serial monthly administrations of gadopentetate dimeglumine in patients with multiple sclerosis: implications for natural history and early-phase treatment trials. *Neurology*, **48**(4), 832–5.

Tweedle M.F. (1997) The ProHance story: the making of a novel MRI contrast agent. *European Radiology*, **7**(Supplement 5), 225–30.

Vander-Elst L., Maton F., Laurent S., Seghi F., Chapelle F. & Muller R.N. (1997) A multinuclear MR study of Gd-EOB-DTPA: comprehensive preclinical characterization of an organ specific MRI contrast agent. *Magnetic Resonance in Medicine*, **38**(4), 604–14.

Wang C., Ahlstrom H., Ekholm S. *et al.* (1997) Diagnostic efficacy of MnDPDP in MR imaging of the liver. A phase III multicentre study. *Acta Radiologica*, **38**(4 Pt 2), 643–9.

Wang C., Gordon P.B., Hustvedt S.O. *et al.* (1997) MR imaging properties and pharmacokinetics of MnDPDP in healthy volunteers. *Acta Radiologica*, **38**(4 Pt 2), 665–76.

Weissleder R. (1996) Can gadolinium be safely given in renal failure? *American Journal of Roentgenology*, **167**(1), 278–9.

Yoshikawa K. & Davies A. (1997) Safety of ProHance in special populations. *European Radiology*, **7**(Supplement 5), 246–50.

Yuh W.T. & Maley J.E. (1998) Contrast dosage in the neuroimaging of brain tumors. Principles and indications. *Magnetic Resonance Imaging Clinics of North America*, **6**(1), 113–24.

Yuh W.T., Parker J.R. & Carvlin M.J. (1997) Indication-related dosing for magnetic resonance contrast media. *European Radiology*, **7**(Supplement 5), 269–75.

HEAD AND NECK

Brain	Pharynx
Temporal lobes	Larynx
Posterior fossa and internal auditory meati	Thyroid and parathyroid glands
Pituitary fossa	Salivary glands
Orbits	Temporomandibular joints
Paranasal sinuses	Vascular imaging

Summary of parameters. The figures given are general and should be adjusted according to the system used.

Spin echo (SE)			**Coherent GRE**		
0.2 T to 0.5 T	short TE	min–30 ms		long TE	15 ms+
	long TE	70 ms+		short TR	<50 ms
	short TR	250–500 ms		low flip	5°–20°
	long TR	2000 ms+		medium flip	20°–40°
				high flip	60°+
1 T to 1.5 T	short TE	min–20 ms	**Incoherent GRE**		
	long TE	70 ms+		short TE	min–5 ms
	short TR	300–600 ms		short TR	<50 ms
	long TR	2000 ms+		medium flip	20°–40°
				high flip	60°+
Fast spin echo (FSE)			**Inversion recovery (IR)**		
	short TE	min–20 ms		short TE	min–20 ms
	long TE	90 ms+		long TE	60 ms+
	short TR	400–600 ms		short TR	1800 ms
	long TR	4000 ms+		long TR	6000 ms+
	short ETL	2–6		short TI	100–175 ms
	long ETL	16+		medium TI	200–600 ms
				long TI	1700–2200 ms
Slice thickness			**Slice numbers**		
2D	thin	2.5–4 mm	Volumes	small	<32
	medium	5–6 mm		medium	64
	thick	8 mm+		large	128+
3D	thin	<1 mm	**Matrix**		
	thick	>3 mm		coarse	256 × 128
				medium	256 × 192
				fine	256 × 256
				very fine	512 × 256

Summary of parameters   *Continued*

FOV			PC-MRA		
	small	<18 cm	2D and 3D	TE	min
	medium	20–26 cm		TR	25–33 ms
	large	30 cm+		flip	30°
				VENC venous	20–40 cm/s
				VENC arterial	60 cm/s
NEX/NSA			**TOF-MRA**		
	short	1 or less	2D	TE	min
	medium	2–3		TR	28–45 ms
	multiple	4+		flip	40°–60°
			3D	TE	min
				TR	25–50 ms
				flip	20°–30°

Brain

Basic anatomy (Figs 8 and 9)

parietal lobe

corpus callosum

thalamus

frontal lobe

occipital lobe

pineal gland

intermediate mass

sylvian fissure

hypothalamus

fourth ventricle

cerebellum

pituitary gland

pons

medulla oblongata
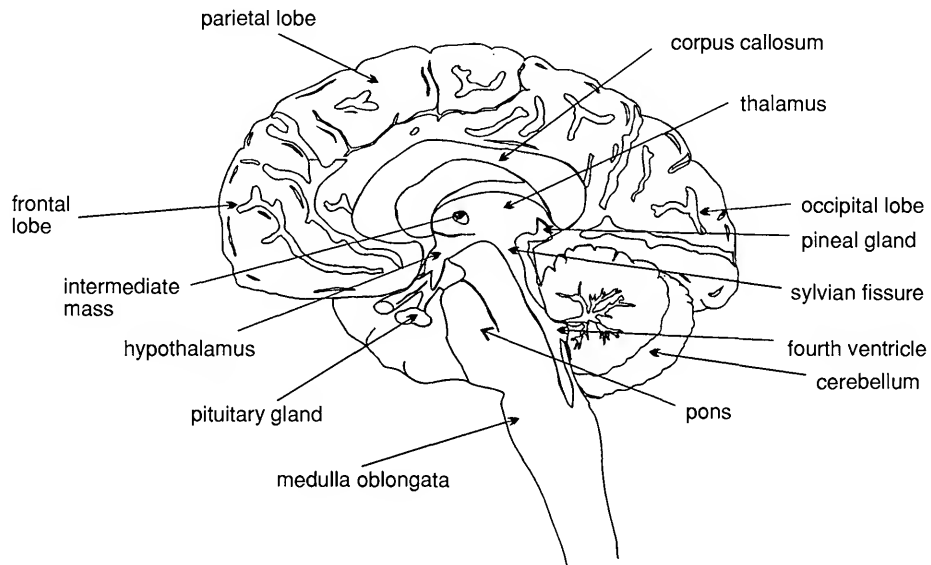
Fig. 8. Sagittal section through the brain showing midline structures.

cerebrum

olfactory bulb

optic tract

optic nerve

cerebral peduncle

trigeminal nerve

pons

middle cerebellar peduncle

medulla oblongata

cerebellum

spinal cord
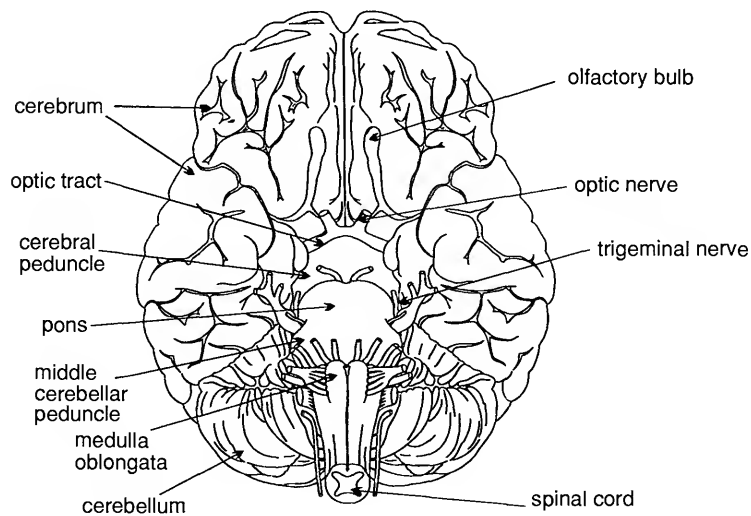
Fig. 9. Transverse section through the brain showing inferior structures.

Common indications

- Multiple sclerosis (MS).
- Primary tumour assessment and/or metastatic disease.
- AIDS (toxoplasmosis).
- Infarction (cerebral vascular accident (CVA) vs transient ischaemic attack (TIA)).
- Haemorrhage.
- Hearing loss.
- Visual disturbances.
- Infection.
- Trauma.
- Unexplained neurological symptoms or deficit.

Equipment

- Head coil (quadrature or phased array).
- Immobilization pads and straps.
- Ear plugs.
- High-performance gradients for EPI, diffusion and perfusion imaging.

Patient positioning

The patient lies supine on the examination couch with their head within the head coil. The head is adjusted so that the interpupillary line is parallel to the couch and the head is straight. The patient is positioned so that the longitudinal alignment light lies in the midline, and the horizontal alignment light passes through the nasion. Straps and foam pads are used for immobilization.

Suggested protocol

Sagittal SE/FSE/incoherent (spoiled) GRE T1 (Fig. 10)

Medium slices/gap are prescribed on either side of the longitudinal alignment light from one temporal lobe to the other. The area from the foramen magnum to the top of the head is included in the image.

L 37 mm to R 37 mm
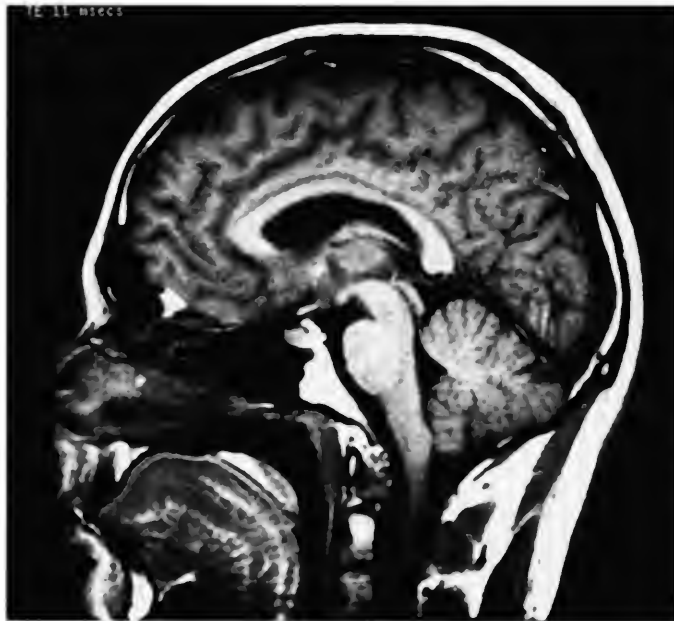
Fig. 10. Sagittal SE T1 midline slice of the brain.

Fig. 11. Sagittal SE T1 weighted midline slice of the brain showing the axis of the anterior and posterior commissures.

Fig. 12.   Sagittal SE T1 weighted midline slice of the brain showing slice prescription boundaries and orientation for axial/oblique imaging.

Axial/oblique SE/FSE PD/T2 (Fig. 13)

Medium slices/gap are prescribed from the foramen magnum to the superior surface of the brain. Slices may be angled so that they are parallel to the anterior–posterior commissure axis. This enables precise localization of lesions from reference to anatomy atlases (Figs 11 and 12). Many sites have replaced the PD sequence with FLAIR (see below). SS-FSE or SS-EPI may be a necessary alternative for a rapid examination in uncooperative patients.

Coronal SE/FSE PD/T2 (Figs 15 and 16)

As for Axial PD/T2,
except   prescribe slices from the cerebellum to the frontal lobe (Fig. 14).

Additional sequences

Axial/oblique IR T1 (Fig. 17)

Slice prescription as for Axial/oblique T2.
   This sequence is especially useful in imaging the paediatric brain (see *Paediatric imaging* later in Part 2). White matter does not fully myelinate until approximately
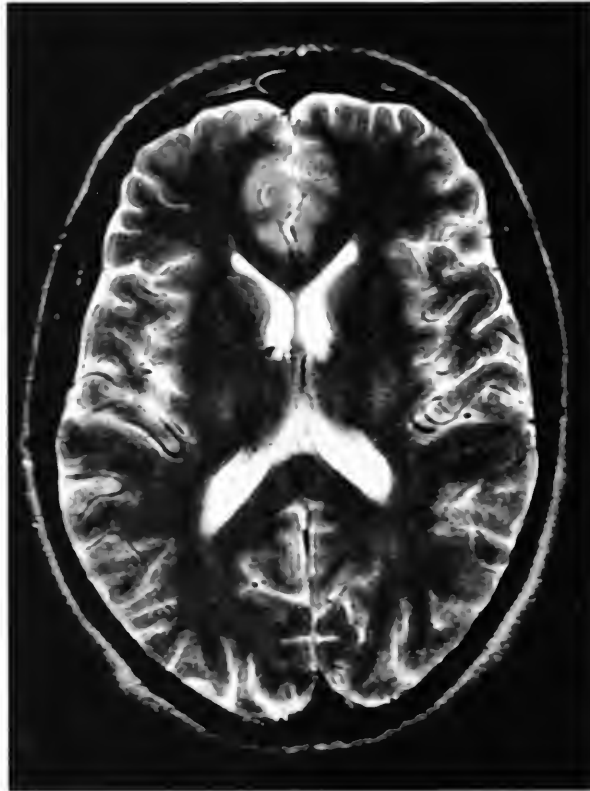
Fig. 13. Axial/oblique FSE T2 weighted image of the brain showing normal appearances.
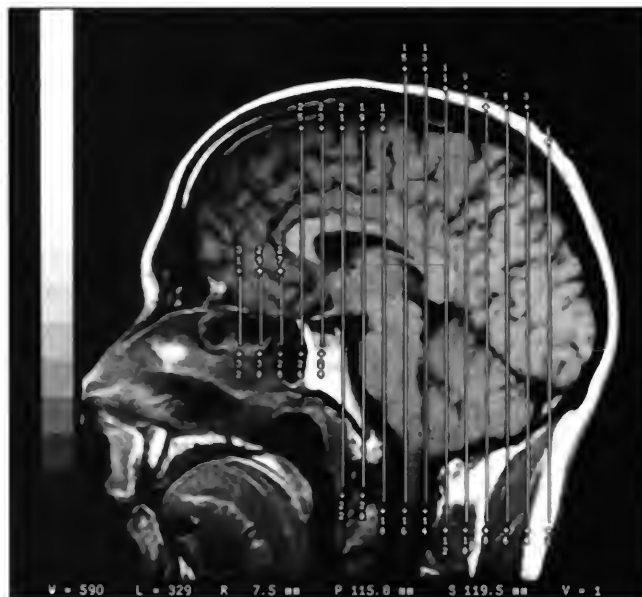
Fig. 14. Sagittal SE T1 weighted image showing slice prescription boundaries and orientation for coronal imaging.
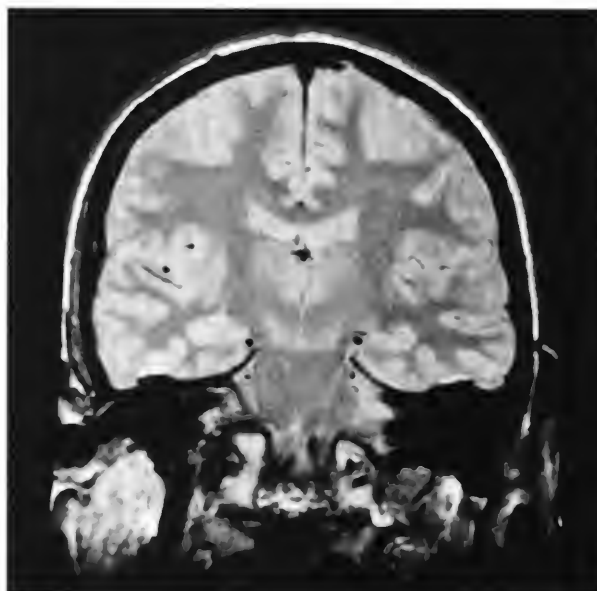
Fig. 15.   Coronal FSE PD weighted image of the brain.
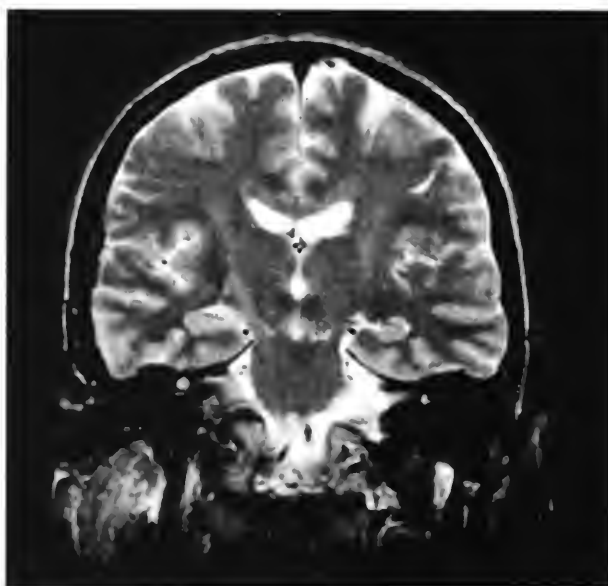
Fig. 16.   Coronal FSE T2 weighted image of the brain showing normal appearances.
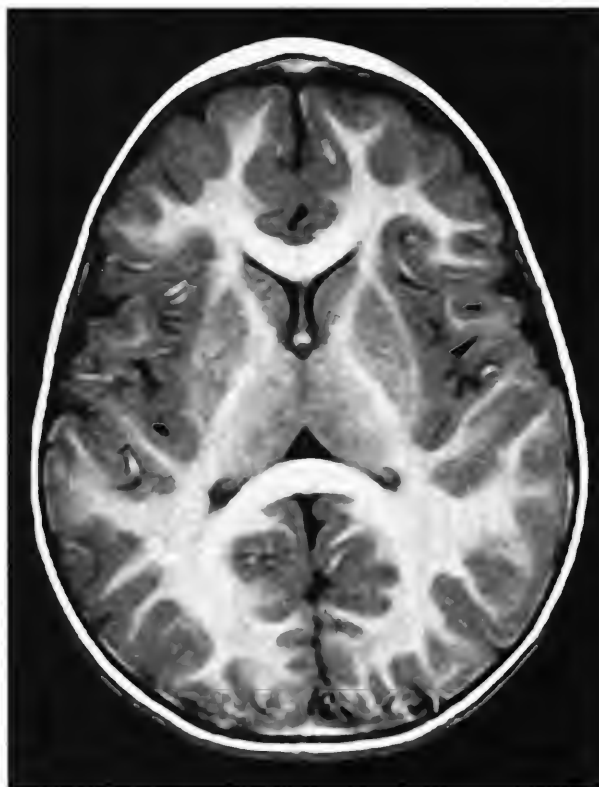
Fig. 17. Axial IR T1 weighted image using a TI of 700 ms. Note the exquisite contrast between grey and white matter.

5 years of age, therefore in the very young patient, grey and white matter have very similar T1 relaxation times, and the CNR between these tissues is small on SE T1 sequences.

Axial/oblique FLAIR/EPI (Fig. 18)

Slice prescription as for Axial/oblique T2.

This sequence provides a rapid acquisition with suppression of CSF signal. It may be useful when examining periventricular or cord lesions such as MS plaques.

Axial/oblique SE/FSE/incoherent (spoiled) GRE T1 (Fig. 19)

Slice prescription as for Axial/oblique T2.

Pre- and post-contrast scans are common especially for tumour assessment.

Fig. 18. Axial/oblique FLAIR image of the brain. Periventricular abnormalities will have a high signal intensity in contrast to the low signal of CSF which has been nulled using a long TI.

SS-FSE T2 (Fig. 20)

Useful for rapid imaging in uncooperative patients.

Axial 3D incoherent (spoiled) GRE T1

This sequence is useful for high-resolution imaging of small structures within the brain. If reformatting of slices is desired, an isotropic dataset must be acquired (see *Volume imaging* under *Parameters and trade-offs* in Part 1).

Axial/oblique GRE/EPI T1/T2 (Fig. 21)

Due to sensitivity to magnetic susceptibilities, these sequences demonstrate haemorrhage better than SE and FSE.

Axial/oblique SE + MT

Slice prescription as for Axial/oblique T2.
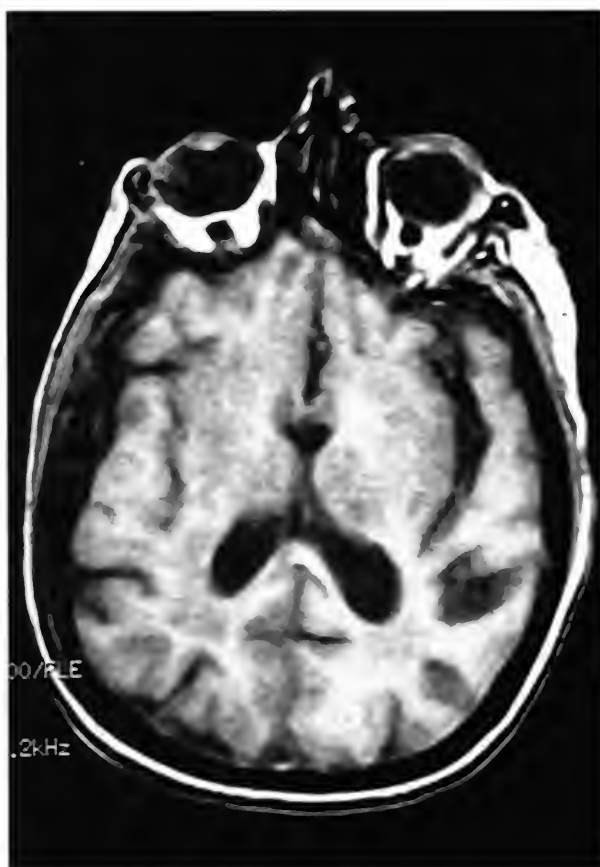
Fig. 19. Axial/oblique incoherent (spoiled) GRE image of the brain.

MT is a useful sequence to improve visualization of lesions such as metastasis, and some low-grade tumours, as grey and white matter loses 30–40% of its signal when a MT pulse sequence is utilized. The CNR between lesions and the surrounding brain is therefore increased (see *Pulse sequences* in Part 1).

Axial DWI

Slice prescription as for Axial/oblique T2.

This sequence is important in the investigation of early stroke. It is also utilized in paediatric patients to investigate the effects of hypoxia and myelination patterns (see *Paediatric imaging* later in Part 2). A b-value of 800–1000 s/mm^2 is selected (the higher the b-value, the more diffusion weighting). Isotropic diffusion should be acquired (i.e. diffusion gradients applied in all three axis) (see *Pulse sequences* in Part 1).
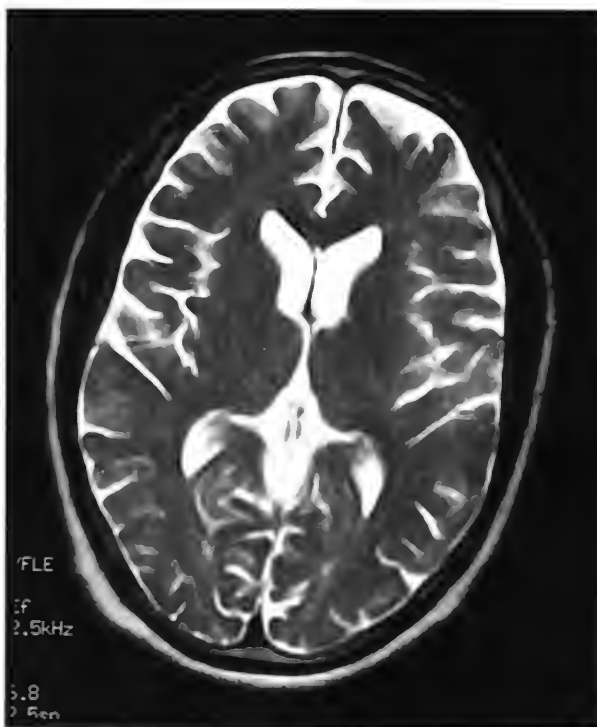
Fig. 20.   SS-FSE T2 weighted image of the brain. The entire brain was scanned in 40 s.

Axial perfusion imaging (Fig. 22)

Slice prescription as for Axial/oblique T2.

This sequence provides temporal resolution of enhancing lesions and indicates activity. Injection of a gadolinium bolus should begin immediately after the scan is initiated. Post-enhancement T1 imaging follows the perfusion series (*see Pulse sequences* and its subheading *Dynamic imaging* in Part 1).

Image optimization

Technical issues

The SNR and contrast characteristics of the brain are usually good. The quadrature head coil and phased array coil yield high and uniform signal, and spatial resolution is achievable in relatively short scan times. FSE can be utilized to produce images with good grey matter/white matter contrast in a short scan time. As the TR is increased above 2000 ms, the signal intensity of CSF increases due to its high proton density. This may reduce contrast between some periventricular lesions (such as MS) and CSF. In order to optimize contrast, two separate acquisitions may be necessary, one for PD, the other for T2 weighted images. In such an acquisition, a TR of 2000–2400 ms may be selected along with an ETL of no higher than 4.
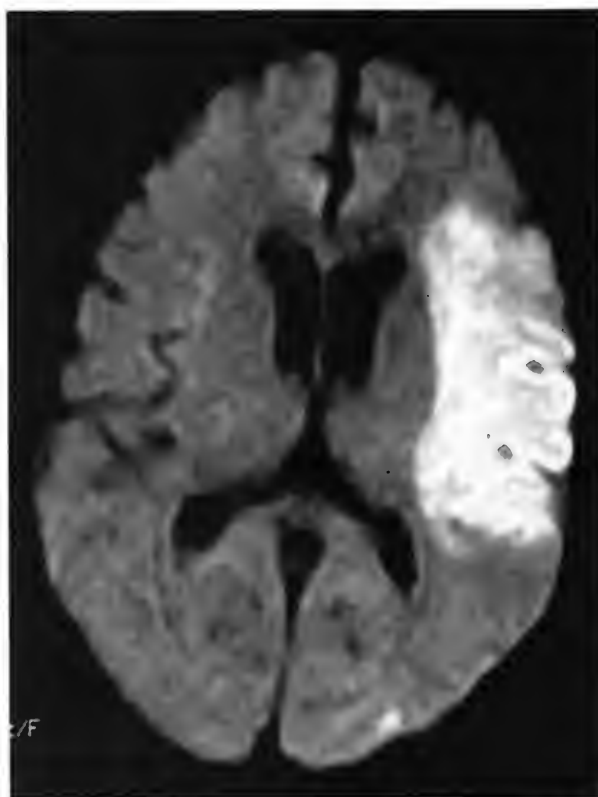
Fig. 21.   Single shot EPI image of the brain. The entire brain was scanned in 14 s.

For the T2 weighted images, a TR of 4000 ms or higher may be selected along with an ETL of 16 or more. However, as the ETL increases, image blurring also increases. Despite the advantages of using FSE in the brain, if haemorrhage is suspected it may still be necessary to utilize SE, as the application of several 180° pulses in FSE reduces the magnetic susceptibility of blood. Due to the relatively high SNR, only a few NEX/NSA are usually required to achieve optimum image quality. However, this is not necessarily true when examining small structures with thin slices, as the associated SNR reduction often necessitates the use of multiple NEX/NSA. As the brain contains no fat (only small amounts in the scalp), the receive bandwidth can be decreased to improve the SNR without significantly increasing chemical shift artefact. A rectangular/asymmetric FOV can be used effectively to reduce scan times in axial and coronal imaging with the phase axis R to L.

Diffusion

Increasing the b-value will increase the amplitude of the diffusion gradients making the acquisition more sensitive to the diffusion of water in normal brain. As this
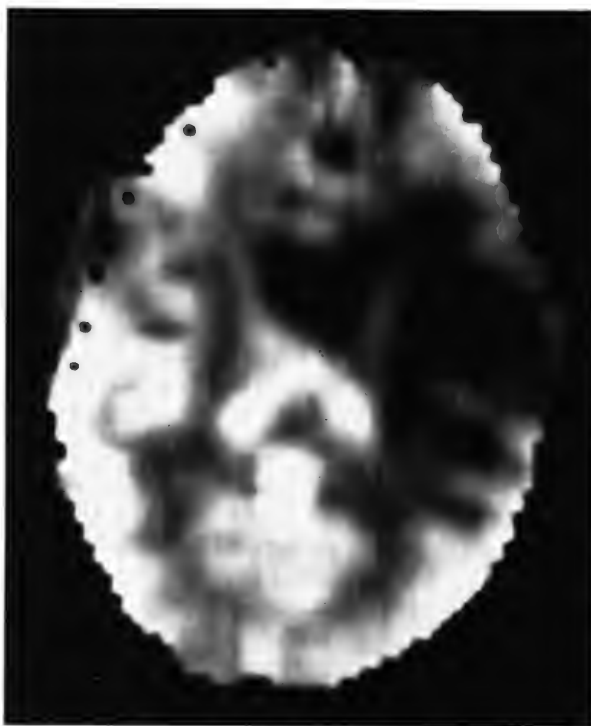
Fig. 22. Perfusion weighted image of pathology in the left parietal area.

occurs, the signal from areas with normal diffusion decreases, increasing the contrast between areas of normal and restricted diffusion. With some MR systems, an image with a b-value of 0 will be displayed. Depending on the type of sequence used for the diffusion acquisition (i.e. T2 weighted EPI, FLAIR EPI, etc.), these images may be substituted for one of the axial sequences.

Perfusion

The use of a MR compatible contrast injector greatly increases the consistency of the injection rate. Furthermore, in order to maximize the perfusion effect, a very rapid bolus of contrast must be delivered. An injection rate of 2–3 ml/s is preferrable. The volume injected can be between 0.1 mmol/kg and 0.3 mmol/kg.

With some MR systems, either SE-EPI or GRE-EPI may be available to acquire perfusion images. The GRE-EPI sequences greatly increase sensitivity to susceptibility effects of the bolus of gadolinium as it enters the brain on the first pass. However, air/tissue interface susceptibility artefacts are much more severe with a GRE-EPI than with a SE-EPI sequence. If the area under investigation is large and in the parietal area, a GRE-based sequence may be the best choice. However, if the area of question is lower in the brain and/or relatively small, a SE-based sequence may be more optimal. Because the SE-EPI is not as sensitive to the susceptibility of gadolinium, a higher dose (i.e. 0.2–0.3 mmol/kg) may be necessary.

Artefact problems

The main source of artefact in the brain is from flow motion of the carotids and vertebral arteries. A spatial pre-saturation pulse placed I to the FOV reduces this significantly. In large FOV imaging, there is no need to place spatial pre-saturation pulses anywhere other than I, as there is no flow coming into the FOV from any other direction. If a small FOV is used, S or R and L spatial pre-saturation pulses are sometimes necessary.

GMN also minimizes artefact especially in the posterior fossa. However, it not only increases the signal in vessels but also the minimum TE available, and is therefore usually reserved for T2 and T2* weighted sequences. Pe gating minimizes artefact even further but, as the scan time is dependent on the patient's heart rate, it is rather time-consuming and is not therefore commonly used. Ghosting occurs along the phase encoding axis which may be swapped in order to remove the artefact away from the ROI. An example of this is in coronal imaging of the temporal lobes (see later in Fig. 29). However, in most examinations of the brain, this strategy is unnecessary as flow suppression techniques are satisfactory.

Uncooperative patients are likely to cause motion artefacts unless very rapid sequences are employed. FSE, while faster than SE, often produces more severe motion artefacts because one of the central lines of K space is being filled during each TR period. SS-FSE techniques greatly reduce the effects of motion and allow the whole brain to be examined in approximately 30 s by using ETLs as high as 128. SS-FSE sequences, although very rapid, may still show some degree of patient motion. In order to completely eliminate the effect of patient motion, SS-EPI techniques should be used. However, EPI sequences are prone to air/tissue magnetic susceptibility artefact (see *Pulse sequences* in Part 1).

Patient considerations

Claustrophobia is often troublesome because of the enclosing nature of the head coil. In addition, neurological factors may increase the likelihood of patient movement. Examples of these are epilepsy, Parkinson's disease and reduced awareness or consciousness. Reassurance, and in extreme circumstances sedation or general anaesthesia, is sometimes required (see *Paediatric imaging* later in Part 2).

Due to excessively loud gradient noise associated with some sequences, ear plugs must always be provided to prevent hearing impairment.

EPI sequences employ very rapid gradient rise times. The faster the rise times, the greater the chance for inducing peripheral nerve stimulation. To reduce this probability, the frequency encoding direction should be R to L for all axial EPI sequences in the brain. This is not necessary with SS-FSE sequences. Additionally, patients should be instructed to place their arms by their sides and to not cross their ankles to prevent creating a loop that could precipitate excessive induction of current.

Contrast usage

Contrast has several uses in standard brain imaging. It is usually required for tumour assessment such as meningiomas and neuromas. Active MS plaques and metastases also enhance, especially after high dosage. Infectious processes, such as abscesses, are very susceptible to enhancement. In addition, the meninges enhance so that infectious tuberculosis, leptomeningeal tumour spread, and post-trauma meningeal irritation can be visualized. Contrast is also used to ascertain the age of an infarct. Very recent infarcts may enhance to some degree, but maximum response to contrast usually occurs after the blood–brain barrier has been breached. Old or chronic infarcts do not enhance. Either SE or incoherent (spoiled) GRE T1 are the sequences of choice after contrast. If a 3D incoherent (spoiled) GRE sequence is acquired using isotropic voxels, the dataset may be reformatted in other planes and/or slice locations. Perfusion imaging, with a rapidly infused bolus of gadolinium, is useful for measuring the activity of a lesion. In these cases rapid acquisitions such as SS-FSE or EPI are required.

Further reading

Bandettini P.A. & Wong E.C. (1997) Magnetic resonance imaging of human brain function. Principles, practicalities, and possibilities. *Neurosurgery Clinics of North America*, **8**(3), 345–71.

Blackband S.J., Bui J.D., Buckley D.L. *et al.* (1997) MR microscopy of perfused brain slices. *Magnetic Resonance in Medicine*, **38**(6), 1012–15.

Ebisu T., Tanaka C., Umeda M. *et al.* (1997) Hemorrhagic and nonhemorrhagic stroke: diagnosis with diffusion-weighted and T2-weighted echo-planar MR imaging. *Radiology*, **203**(3), 823–8.

Filippi M., Gawne-Cain M.L., Gasperini C. *et al.* (1998) Effect of training and different measurement strategies on the reproducibility of brain MRI lesion load measurements in multiple sclerosis. *Neurology*, **50**(1), 238–44.

Franconi F., Lethimonnier F., Sonier C.B., Pourcelot L. & Akoka S. (1997) Diffusion imaging with a multi-echo MISSTEC sequence. *Journal of Magnetic Resonance Imaging*, **7**(2), 399–404.

Gasperini C., Pozzilli C., Bastianello S. *et al.* (1998) Effect of steroids on Gd-enhancing lesions before and during recombinant beta interferon 1a treatment in relapsing remitting multiple sclerosis. *Neurology*, **50**(2), 403–6.

Gawne-Cain M.L., O'Riordan J.I., Coles A., Newell B., Thompson A.J. & Miller D.H. (1998) MRI lesion volume measurement in multiple sclerosis and its correlation with disability: a comparison of fast fluid attenuated inversion recovery (fFLAIR) and spin echo sequences. *Journal of Neurology Neurosurgery and Psychiatry*, **64**(2), 197–203.

Grant P.E., Vigneron D.B. & Barkovich A.J. (1998) High-resolution imaging of the brain. *Magnetic Resonance Imaging Clinics of North America*, **6**(1), 139–54.

Gray L. & MacFall J. (1998) Overview of diffusion imaging. *Magnetic Resonance Imaging Clinics of North America*, **6**(1), 125–38.

Hamatake S., Korogi Y., Sakamoto Y., Ikushima I., Hirai T. & Takahashi M. (1997) Value of magnetization transfer contrast in intracranial enhancing and nonenhancing lesions with paramagnetic contrast agents. *Radiation Medicine*, **15**(5), 295–303.

Jackson E.F., Ginsberg L.E., Schomer D.F. & Leeds N.E. (1997) A review of MRI pulse sequences and techniques in neuroimaging. *Surgical Neurology*, **47**(2), 185–99.

Jezzard P. & Song A.W. (1996) Technical foundations and pitfalls of clinical fMRI. *Neuroimage*, **4**(3 Pt 3), 63–75.

Kollias S.S., Bernays R., Marugg R.A., Romanowski B., Yonekawa Y. & Valavanis A. (1998) Target definition and trajectory optimization for interactive MR-guided biopsies of brain tumors in an open configuration MRI system. *Journal of Magnetic Resonance Imaging*, **8**(1), 143–59.

Krabbe K., Gideon P., Wagn P., Hansen U., Thomsen C. & Madsen F. (1997) MR diffusion imaging of human intracranial tumours. *Neuroradiology*, **39**(7), 483–9.

Maeda M., Maley J.E., Crosby D.L. *et al.* (1997) Application of contrast agents in the evaluation of stroke: conventional MR and echo-planar MR imaging. *Journal of Magnetic Resonance Imaging*, **7**(1), 23–8.

Molyneux P.D., Filippi M., Barkhof F. *et al.* (1998) Correlations between monthly enhanced MRI lesion rate and changes in T2 lesion volume in multiple sclerosis. *Annals of Neurology*, **43**(3), 332–9.

Narayana P.A., Doyle T.J., Lai D. & Wolinsky J.S. (1998) Serial proton magnetic resonance spectroscopic imaging, contrast-enhanced magnetic resonance imaging, and quantitative lesion volumetry in multiple sclerosis. *Annals of Neurology*, **43**(1), 56–71.

Nichols J.S., Elger C., Hemminger L. *et al.* (1997) Magnetic resonance imaging: utilization in the management of central nervous system trauma. *Journal of Trauma*, **42**(3), 520–4.

Redpath T.W. (1997) MRI developments in perspective. *British Journal of Radiology*, **70**(1), 70–80.

Reimer P., Bremer C., Horch C., Morgenroth C., Allkemper T. & Schuierer G. (1998) MR-monitored LITT as a palliative concept in patients with high grade gliomas: preliminary clinical experience. *Journal of Magnetic Resonance Imaging*, **8**(1), 240–4.

Reith W., Heiland S., Erb G., Benner T., Forsting M. & Sartor K. (1997) Dynamic contrast-enhanced T2*-weighted MRI in patients with cerebrovascular disease. *Neuroradiology*, **39**(4), 250–57.

Rovaris M., Sormani M.P., Rocca M.A., Comi G. & Filippi M. (1997) The influence of slice orientation on brain MRI lesion load measurement in multiple sclerosis. *Multiple Sclerosis*, **3**(6), 382–4.

Sargent M.A. & Poskitt K.J. (1997) Fast fluid-attenuated inversion recovery (FLAIR) magnetic resonance imaging of the brain: a comparison of multi-shot echo-planar and fast spin-echo techniques. *Pediatric Radiology*, **27**(6), 545–9.

Schick F. (1997) SPLICE: sub-second diffusion-sensitive MR imaging using a modified fast spin-echo acquisition mode. *Magnetic Resonance in Medicine*, **38**(4), 638–44.

Schwarzmaier H.J., Yaroslavsky I.V., Yaroslavsky A.N., Fiedler V., Ulrich F. & Kahn T. (1998) Treatment planning for MRI-guided laser-induced interstitial thermotherapy of brain tumors – the role of blood perfusion. *Journal of Magnetic Resonance Imaging*, **8**(1), 121–7.

Singer M.B., Chong J., Lu D., Schonewille W.J., Tuhrim S. & Atlas S.W. (1998) Diffusion-weighted MRI in acute subcortical infarction. *Stroke*, **29**(1), 133–6.

Sorensen A.G., Tievsky A.L., Ostergaard L., Weisskoff R.M. & Rosen B.R. (1997) Contrast agents in functional MR imaging. *Journal of Magnetic Resonance Imaging*, **7**(1), 47–55.

Weiss K.L., Figueroa R.E. & Allison J. (1998) Functional MR imaging in patients with epilepsy. *Magnetic Resonance Imaging Clinics of North America*, **6**(1), 95–112.

Xing D., Papadakis N.G., Huang C.L., Lee V.M., Carpenter T.A. & Hall L.D. (1997) Optimised diffusion-weighting for measurement of apparent diffusion coefficient (ADC) in human brain. *Magnetic Resonance Imaging*, **15**(7), 771–84.

Zur Y., Bosak E. & Kaplan N. (1997) A new diffusion SSFP imaging technique. *Magnetic Resonance in Medicine*, **37**(5), 716–22.

Temporal lobes

Basic anatomy (Fig. 23)
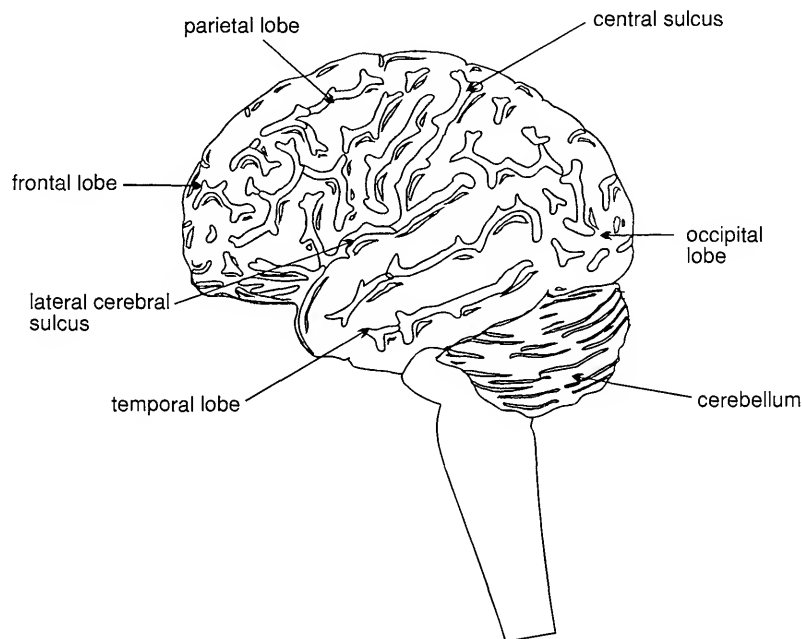
Fig. 23. The temporal lobe and its relationships.

Common indications

- Diagnosis and evaluation of a lesion specifically in the temporal lobes (tumours, vascular malformations, leukodystrophies and atrophic processes).
- Temporal lobe epilepsy.
- Evaluation of signal change in the hippocampus and the temporal lobe.
- Measurement of the hippocampal volume (hippocampal atrophy is presently considered the most sensitive indicator of hippocampal disease especially in Alzheimer's disease and schizophrenia).

Equipment

- Head coil (quadrature, or phased array).
- Immobilization pads and straps.
- Ear plugs.

Patient positioning

The patient lies supine on the examination couch with their head within the head coil. The head is adjusted so that the interpupillary line is parallel to the couch and the head is straight. The patient is positioned so that the longitudinal alignment light lies in the midline, and the horizontal alignment light passes through the nasion. Straps and foam pads are used for immobilization.

Suggested protocol

Sagittal SE T1

Medium slices/gap are prescribed on either side of the longitudinal alignment light through the whole head. The area from the foramen magnum to the top of the head is included in the image.

L 37 mm to R 37 mm

Axial/oblique SE/FSE T2

Thin slices/gap or interleaved are angled parallel to the temporal lobe that can be seen on a lateral slice on the sagittal images (Fig. 24). Prescribe the slices from the inferior aspect of the temporal lobes to the superior border of the body of the corpus callosum.

Coronal/oblique SE/FSE T1

As for the Axial/oblique T2,
except   thin slices interleaved are angled perpendicular to the axials (Fig. 25).
   Slices are prescribed from the posterior portion of the cerebellum to the anterior border of the genu of the corpus callosum.

Coronal 3D incoherent (spoiled) GRE T1 (Fig. 26)

Thin slices are either prescribed through the temporal lobes only (medium number of slice locations), or the whole head (large number of slice locations).
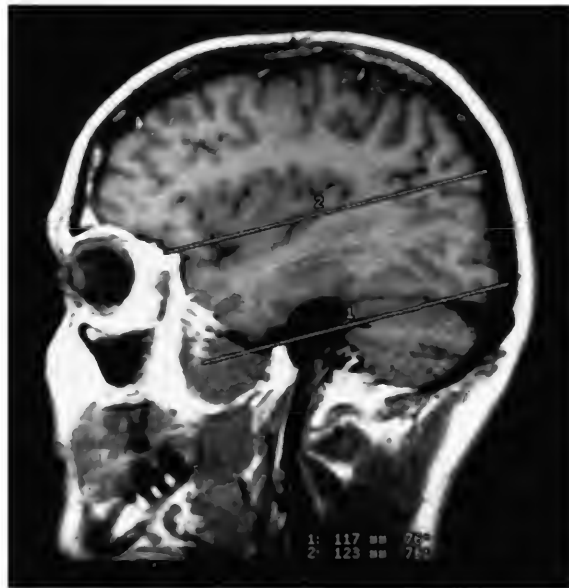
Fig. 24. Sagittal SE T1 weighted image through a temporal lobe showing slice prescriptions boundaries and orientation for axial/oblique imaging of the temporal lobes.
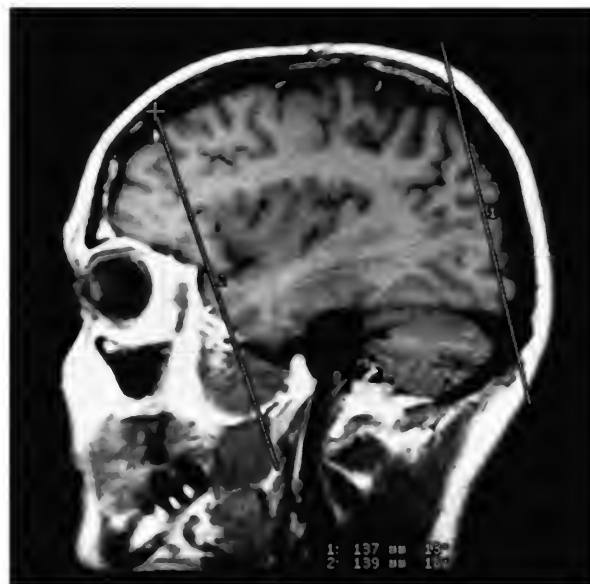
Fig. 25. Sagittal SE T1 weighted image through a temporal lobe showing slice prescriptions boundaries and orientation for coronal/oblique imaging of the temporal lobes.
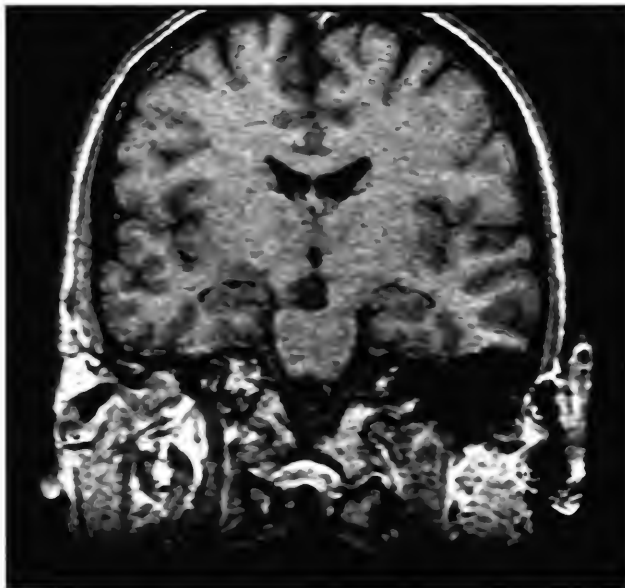
Fig. 26.   Coronal incoherent (spoiled) T1 weighted GRE image through the hippocampi acquired as part of a 3D acquisition.

For hippocampal measurements, slices are prescribed from the posterior portion of the cerebellum to the anterior border of the genu of the corpus callosum. Hippocampal volumes are measured by using system software to calculate the area of the hippocampus on each slice and multiplying this by the depth of the slice slab. If reformatting of slices is desired, then an isotropic dataset should be acquired (see *Volume imaging* under *Parameters and trade-offs* in Part 1).

Axial/oblique/Coronal/oblique IR-FSE T2 (Figs 27 and 28)

Slice precription as for Axial/oblique/Coronal/oblique FSE T2.

This sequence often provides images with high contrast between grey matter and white matter. A TI selected to null the signal from white matter (about 300 ms) can be used to increase the grey/white contrast in the hippocampal region. Images may be video-inverted so that white matter appears white and grey matter apears grey. This is sometimes useful to increase the conspicuity of white matter lesions which have a low signal intensity when using this technique.

Image optimization

Technical issues

The SNR and contrast characteristics of the temporal lobes are usually excellent as the quadrature head coil and phased array coil yield high and uniform signal. Good spatial resolution is therefore achievable in relatively short scan times.
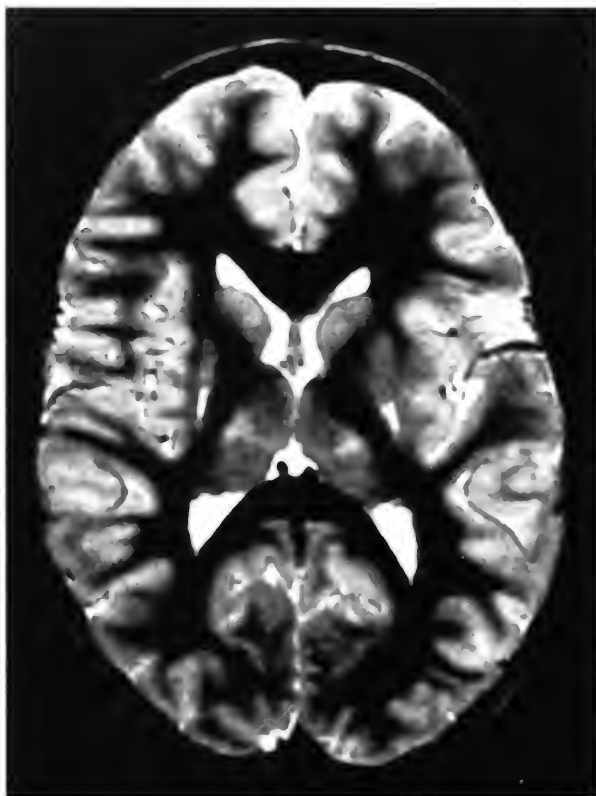
Fig. 27. Axial IR-FSE T2 weighted image with a TI selected to null the signal from white matter (300 ms).

Surface coils placed directly onto the patient's head increase local SNR and resolution, especially in children. However, using this method, other areas of the brain cannot be imaged due to signal fall-off. As lesions within the temporal lobes are often quite small, volume acquisitions are useful as they allow for very thin slices and no gap. As they are mainly utilized to demonstrate anatomy or contrast enhancement, an incoherent (spoiled) GRE that produces PD and T1 contrast is desirable. Alternatively, angling the slices perpendicular to the sylvian fissure in 2D acquisitions often improves visualization of the temporal lobes.

FSE is a useful pulse sequence especially for T2 weighted images, as FSE in conjunction with fine matrices acquires high-resolution images of the temporal lobes in a relatively short scan time. However, IR sequences can also be utilized to great effect. FLAIR sequences usually demonstrate subtle areas of increased T2 signal intensity better than T2 weighted SE or FSE sequences. As the brain contains no fat (only small amounts occur in the scalp), reducing the receive bandwidth significantly improves the SNR without significantly increasing chemical shift artefact (see *Flow phenomena and artefacts* in Part 1). A rectangular/asymmetric FOV can be effectively used to reduce scan times in axial and coronal imaging with the phase axis R to L.
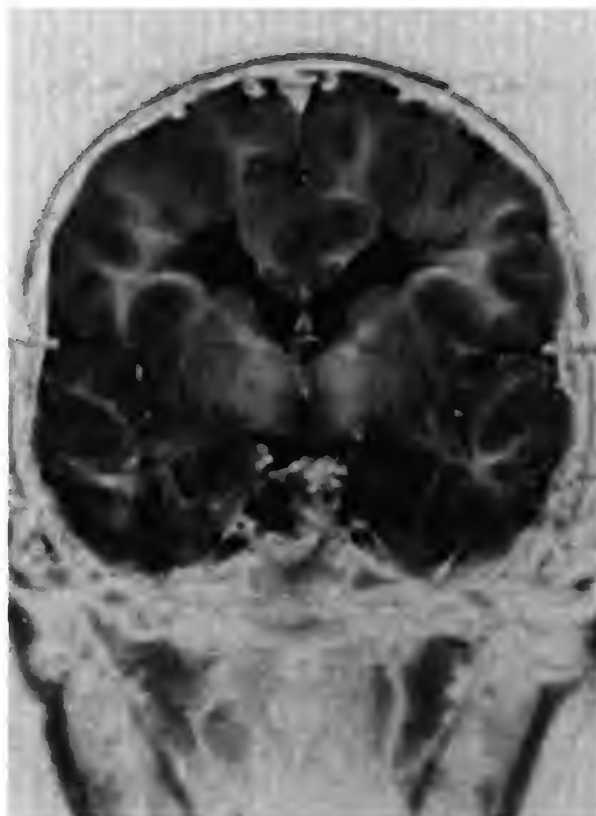
Fig. 28.   Axial IR-FSE T2 weighted image video inverted to better demonstrate white matter lesions which appear as a low signal intensity.

Artefact problems

The main source of artefact in the temporal lobes is from flow motion of the carotids and vertebral arteries. A spatial pre-saturation pulse placed I to the FOV reduces this significantly. In large FOV imaging, there is no need to place spatial pre-saturation pulses anywhere other than I, as there is no flow coming into the FOV from any other direction. On coronal images, phase artefact from the carotid and vertebral vessels is often troublesome. Swapping the phase axis so that it lies S to I instead of R to L removes artefact away from the laterally situated temporal lobes, but oversampling is necessary to prevent the neck and the top of the head wrapping into the FOV along the phase axis. This method of swapping the phase direction is used most effectively to reduce artefact in the lateral portion of the temporal lobes. However, phase ghosting can still interfere with the more medially situated hippocampi, and if they are the ROI there is probably no benefit in swapping the phase axis (Fig. 29).
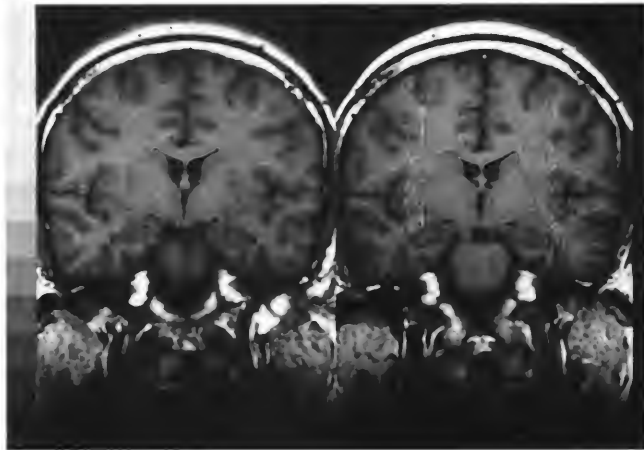
Fig. 29. Coronal FSE T1 weighted images through the temporal lobes. The image on the left has the phase encoding axis R to L. The image on the right has the phase encoding axis S to I. Artefact is removed from the lateral portion of the temporal lobes on this image but interferes with the hippocampal region.

GMN also minimizes artefact in the temporal lobes. However, it not only increases the signal in vessels but also the minimum TE available, and is therefore usually reserved for T2 and T2* weighted sequences. Magnetic susceptibility is often seen at high field strengths on the coronal incoherent (spoiled) GRE images, especially at the border of the petrous ridge and the brain. If slices are prescribed through the temporal lobe only, spatial pre-saturation pulses are brought into the FOV in the volume acquisition to reduce aliasing along the slice select axis (see *Volume imaging* under *Parameters and trade-offs* in Part 1).

Patient considerations

Claustrophobia is often troublesome because of the enclosing nature of the head coil. Careful explanation of the procedure and reassurance is necessary. As many of these patients have drug-resistant epilepsy, careful observation of the patient throughout the examination is important. The gradient noise and bore and alignment lights are potential sources of epileptic stimuli. If the patient fits during the examination stop scanning immediately, withdraw the patient from the magnet, call a physician and instigate first-aid measures.

Due to excessively loud gradient noise associated with some sequences, ear plugs must always be provided to prevent hearing impairment.

Contrast usage

Contrast is sometimes helpful to demonstrate small lesions in the temporal lobes.

HEAD AND NECK

Further reading

Andreasen N.C., Rajarethinam R., Cizadlo T. *et al.* (1996) Automatic atlas-based volume estimation of human brain regions from MR images. *Journal of Computer Assisted Tomography*, **20**(1), 98–106.

Cendes F., Stanley J.A., Dubeau F., Andermann F. & Arnold D.L. (1997) Proton magnetic resonance spectroscopic imaging for discrimination of absence and complex partial seizures. *Annals of Neurology*, **41**(1), 74–81.

Chan S., Chin S.S., Kartha K. *et al.* (1996) Reversible signal abnormalities in the hippocampus and neocortex after prolonged seizures. *American Journal of Neuroradiology*, **17**(9), 1725–31.

Davies K.G., Phillips B.L. & Hermann B.P. (1996) MRI confirmation of accuracy of freehand placement of mesial temporal lobe depth electrodes in the investigation of intractable epilepsy. *British Journal of Neurosurgery*, **10**(2), 175–8.

DeLisi L.E., Sakuma M., Tew W., Kushner M., Hoff A.L. & Grimson R. (1997) Schizophrenia as a chronic active brain process: a study of progressive brain structural change subsequent to the onset of schizophrenia. *Psychiatry Research*, **74**(3), 129–40.

Gur R.E., Cowell P., Turetsky B.I. *et al.* (1998) A follow-up magnetic resonance imaging study of schizophrenia. Relationship of neuroanatomical changes to clinical and neurobehavioral measures. *Archives of General Psychiatry*, **55**(2), 145–52.

Holopainen I.E., Lundbom N.M., Metsahonkala E.L. *et al.* (1997) Temporal lobe pathology in epilepsy: proton magnetic resonance spectroscopy and positron emission tomography study. *Pediatric Neurology*, **16**(2), 98–104.

Pantel J., Schroder J., Schad L.R. *et al.* (1997) Quantitative magnetic resonance imaging and neuropsychological functions in dementia of the Alzheimer type. *Psychology in Medicine*, **27**(1), 221–9.

Strassburger T.L., Lee H.C., Daly E.M. *et al.* (1997) Interactive effects of age and hypertension on volumes of brain structures. *Stroke*, **28**(7), 1410–17.

Woods B.T., Yurgelun-Todd D., Goldstein J.M., Seidman L.J. & Tsuang M.T. (1996) MRI brain abnormalities in chronic schizophrenia: one process or more? *Biology & Psychiatry*, **40**(7), 585–96.

Yurgelun-Todd D.A., Waternaux C.M., Cohen B.M., Gruber S.A., English C.D. & Renshaw P.F. (1996) Functional magnetic resonance imaging of schizophrenic patients and comparison subjects during word production. *American Journal of Psychiatry*, **153**(2), 200–295.

Posterior fossa and internal auditory meati
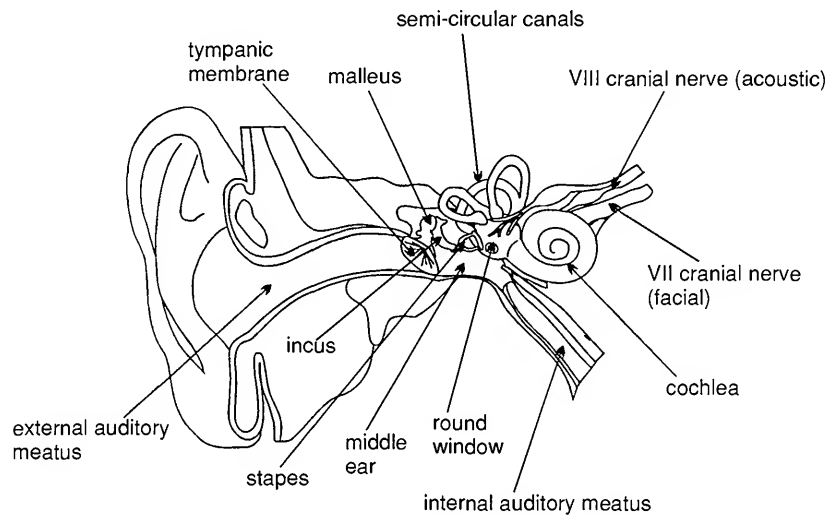
Basic anatomy (Fig. 30)

Fig. 30. The anatomy of the inner ear.

Common indications

- Symptoms that require the exclusion of an acoustic neuroma (vertigo, unilateral sensory hearing loss, tinnitis).
- Facial palsy/numbness.
- Diagnosis of a posterior fossa lesion.
- Hemifacial spasm.
- Trigeminal neuralgia.

Equipment

- Head coil (quadrature or phased array).
- Immobilization pads and straps.
- Ear plugs.

Patient positioning

The patient lies supine on the examination couch with their head within the head coil. The head is adjusted so that the interpupillary line is parallel to the couch and the head is straight. The patient is positioned so that the longitudinal alignment light lies in the midline, and the horizontal alignment light passes through the nasion. Straps and foam pads are used for immobilization.

Suggested protocol

*Sagittal SE T1 or coherent GRE T2** (Fig. 31)

Medium slices/gap are either prescribed on either side of the longitudinal alignment light, or through the internal auditory meatus (IAM) on one side only. The area from the foramen magnum to the superior border of the body of the corpus callosum is included in the image.

L 37 mm to L 20 mm (left IAM)
R 37 mm to L 20 mm (right IAM)
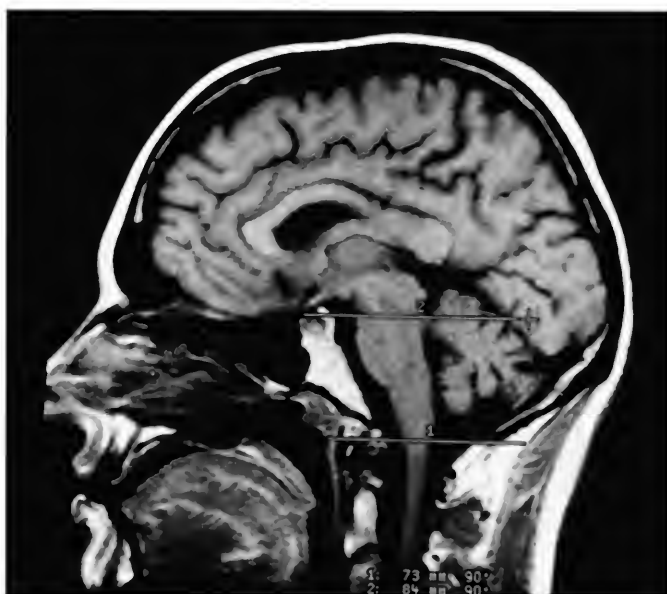
Fig. 31. Sagittal SE T1 weighted midline slice through the brain showing slice prescription boundaries and orientation for axial imaging of the internal auditory meatus (IAM).

Axial SE/FSE T1 (Fig. 32)

Thin slices/gap or interleaved are prescribed through the posterior fossa from the foramen magnum to the superior border of the petrous ridge. Coverage is increased if a large posterior fossa tumour is present (Fig. 31).

Axial SE/FSE T1 with contrast

Slice prescription as for Axial T1.

Additional sequences

Coronal SE/FSE T1 +/− contrast

As for Axial T1,

except slices are prescribed from the posterior border of the cerebellum to the clivus (Fig. 33).

3D incoherent (spoiled) GRE T1 +/− contrast

Thin slices and a small or medium number of slice locations are prescribed to cover the area as above (axially or coronally).

Fig. 32. Axial SE T1 weighted image through the internal auditory meati (IAM).

Fig. 33. Sagittal SE T1 weighted midline slice through the brain showing slice prescription boundaries and orientation for coronal imaging of the internal auditory meati (IAM).

High-resolution technique

Axial FSE T2 (Figs 34 and 35)

Slices prescribed as for Axial T1.

Thin slices/gap or interleaved	3 mm
Long TE	100 ms
Long TR	4000 ms+
Long ETL	16
Matrix	512 × 256
NEX/NSA	4
FOV	20 cm

Coronal FSE T2

As for Axial high resolution T2,
except prescribe slices from the posterior border of the cerebellum to the clivus.

3D FSE T2

This sequence produces images with high contrast and SNR. Additionally, the images are contiguous and will not suffer from cross-excitation. An isotropic acquisition allows multiplanar reformatting (see *Volume imaging* under *Parameters and trade-offs* in Part 1).
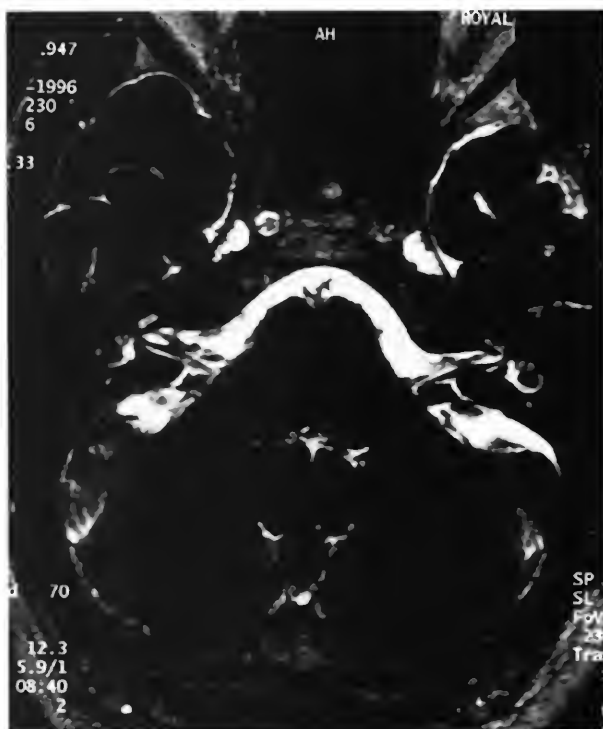
Fig. 34. Axial FSE T2 weighted high resolution image of the internal auditory meati (IAM) demonstrating the facial and acoustic nerves with the canal.
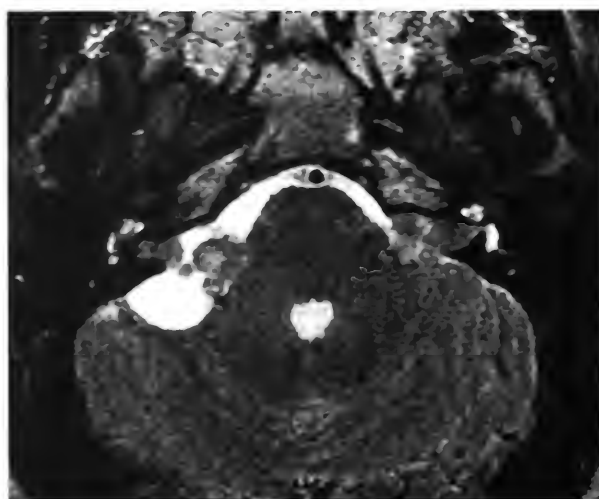
Fig. 35. Axial FSE T2 weighted high resolution image of the internal auditory meati (IAM) demonstrating large bilateral acoustic neuromas. This examination did not require contrast to confirm the diagnosis.

Image optimization

Technical issues

The IAM are very small structures and this examination is usually carried out to exclude a small acoustic neuroma situated within the canal. Therefore it is important to achieve the highest spatial resolution possible in keeping with good SNR. The inherent SNR is usually excellent due to the high proton density of the brain tissue and the quality of the head coil. However, in the region of the IAM, the low proton density of the petrous bones and mastoids reduces the SNR. The thinnest slices and smallest gap or interleaving are used to optimize spatial resolution and visualization of the IAM. A very fine matrix is advisable, although increasing this too much can reduce the SNR to unacceptable levels. To optimize spatial resolution even further, the FOV is reduced compared to standard brain imaging. As a result of all these measures, the NEX/NSA may have to be increased to maintain SNR.

A high-resolution T2 FSE technique often negates the use of contrast enhancement and the T1 sequence, especially when examining the IAM. When FSE is used in conjunction with a 512 frequency encoding matrix, extremely good resolution and contrast are achievable. The T2 weighting of the sequence produces excellent contrast between the high signal of the CSF and the relatively low signal of the nerve. The 512 frequency encoding matrix gives very good resolution of many of the cranial nerves and vessels in the posterior fossa. The facial and auditory nerves can usually be seen as distinct from each other within the canal, and under these circumstances contrast may not be necessary. The NEX/NSA is increased to maintain the SNR, but the scan times are still only in the order of a few minutes due to the implementation of FSE. However, at lower field strengths more NEX/NSA are usually required to achieve satisfactory SNR. This sequence is also useful in the coronal plane when looking specifically at the posterior fossa.

Volume acquisitions eliminate the slice gap and enable very thin slices to be acquired. Incoherent (spoiled) GRE sequences after contrast enhancement are common, but heavily T2 weighted acquisitions using FSE are often superior. Magnetization prepared sequences may also be of value. If the whole of the posterior fossa is under examination, spatial resolution may not be as important as with the IAM. If the ROI is large (such as a tumour invading the fossa), slightly thicker slices/gap are employed, and a routine brain protocol is often required.

Artefact problems

Flow motion from the venous sinuses is often troublesome in the posterior fossa. GMN minimizes this artefact but it not only increases the signal in vessels but also the minimum TE available, and is therefore reserved for T2 weighted sequences. Spatial pre-saturation pulses placed S and I to the FOV are also beneficial. Pe gating reduces artefact even further but, as the scan time is dependent on the patient's heart rate, it is sometimes rather time-consuming. The implementation of Pe gating is, therefore, best reserved for cases of severe flow artefact that cannot be reduced to tolerable levels by other measures.

Patient considerations

Claustrophobia is sometimes troublesome because of the enclosing nature of the head coil, and patients are often very deaf and may not respond to the system intercom. Under these circumstances, careful explanation and reassurance of the patient are important.

Due to excessively loud gradient noise associated with some sequences, ear plugs must always be provided to prevent hearing impairment.

Contrast usage

As T1 weighted sequences yield low inherent contrast between the petrous ridge and the IAM and acoustic neuromas demonstrate good enhancement, contrast is usually necessary. However, the high-resolution technique and/or the 3D FSE sequence often diagnoses or rules out an acoustic neuroma without contrast.

Further reading

Allen R.W., Harnsberger H.R., Shelton C. *et al.* (1996) Low-cost high-resolution fast spin-echo MR of acoustic schwannoma: an alternative to enhanced conventional spin-echo MR? *American Journal of Neuroradiology*, **17**(7), 1205–10.

Arnold B., Jager L. & Grevers G. (1996) Visualization of inner ear structures by three-dimensional high-resolution magnetic resonance imaging. *American Journal of Otology*, **17**(3), 480–85.

Carrier D.A. & Arriaga M.A. (1997) Cost-effective evaluation of asymmetric sensorineural hearing loss with focused magnetic resonance imaging. *Otolaryngology, Head & Neck Surgery*, **116**(6 Pt 1), 567–74.

Dahm M.C., Mack M.G., Tykocinski M. & Vogl T.J. (1997) Submillimeter imaging and reconstruction of the inner ear. *American Journal of Otology*, **18**(6 Supplement), S54–6.

Fukui M.B., Weissman J.L., Curtin H.D. & Kanal E. (1996) T2-weighted MR characteristics of internal auditory canal masses. *American Journal of Neuroradiology*, **17**(7), 1211–18.

Girard N., Poncet M., Caces F. *et al.* (1997) Three-dimensional MRI of hemifacial spasm with surgical correlation. *Neuroradiology*, **39**(1), 46–51.

Hara A., Takahashi K., Ito Z., Kusakari J. & Kurosaki Y. (1997) Value of fat suppression magnetic resonance imaging in the diagnosis of lipomas of the internal auditory canal. *Annals of Otology, Rhinology and Laryngology*, **106**(4), 343–7.

Held P., Fellner C., Fellner F. *et al.* (1997) MRI of inner ear and facial nerve pathology using 3D MP-RAGE and 3D CISS sequences. *British Journal of Radiology*, **70**(834), 558–66.

Kremer P., Forsting M., Hamer J. & Sartor K. (1998) MR enhancement of the internal auditory canal induced by tissue implant after resection of acoustic neurinoma. *American Journal of Neuroradiology*, **19**(1), 115–18.

Lee J.N., King B.D., Parker D.L., Buswell H.R. & Harnsberger H.R. (1996) High resolution 3D imaging of the inner ear with a modified fast spin-echo pulse sequence. *Journal of Magnetic Resonance Imaging*, **6**(1), 223–5.

Naganawa S., Yamakawa K., Fukatsu H. *et al.* (1996) High-resolution T2-weighted MR imaging of the inner ear using a long echo-train-length 3D fast spin-echo sequence. *European Radiology*, **6**(3), 369–74.

Naito Y., Miura M., Funabiki K., Naito E. & Honjo I. (1997) Application of parasagittal surface coil MRI to otoneurological diagnosis. *Acta Otolaryngologica*, Supplement Stockholm (528), 85–90.

Omojola M.F., al Hawashim N.S., Zuwayed M.A. & al Ferayan A. (1997) CT and MRI features of cavernous haemangioma of internal auditory canal. *British Journal of Radiology*, **70**(839), 1184–7.

Shelton C., Harnsberger H.R., Allen R. & King B. (1996) Fast spin echo magnetic resonance imaging: clinical application in screening for acoustic neuroma. *Otolaryngology, Head & Neck Surgery*, **114**(1), 71–6.

Stone J.A., Chakeres D.W. & Schmalbrock P. (1998) High-resolution MR imaging of the auditory pathway. *Magnetic Resonance Imaging Clinics of North America*, **6**(1), 195–217.

Swartz J.D. (1996) Sensorineural hearing deficit: a systematic approach based on imaging findings. *Radiographics*, **16**(3), 561–74.

Weissman J.L., Hirsch B.E., Fukui M.B. & Rudy T.E. (1997) The evolving MR appearance of structures in the internal auditory canal after removal of an acoustic neuroma. *American Journal of Neuroradiology*, **18**(2), 313–23.

Pituitary fossa

Basic anatomy (Fig. 36)
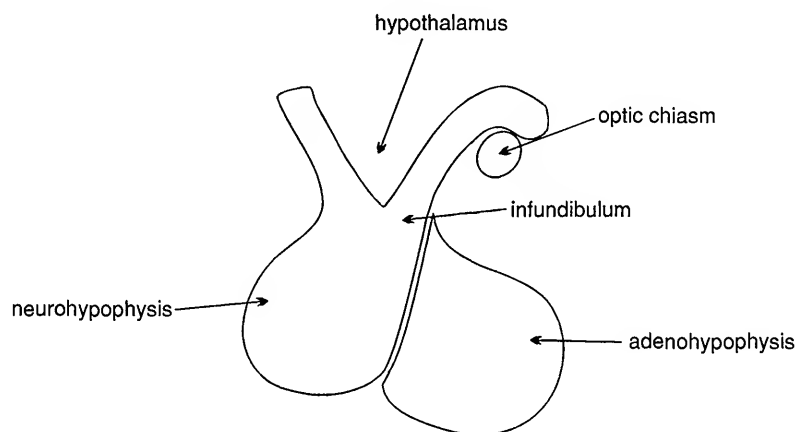
Fig. 36. The components of the pituitary gland.

Common indications

- Investigation of diseases related to pituitary function (hyperprolactinaemia, Cushing's disease, acromegaly, hypopituitarism, diabetes insipidus, amenorrhoea).
- Hypothalamic disorders.
- Visual field defect.
- Post-operative assessment of pituitary adenomas.

Equipment

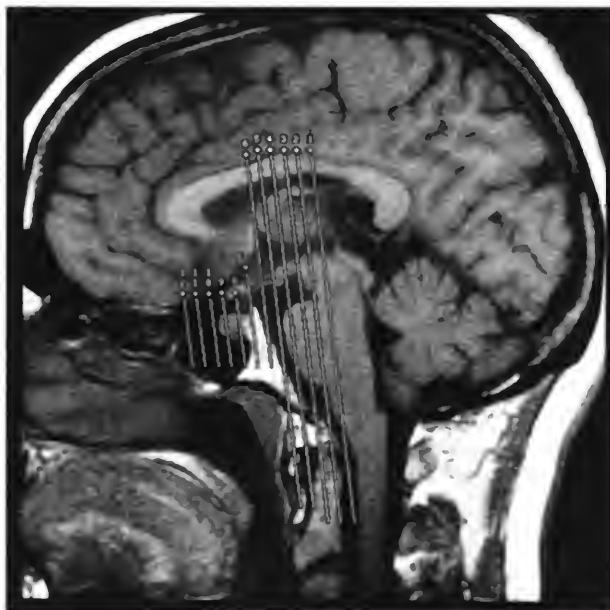- Head coil (quadrature or phased array).
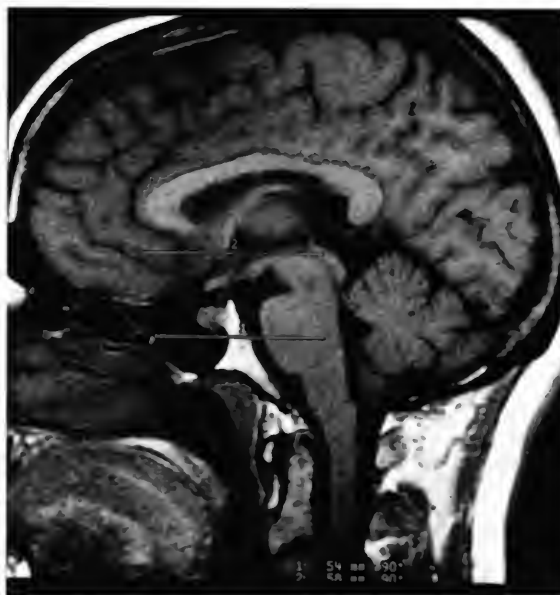- Immobilization pads and straps.
- Ear plugs.

Fig. 37. Sagittal SE T1 weighted midline slice through the brain showing slice prescription boundaries and orientation for coronal imaging of the pituitary fossa.

Patient positioning

The patient lies supine on the examination couch with their head within the head coil. The head is adjusted so that the interpupillary line is parallel to the couch and the head is straight. The patient is positioned so that the longitudinal alignment light lies in the midline, and the horizontal alignment light passes through the nasion. Straps and foam pads are used for immobilization.

Suggested protocol

Sagittal SE T1 (Fig. 37)

Thin slices/gap or interleaved are prescribed from the left to the right lateral borders of the pituitary fossa. The area from the inferior edge of the sphenoid sinus to the superior portion of the lateral ventricles is included in the image.

L 10 mm to R 10 mm

Coronal SE/FSE T1 (Fig. 38)

Thin slices/gap or interleaved are prescribed from the posterior clinoids to the anterior clinoids. The inferior border of the sphenoid sinus to the superior
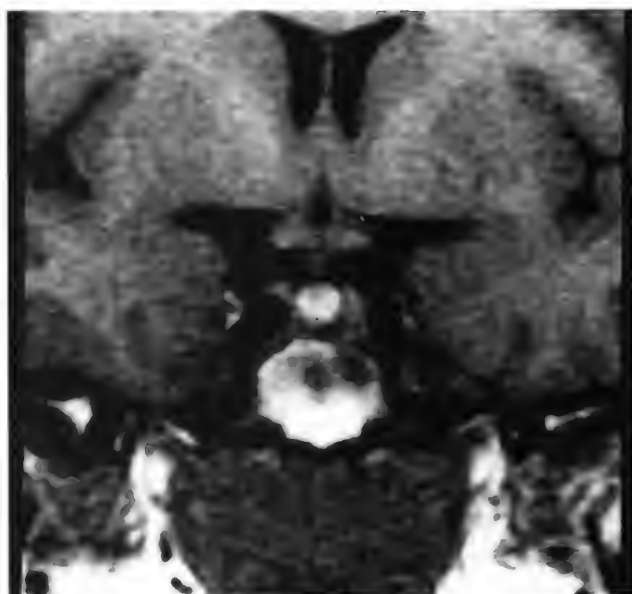
Fig. 38. Coronal FSE T1 weighted image through the pituitary fossa.

portion of the lateral ventricles is included in the image (Fig. 37). Use chemical/ spectral pre-saturation if a high signal mass is seen to exclude intrasellar dermoid.

Additional sequences

Coronal SE/FSE T1 + contrast

Slice prescription as for Coronal T1 without contrast.

Sagittal SE/FSE T1 +/− contrast

Slice prescription as for Sagittal T1 without contrast.

3D incoherent (spoiled) GRE T1 +/− contrast

Thin slices and a small number of slice locations are prescribed through the pituitary fossa. Extend coverage anteriorly and posteriorly to allow for slice wrap.

Axial SE/FSE T1 +/− contrast

As for Coronal T1,
except slices prescribed from the floor of the pituitary fossa to the circle of Willis (Fig. 39).

Fig. 39. Sagittal SE T1 weighted midline slice through the brain showing slice prescription boundaries and orientation for axial imaging of the pituitary fossa.

Image optimization

Technical issues

The pituitary fossa is a relatively small structure and, in addition, microadenomas are often difficult to visualize. As a result spatial resolution is important. To optimize this use thin slices interleaved and the smallest FOV possible in keeping with good SNR. In addition, a fine matrix used in conjunction with multiple NEX/NSA is necessary to maintain SNR. Volume acquisitions allow for thinner slices and no gap and are therefore sometimes useful in this area. As anatomical detail and contrast enhancement are important, an incoherent (spoiled) GRE sequence is required.

Artefact problems

The pituitary fossa is located just anterior and inferior to the circle of Willis and therefore flow artefact is often more troublesome than in standard brain imaging. In addition, the smaller FOV increases the likelihood of aliasing, so oversampling is necessary if anatomy exists outside the FOV in the phase direction. Spatial pre-saturation bands are placed S, I, and L and R of the FOV to reduce artefact and aliasing, but this often increases the SAR so that the slice number available per TR decreases. In extreme circumstances Pe gating may be required but, as the scan time depends on the proficiency of gating and the patient's heart rate, scan times are often considerably lengthened.

In volume acquisitions only a small slice slab is required and, therefore, slice wrap is usually troublesome. When prescribing slices always increase coverage to compensate for this. Spatial pre-saturation bands placed A and P to the edges of the slice slab help to reduce aliasing of this type (see *Flow phenomena and artefacts in Part 1*). GMN minimizes flow artefact in the pituitary region; however it not only increases the signal in vessels but also the minimum TE available, and is therefore not usually beneficial in T1 weighed sequences. Incoherent (spoiled) GRE sequences through the pituitary fossa may suffer from excessive magnetic susceptibility artefacts when acquired on high field systems (1.0 T and above). Lower field strengths, however, can benefit from the increased SNR provided by 3D acquisitions while taking advantage of reduced magnetic susceptibility artefacts.

Patient considerations

Claustrophobia is often troublesome due to the enclosing nature of the head coil. Careful explanation of the procedure and reassurance are required to avoid the necessity of sedation.

Due to excessively loud gradient noise associated with some sequences, ear plugs must always be provided to prevent hearing impairment.

Contrast usage

Contrast is not routinely required except for diabetes insipidus and hypothalamic disorders. Contrast is sometimes necessary for Cushing's disease because microadenomas are often very small, and not seen on unenhanced scans. However, it should be noted that eventually all the pituitary gland enhances as well as the microadenoma itself, and therefore careful timing of post-contrast scans is important. It is common to see a high signal intensity in the posterior lobe of the pituitary on unenhanced images, especially in patients with diabetes. At present, the causes and clinical significance of this have not been fully evaluated. In addition, studies have shown that half-dose gadolinium may be optimal for imaging the pituitary.

Further reading

Araki Y., Ashikaga R., Takahashi S., Ueda J. & Ishida O. (1997) High signal intensity of the infundibular stalk on fluid-attenuated inversion recovery MR. *American Journal of Neuroradiology*, **18**(1), 89–93.

Bartynski W.S. & Lin T. (1997) Dynamic and conventional spin-echo MR of pituitary microlesions. *American Journal of Neuroradiology*, **18**(5), 965–72.

Giacometti A.R., Joseph G.J., Peterson J.E. & David P.C. (1993) Comparison of full- and half-dose gadolinium-DTPA: MR imaging of the normal sella. *American Journal of Neuroradiology*, **14**(1), 123–7.

Holder C.A. & Elster A.D. (1997) Magnetization transfer imaging of the pituitary: further insights into the nature of the posterior 'bright spot'. *Journal of Computer Assisted Tomography*, **21**(2), 171–4.

Kornreich L., Horev G., Lazar L., Josefsberg Z. & Pertzelan A. (1997) MR findings in hereditary isolated growth hormone deficiency. *American Journal of Neuroradiology,* **18**(9), 1743–7.

Kurokawa H., Fujisawa I., Nakano Y. *et al.* (1998) Posterior lobe of the pituitary gland: correlation between signal intensity on T1-weighted MR images and vasopressin concentration. *Radiology,* **207**(1), 79–83.

Maghnie M., Genovese E., Bernasconi S., Binda S. & Arico M. (1997) Persistent high MR signal of the posterior pituitary gland in central diabetes insipidus. *American Journal of Neuroradiology,* **18**(9), 1749–52.

Maghnie M., Genovese E., Villa A., Spagnolo L., Campan R. & Severi F. (1996) Dynamic MRI in the congenital agenesis of the neural pituitary stalk syndrome: the role of the vascular pituitary stalk in predicting residual anterior pituitary function. *Clinical Endocrinology,* **45**(3), 281–90.

Magnaldi S., Frezza F., Longo R., Ukmar M., Razavi I.S. & Pozzi-Mucelli R.S. (1997) Assessment of pituitary microadenomas: comparison between 2D and 3D MR sequences. *Magnetic Resonance Imaging,* **15**(1), 21–7.

Manfre L., Midiri M., Rosato F., Janni A. & Lagalla R. (1997) Perfusion MRI in normal and abnormal pituitary gland. A preliminary study. *Clinical Imaging,* **21**(5), 311–18.

Marro B., Zouaoui A., Sahel M. *et al.* (1997) MRI of pituitary adenomas in acromegaly. *Neuroradiology,* **39**(6), 394–9.

Rand T., Kink E., Sator M. *et al.* (1996) MRI of microadenomas in patients with hyperprolactinaemia. *Neuroradiology,* **38**(8), 744–6.

Tsuda M., Takahashi S., Higano S., Kurihara N., Ikeda H. & Sakamoto K. (1997) CT and MR imaging of craniopharyngioma. *European Radiology,* **7**(4), 464–9.
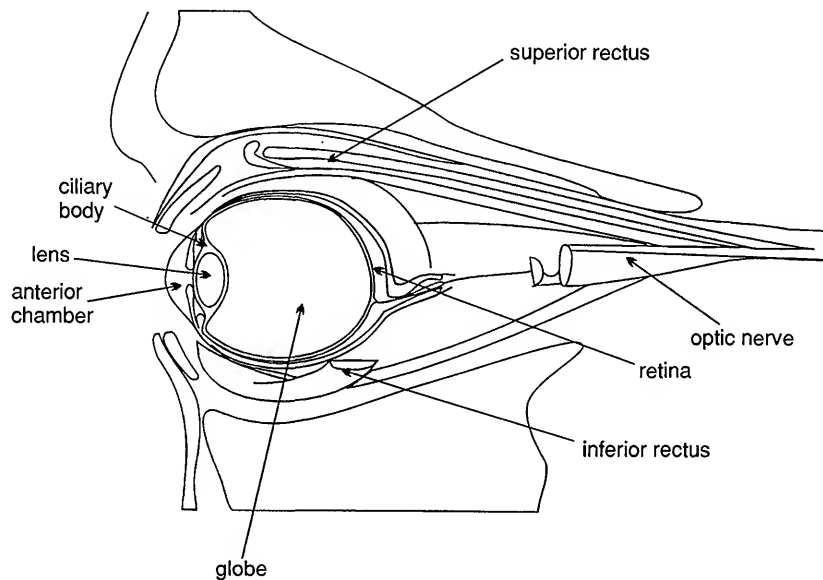
Orbits

Basic anatomy (Fig. 40)

Fig. 40. The structures of the orbit in sagittal section.

Common indications

- Proptosis.
- Visual disturbance.
- Evaluation of orbital or ocular mass lesions.

Equipment

- Small surface coil for globe and orbit.
- Quadrature head coil or phased array coil for orbital apex, chiasm and intracranial optic pathways.
- Immobilization straps and foam pads.
- Ear plugs.

Patient positioning

The patient lies supine on the examination couch. Both orbits are usually examined at the same time. If surface coils are used, these are placed over each orbit but should not touch the patient. Special holders are often provided by the manufacturers to enable the coils to be placed anteriorly over the eyes. Ensure that the receiving side of the coils faces the orbits, i.e. towards the table. The patient assumes a fixed gaze, straight ahead, with the eyes open. This enables the patient to focus and keeps the eyes still, thereby reducing motion artefact. Any eye make-up is removed prior to the examination as this causes image artefact and patient discomfort, especially if it contains metal.

The patient is positioned so that the longitudinal alignment light lies in the midline, and the horizontal alignment light passes through the orbits. If surface coils are used, this corresponds to the centre of the coils. Straps and foam pads are used for immobilization.

Suggested protocol

Sagittal SE/FSE T1 (Figs 41 and 42)

Medium slices/gap are prescribed on either side of the longitudinal alignment light through the whole head. The area from the foramen magnum to the top of the head is included in the image.

L 37 mm to R 37 mm
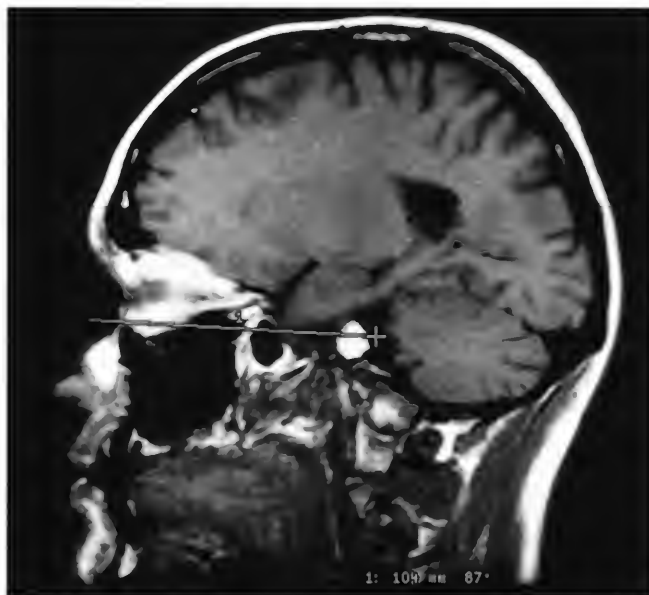
Fig. 41.   Sagittal SE T1 weighted image of the orbit and optic nerve showing the correct orientation of axial/oblique slices parallel to the optic nerve.
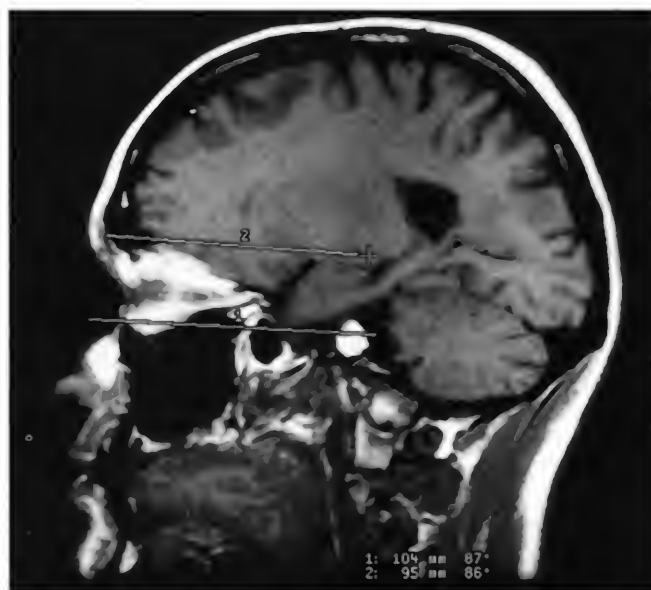
Fig. 42. Sagittal SE T1 weighted slice through the orbit showing slice prescription boundaries and orientation for axial/oblique imaging of the orbits and optic nerve.

Axial/oblique SE/FSE T1 or T2 (Fig. 43)

Thin slices/gap or interleaved are prescribed either in the true axial plane, or angled to the optic nerve from the inferior margin of the orbit to above the chiasm (Fig. 42).

Coronal SE/FSE T2 or STIR

As for Axial/oblique T1,
except prescribe slices from the posterior border of the globe to the posterior aspect of the chiasm.
  Use chemical/spectral pre-saturation on SE/FSE sequences (Fig. 44).

Additional sequences

Coronal/Axial SE/FSE T1

As for Axial/Coronal above,
except use contrast and chemical/spectral pre-saturation.
  If optic neuritis is suspected, scan the whole brain.

Image optimization

Technical issues

If surface coils are used, the SNR in the region of the globe and the anterior aspect of the orbit is high. This allows for excellent spatial resolution of small structures
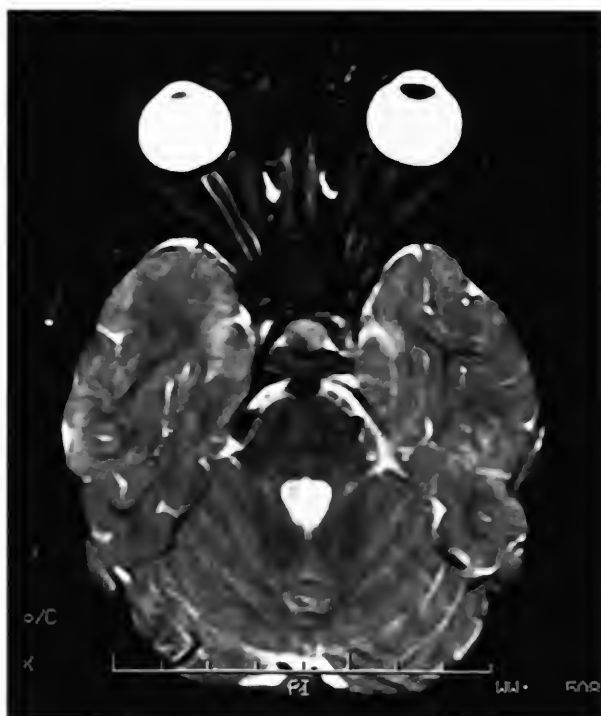
Fig. 43.   Axial/oblique FSE T2 of the orbits clearly demonstrating the lens of the eye, the globe, the optic nerves and the chiasm.
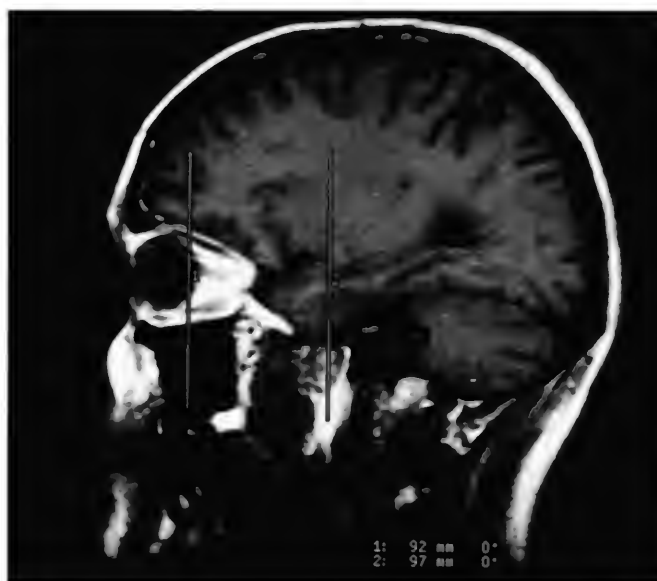

Fig. 44.   Sagittal SE T1 weighted slice through the orbits showing slice prescription boundaries and orientation for coronal imaging of the orbits and optic nerve.

such as the optic nerve, but there is signal fall-off at the orbital apex. Therefore the choice of coil largely depends on the coverage required. If the globe, the retro-orbital area and the portion of the optic nerve within the orbit are of interest, a surface coil is the best choice. If, however, information about the chiasm and intracranial optic pathways is required, the head coil is necessary. Thin interleaved slices or a very small gap are needed to obtain the resolution within the orbit and chiasm. Fine matrices and a small FOV are also required to maintain resolution, and therefore multiple NEX/NSA are necessary to preserve SNR.

FSE is probably the ideal sequence, especially for T2 weighted images, as speed is important due to motion artefact from blinking and eye movement. Due to the high fat content within the orbit, chemical/spectral pre-saturation/STIR are often necessary to visualize orbital structures adequately. This is especially true on the FSE T2 sequences, where fat returns a signal similar to the CSF surrounding the optic nerve.

Artefact problems

The main source of artefact is from eye movement. Instruct the patient to focus on the roof of the bore of the magnet and to blink as little as possible. Use the fastest sequence possible in keeping with good contrast, resolution and SNR. FSE is a valuable pulse sequence in achieving this. Flow motion in the circle of Willis is often troublesome in the chiasm, which lies just beneath it. Use spatial pre-saturation bands placed S and P to the FOV to reduce this. In addition, spatial pre-saturation bands placed I to the FOV reduce flow motion from the carotids. GMN also minimizes flow motion but, as it increases the signal in vessels and the minimum TE, it is usually reserved for the T2 weighted sequences.

As a small FOV is commonly used in this area, aliasing is a problem especially if the head coil is employed, because tissue outside the FOV in the phase axis produces signal. Oversampling is therefore required to eliminate this. If any magnetic susceptibility artefact is seen, especially superiorly to the orbit, this may be due to eye make-up left on the eyelid. This must be totally removed prior to the examination. Chemical shift artefact can occur on high field strength systems due to the presence of intraorbital fat. Fat suppression techniques reduce this and if they are used, the receive bandwidth can be reduced to increase the SNR. Additional shimming may be required before chemical/spectral pre-saturation sequences.

Patient considerations

Some patients may be blind or partially sighted and consideration should be given to this. The patient is carefully instructed on the importance of keeping the eyes still. Focusing is practised before the examination and the patient told when, during the examination, blinking is undesirable and when it is allowed. Obviously if the patient is blind, focusing is not possible and so the technique is adapted to ensure that the sequences are as fast as possible. All eye make-up must be removed prior

to the examination to avoid artefact and to reduce discomfort, as some make-up can heat up during the examination.

Due to excessively loud gradient noise associated with some sequences, ear plugs must always be provided to prevent hearing impairment.

Contrast usage

Contrast is valuable in assessing the optic nerve and chiasm as well as intraorbital masses. However, due to the presence of orbital fat, the administration of contrast only serves to increase the signal of these structures so that they are isointense with fat on T1 weighted images. Therefore some means of suppressing the fat signal is required when using contrast enhancement. It is important to note that STIR cannot be used for this purpose, as contrast decreases the T1 recovery time of the tissue so that it is similar to that of fat. Therefore, the inverting pulse used in STIR sequences sometimes nullifies the signal from enhancing tissues as well as fat. If fat suppression is required use chemical/spectral pre-saturation.

Further reading

Borges A.R., Lufkin R.B., Huang A.Y., Farahani K. & Arnold A.C. (1997) Frequency-selective fat suppression MR imaging. Localized asymmetric failure of fat suppression mimicking orbital disease. *Journal of Neuroophthalmology*, **17**(1), 12–17.

Cytryn A.S., Putterman A.M., Schneck G.L., Beckman E. & Valvassori G.E. (1997) Predictability of magnetic resonance imaging in differentiation of orbital lymphoma from orbital inflammatory syndrome. *Ophthalmology, Plastic & Reconstructive Surgery*, **13**(2), 129–34.

Gufler H., Laubenberger J., Gerling J., Nesbitt E., Kommerell G. & Langer M. (1997) MRI of lymphomas of the orbits and the paranasal sinuses. *Journal of Computer Assisted Tomography*, **21**(6), 887–91.

Herrick R.C., Hayman L.A., Maturi R.K., Diaz-Marchan P.J., Tang R.A. & Lambert H.M. (1998) Optimal imaging protocol after intraocular silicone oil tamponade. *American Journal of Neuroradiology*, **19**(1), 101–8.

Krzizoh T.H., Kaufmann H. & Traupe H. (1997) Elucidation of restrictive motility in high myopia by magnetic resonance imaging. *Archives of Ophthalmology*, **115**(8), 1019–27.

Shinaver C.N., Mafee M.F. & Choi K.H. (1997) MRI of mesenchymal chondrosarcoma of the orbit: case report and review of the literature. *Neuroradiology*, **39**(4), 296–301.

Paranasal sinuses
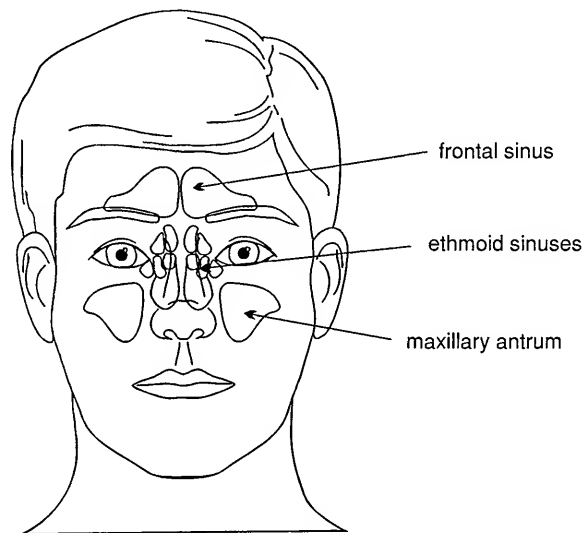
Basic anatomy (Fig. 45)

Fig. 45. Anterior view of the paranasal sinuses.

Common indications

- Staging of neoplasms prior to resection.
- Distinction of inflammation from neoplasm.

Equipment

- Head coil (quadrature or phased array).
- Immobilization foam pads and straps.
- Ear plugs.

Patient positioning

The patient lies supine on the examination couch with their head within the head coil. The head is adjusted so that the interpupillary line is parallel to the couch and

the head is straight. The patient is positioned so that the longitudinal alignment light lies in the midline, and the horizontal alignment light passes through the nasion. Straps and foam pads are used for immobilization.

Suggested protocol

Sagittal SE T1

Medium slices/gap are prescribed on either side of the longitudinal alignment light through the whole head. The area from the foramen magnum to the top of the head is included in the image.

L 37 mm to R 37 mm

Coronal SE/FSE T1

Medium slices/gap are prescribed from the posterior portion of the sphenoid sinus to the tip of the nose. All of the paranasal sinuses are included in the image from the inferior margin of the maxillary sinuses to the superior border of the frontal sinuses (Fig. 46).

Axial SE/FSE T1

As for Coronal T1,

except prescribe slices from the inferior border of the maxillary sinuses to the superior edge of the frontal sinuses (Fig. 47).

Fig. 46. Sagittal SE T1 weighted midline slice through the brain showing slice prescription boundaries and orientation for coronal imaging of the paranasal sinuses.

Fig. 47. Sagittal SE T1 weighted midline slice through the brain showing slice prescription boundaries and orientation for axial imaging of the paranasal sinuses.

Coronal/Axial SE/FSE PD/T2

Slice prescription as for Axial and Coronal T1.

Additional sequences

The use of MR to image the sinuses has recently extended into interventional procedures. The use of open magnet systems that allow near real-time imaging has proved beneficial in functional endoscopic sinus surgery. The multiplanar capabilities of MR enable rapid visualization of the optic nerve in three planes so that this type of surgery has become safer and quicker.

Image optimization

Technical issues

The SNR and CNR of the sinuses are often poor due to the low proton density of the air-filled cavities. MRI does not demonstrate bony resolution as well as computer tomography (CT), but is useful for visualizing the nature and extent of soft tissue masses. Spatial resolution is not usually as important as good SNR in this region. Medium slices are selected to maintain SNR, and multiple NEX/NSA are employed as long as the scan time is kept within reasonable limits. The use of FSE enables

the implementation of fine matrices and multiple NEX/NSA whilst maintaining relatively short scan times.

Artefact problems

The main source of artefact is from the carotid, vertebral and jugular vessels. The use of spatial pre-saturation pulses placed I to the FOV usually reduces this to acceptable levels. GMN may be employed but as it increases the signal in vessels and the minimum TE, it is not usually beneficial in T1 weighted sequences. On the axial and coronal images, phase artefact occurs in the R to L direction which may obscure the maxillary sinuses. However, the strategy of swapping the phase direction places this artefact S and I, which can then interfere with the frontal, ethmoid and sphenoid sinuses. Under these circumstances, swapping the phase axis rarely has merits unless the maxillary sinuses are under examination and flow artefact is a particular problem. If the phase axis is swapped on the coronal images, oversampling is necessary to prevent wrap from the neck and top of the head. Magnetic susceptibility artefact from dental fillings sometimes interferes with the maxillary sinuses but is not easily remedied, other than to avoid GRE sequences.

Patient considerations

Claustrophobia is often troublesome because of the enclosing nature of the head coil. Under these circumstances reassurance and a careful explanation of the procedure is required. Some patients may have profuse nasal secretions so that they need to swallow or blow their nose frequently during the examination.

Due to excessively loud gradient noise associated with some sequences, ear plugs must always be provided to prevent hearing impairment.

Contrast usage

Contrast enhances the mucous lining of the sinuses but it is not commonly used for sinus disease. It is, however, useful to distinguish between enhancing tumour and non-enhancing effusion.

Further reading

Bangert B.A. (1997) Imaging of paranasal sinus disease. *Pediatric Clinics of North America*, **44**(3), 681–99.

Feyh J., Gutmann R., Leunig A. *et al.* (1996) MRI-guided laser interstitial thermal therapy (LITT) of head and neck tumors: progress with a new method. *Journal of Clinical Lasers in Medicine & Surgery*, **14**(6), 361–6.

Gufler H., Laubenberger J., Gerling J., Nesbitt E., Kommerell G. & Langer M. (1997) MRI of lymphomas of the orbits and the paranasal sinuses. *Journal of Computer Assisted Tomography*, **21**(6), 887–91.

Gunkel A.R., Freysinger W. & Thumfart W.F. (1997) Computer-assisted surgery in the frontal and maxillary sinus. *Laryngoscope*, **107**(5), 631–3.

Hightower D.J., Bui-Mansfield L.T. & Coughlin W.F. (1997) Osseous hamartoma of the maxillary sinus: MR and CT characteristics. *Journal of Computer Assisted Tomography*, **21**(6), 905–906.

Hudgins P.A. (1996) Sinonasal imaging. *Neuroimaging Clinics of North America*, **6**(2), 319–31.

Iwabuchi Y., Hanamure Y., Ueno K., Fukuda K. & Furuta S. (1997) Clinical significance of asymptomatic sinus abnormalities on magnetic resonance imaging. *Archives in Otolaryngology, Head & Neck Surgery*, **123**(6), 602–604.

Lund V.J., Lloyd G.A., Howard D.J., Cheesman A.D. & Phelps P.D. (1996) Enhanced magnetic resonance imaging and subtraction techniques in postoperative evaluation of craniofacial resection for sinonasal malignancy. *Laryngoscope*, **106**(5 Pt 1), 553–8.

Maroldi R., Farina D., Battaglia G., Maculotti P., Nicolai P. & Chiesa A. (1997) MR of malignant nasosinusal neoplasms. Frequently asked questions. *European Journal of Radiology*, **24**(3), 181–90.

Phillips C.D. (1997) Current status and new developments in techniques for imaging the nose and sinuses. *Otolaryngology Clinics of North America*, **30**(3), 371–87.

Pharynx

Basic anatomy (Fig. 48)

hard palate

tongue

larynx

soft palate
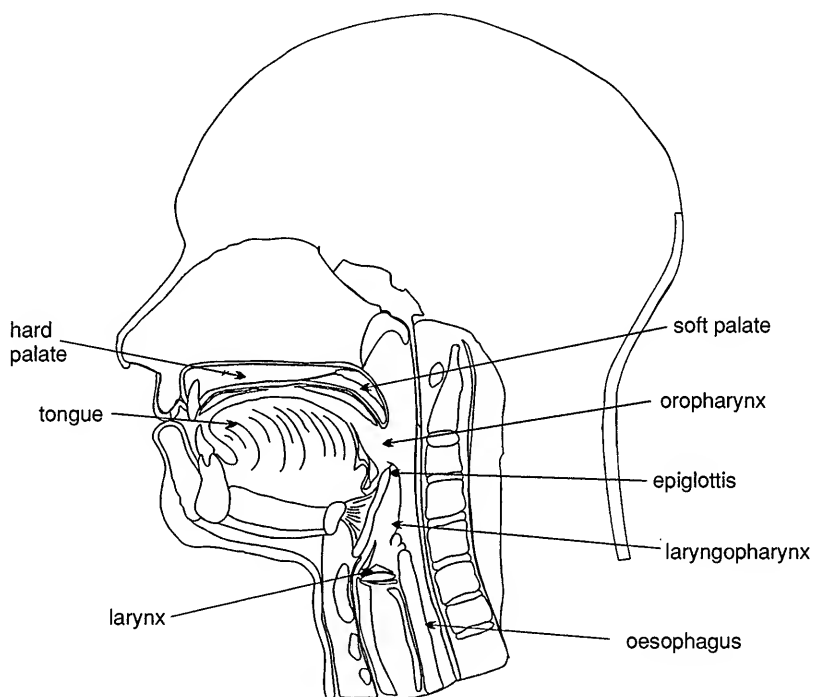
oropharynx

epiglottis

laryngopharynx

oesophagus

Fig. 48. Sagittal section through the mouth and pharynx.

Common indications

- Staging of oropharyngeal carcinoma.
- Pharyngeal and parapharyngeal masses.
- Investigation of sleep apnoea.
- Swallowing disorders.

Equipment

- Anterior neck coil/volume neck coil for cervical nodal involvement.
- Head coil (quadrature or phased array) for pharyngeal area and base of skull.
- Immobilization pads and straps.
- Ear plugs.

Patient positioning

The patient lies supine on the examination couch with their head within the head coil. The head is adjusted so that the interpupillary line is parallel to the couch and the head is straight. If the neck is to be imaged for nodal involvement, the anterior or volume neck coil is placed around or anterior to the patient's neck. Care should be taken to include the base of the skull within the coil. The patient's head is straightened as this usually straightens the neck as well.

The patient is positioned so that the longitudinal alignment light lies in the midline, and the horizontal alignment light passes through the angle of the jaw. When imaging the cervical nodes, the vertical alignment light should be located midway between the posterior and anterior surfaces of the neck. A soft pad may be placed under the patient's neck to facilitate this, although many dedicated coils ensure that the neck naturally assumes the correct position. Straps and foam pads are used for immobilization.

Suggested protocol

Coronal SE/FSE T1 (Fig. 49)

Thin slices/gap are prescribed from the posterior border of the cervical cord to the anterior surface of the neck. This distance is measured relative to the vertical alignment light before the examination. The area from the skull base to the sternoclavicular joints is included in the image.

P 25 mm to A 25 mm

Axial SE/FSE PD/T2 (Fig. 51)

Thin slices/gap are prescribed from the thyroid cartilage to the base of the skull (Fig. 50).

Sagittal SE/FSE PD/T2 (Fig. 53)

As for Axial PD/T2,
except   prescribe slices from the left to the right lateral walls of the pharynx.

The coverage is increased if nodal or parapharyngeal disease is suspected. The area from the skull base to the thyroid cartilage is included in the image (Fig. 52).

Additional sequences

When assessing tumour spread the scan plane and slice coverage is altered depending on the site of the primary tumour as follows:

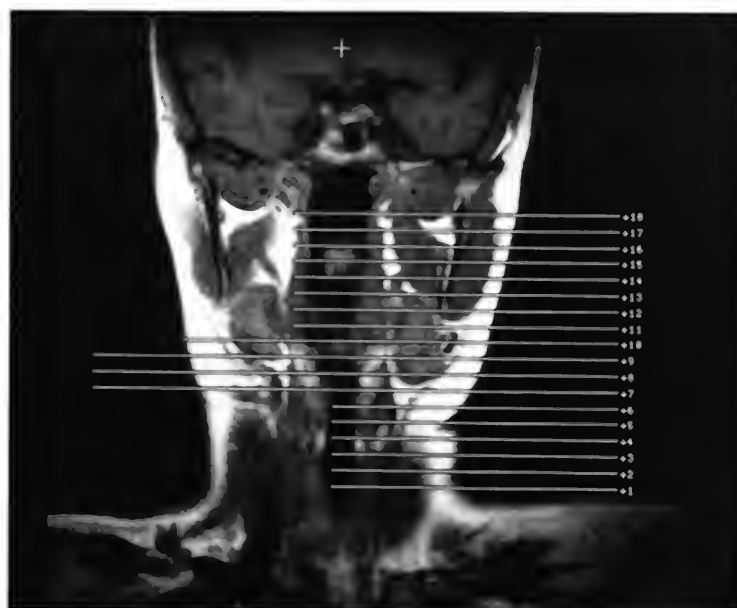**Fig. 49.** Coronal FSE T1 weighted localizer of the pharynx.

Fig. 50. Coronal FSE T1 weighted localizer showing slice prescription boundaries and orientation for axial imaging of the pharynx.
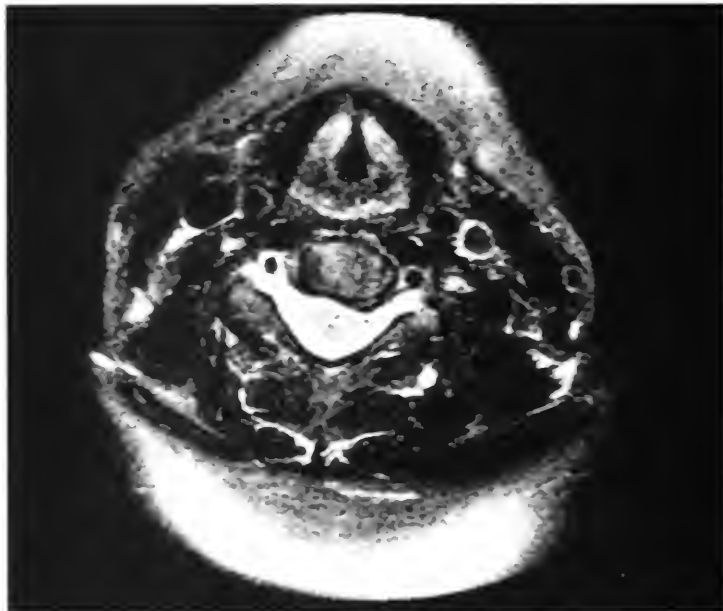
Fig. 51. Axial FSE T2 weighted image through the neck demonstrating the laryngopharynx.
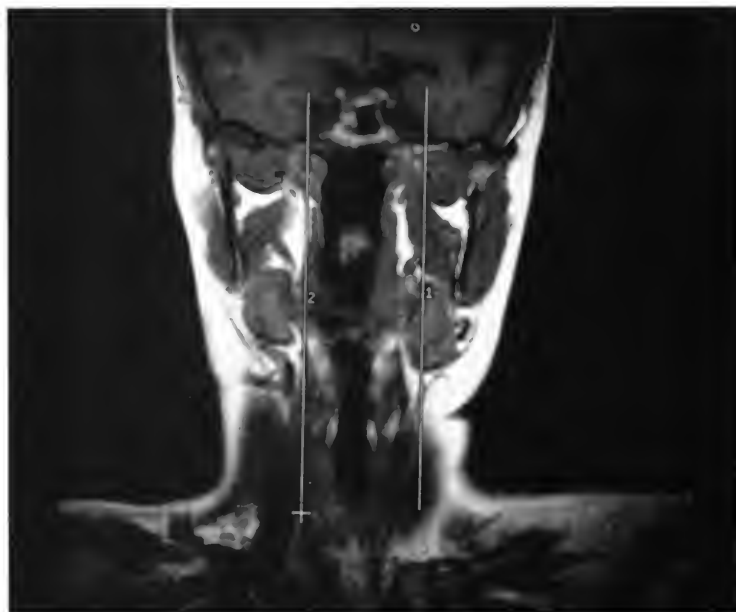

Fig. 52. Coronal FSE T1 localizer showing slice prescription boundaries and orientation for sagittal imaging of the pharynx.

Fig. 53. Sagittal FSE T2 weighted image through the entire pharynx which is clearly seen as low signal intensity. This image also shows the appropriate slice prescription boundaries for axial imaging of the pharynx.

- **Oral tumours** include cervical nodes in the axial and coronal plane.
- **Nasopharyngeal tumours** include the sphenoid sinus in the sagittal and axial plane.
- **Oropharyngeal tumours** include the parapharyngeal space, the base of the middle cranial fossa, and the anterior triangle of the neck in the axial and coronal plane.

Rapid sequences are proving useful in dynamic imaging of the pharynx to assess swallowing. The patient is instructed to swallow bread or mashed potato soaked in gadolinium and the bolus imaged during swallowing. As the upper pharyngeal phase of swallowing is very rapid, sequences such as EPI, which can acquire 20–25 images per second, are necessary in combination with good resolution. In addition, 3D imaging of the pharynx may be utilized to assess anatomy during sleep.

Image optimization

Technical issues

The anterior portion of the neck is a notoriously difficult area to examine. The SNR is often poor, especially if a substandard coil is used. The head coil is probably the best coil for this examination, although an anterior or volume coil moulded to the

face and neck is necessary to best visualize the cervical lymph nodes and inferior tumour spread. However, even with the best coils, multiple NEX/NSA are often necessary to maintain SNR. Spatial resolution is also important in this area, and therefore thin slices/gap and a fairly fine matrix are required to optimize resolution. The use of these matrices and multiple NEX/NSA often leads to long scan times.

A solution to these problems is to use FSE in conjunction with a rectangular/ asymmetric FOV. FSE reduces the scan time significantly and yields higher SNR, especially on the T2 weighted sequences. A rectangular/asymmetric FOV allows the acquisition of fine matrices in shorter scan times. In coronal and axial imaging, the long axis of the rectangle is placed S to I and A to P, respectively.

Artefact problems

Artefact in this region arises from flow motion in the carotid, vertebral and jugular vessels, and from swallowing. Spatial pre-saturation pulses placed S and I to the FOV reduce flow artefact significantly. Bringing the spatial pre-saturation pulses into the FOV increases their effectiveness, but care must be taken that they do not obscure important anatomy. GMN further reduces artefact but, as it also increases the signal in vessels and the minimum TE, it is not usually beneficial in T1 weighted sequences.

Swallowing is a common problem in this area. If the patient swallows too often, motion artefact interferes with the image. Using multiple NEX/NSA to average out this artefact reduces phase ghosting, but leads to longer scan times. If the patient does not swallow at all, pooling of saliva in the pyriform fossae can sometimes lead to difficulties in image interpretation. The patient should be advised to swallow as little as possible during the examination but to try to clear the mouth of saliva when they do. Respiratory motion may move the anterior neck coil during the acquisition of data. If this is a problem, instruct the patient to breathe shallowly. In addition, small foam pads placed between the chest and the coil help to reduce coil movement. Magnetic susceptibility artefact from dental fillings sometimes interferes with important anatomy but is not easily remedied, other than to avoid GRE sequences.

Patient considerations

Some patients with oral or pharyngeal pathology produce copious saliva and have difficulty swallowing. This often leads to choking or major swallowing artefact. Try to calm and reassure the patient as much as possible before the examination. Give the patient plenty of tissues and, in extreme circumstances, consider examining the patient prone. The patient is instructed to swallow as little as possible during the examination but to ensure that they clear the mouth of saliva when they do. This prevents saliva pooling in the pyriform fossae.

Due to excessively loud gradient noise associated with some sequences, ear plugs must always be provided to prevent hearing impairment.

Contrast usage

This is rarely indicated but may be useful to distinguish the extent or nature of a lesion.

Further reading

Mathru M., Esch O., Lang J. *et al.* (1996) Magnetic resonance imaging of the upper airway. Effects of propofol anesthesia and nasal continuous positive airway pressure in humans. *Anesthesiology*, **84**(2), 273–9.

Shellock F.G. (1997) Sleep apnea syndrome: evaluation with dynamic MR imaging of the upper airway. *Radiology*, **204**(1), 281–2.

Suto Y. & Inoue Y. (1996) Sleep apnea syndrome. Examination of pharyngeal obstruction with high-speed MR and polysomnography. *Acta Radiology*, **37**(3 Pt 1), 315–20.

Suto Y., Matsuda E. & Inoue Y. (1996) MRI of the pharynx in young patients with sleep disordered breathing. *British Journal of Radiology*, **69**(827), 1000–1004.

Suto Y., Ohmura N., Inoue Y. & Ohta Y. (1997) Reconstruction of three-dimensional images of the pharynx in patients with sleep apnea using three-dimensional fast low-angle shot MR imaging. *American Journal of Roentgenology*, **168**(5), 1320–1.

Yokoyama M., Yamanaka N., Ishii H., Tamaki K., Yoshikawa A. & Morita R. (1996) Evaluation of the pharyngeal airway in obstructive sleep apnea: study by ultrafast MR imaging. *Acta Otolaryngology*, **523**(Supplement), 242–4.

Larynx

Basic anatomy (see Fig. 48)

Common indications

- Carcinoma of the larynx.
- Assessment prior to reconstruction of the larynx.
- Disorders of the vocal cords and phonation.

Equipment

- Anterior neck coil/volume neck coil.
- Immobilization foam pads and straps.
- Ear plugs.

Patient positioning

The patient lies supine on the examination couch. The coil is placed around or anterior to the patient's neck. The patient's head is straightened as this usually straightens the neck as well. The patient is positioned so that the longitudinal alignment light lies in the midline, and the horizontal alignment light passes through the thyroid cartilage (Adam's apple). The vertical alignment light should be located midway between the posterior and anterior surfaces of the neck. A soft pad may be placed under the patient's neck to facilitate this, although many dedicated coils ensure that the neck naturally assumes the correct posi¨on. Straps and foam pads are used for immobilization.

Suggested protocol

Sagittal SE/FSE T1/T2 (Fig. 54)

Thin slices/gap are prescribed on either side of the longitudinal alignment light from the left to the right lateral skin surfaces of the neck. The area from the superior border of the hard palate to the sternoclavicular joints is included in the image.
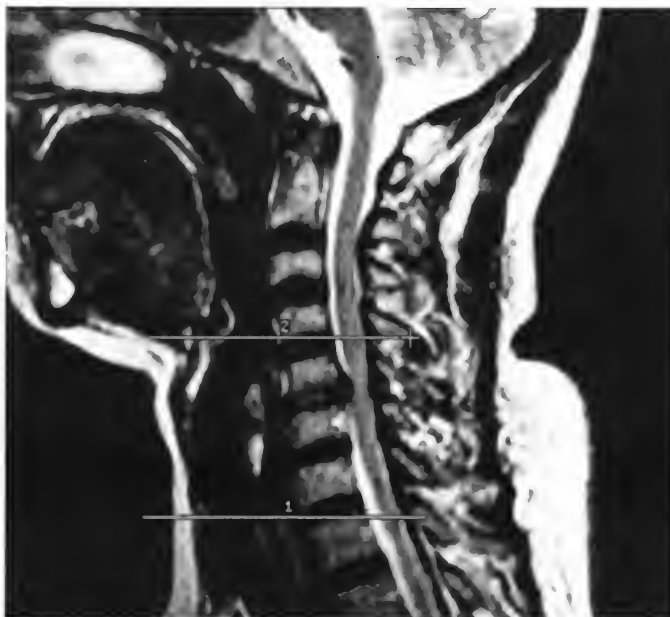
L 25 mm to R 25 mm

Fig. 54. Sagittal FSE T2 weighted image through the neck showing slice prescription boundaries and orientation for axial imaging of the larynx.

Axial SE/FSE T1 (Fig. 55)

Thin slices/gap are prescribed through the laryngeal cartilages and vocal cords (Fig. 54). The slices may be angled parallel to the larynx for tumours limited to the cords.

Coronal SE/FSE T1 (Fig. 57)

As for the Axial T1,

except   prescribe slices from posterior surface of the trachea to anterior surface of the neck.

The slices may be angled so that they are parallel to the larynx for tumours limited to the vocal cords (Fig. 56). The area from the superior border of the hard palate to the sternoclavicular joints is included in the image.

Axial/Coronal SE/FSE PD/T2

Slice prescription as for SE/FSE T1. Useful to distinguish advanced tumour from muscles and the thyroid gland.

Additional sequences

Fast incoherent (spoiled) GRE/EPI T1

During phonation to assess function of the vocal cords.
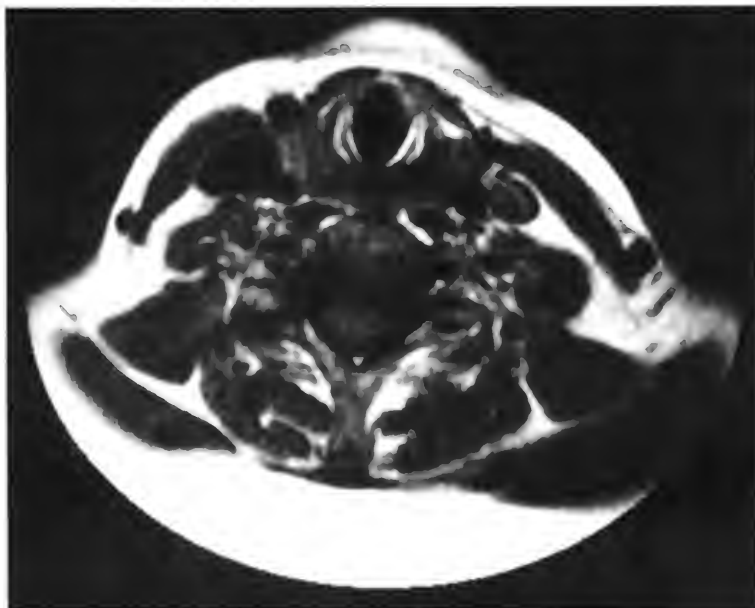
Fig. 55. Axial SE T1 weighted image through the larynx seen anteriorly in the neck.

Fig. 56. Sagittal FSE T2 weighted image through the neck showing slice prescription boundaries and orientation for coronal/oblique imaging of the larynx.
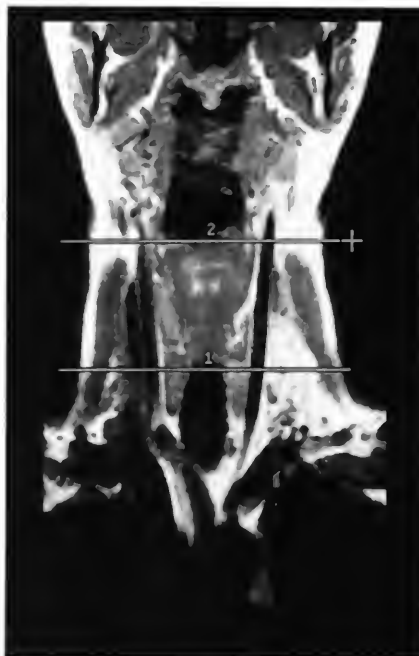
Fig. 57.   Coronal SE T1 weighted image through the larynx. This image also shows slice prescription boundaries for axial imaging.

Image optimization

Technical issues

The anterior portion of the neck is a notoriously difficult area to examine. The SNR is often poor, especially if a substandard coil is used. An anterior neck coil moulded to the face and neck is probably the best coil for this examination. However, even with these coils, multiple NEX/NSA are often necessary to maintain SNR. Spatial resolution is also important in this area, and therefore thin slices/gap and a fairly fine matrix are required to optimize resolution. The use of these matrices and multiple NEX/NSA often leads to long scan times.

A possible solution to these problems is to use FSE in conjunction with a rectangular/asymmetric FOV. FSE reduces the scan time significantly and yields higher SNR, especially on the T2 weighted sequences. A rectangular/asymmetric FOV allows the acquisition of fine matrices in shorter scan times. In coronal and axial imaging, the long axis of the rectangle is placed S to I and A to P, respectively.

Artefact problems

Artefact in this region arises from flow motion in the carotid, vertebral and jugular vessels, and from swallowing. Spatial pre-saturation pulses placed S and I to the

FOV reduce flow artefact significantly. Bringing the spatial pre-saturation pulses into the FOV increases their effectiveness but care must be taken that they do not obscure important anatomy. GMN further reduces artefact but, as it also increases the signal in vessels and the minimum TE, it is not usually beneficial in T1 weighted sequences.

The patient should be advised to swallow as little as possible during the examination. The implementation of multiple NEX/NSA averages out any phase ghosting but leads to longer scan times. Respiratory motion may move the anterior neck coil during the acquisition of data. If this is a problem, instruct the patient to breathe shallowly. In addition, small foam pads placed between the chest and the coil help to reduce coil movement.

Patient considerations

A careful explanation of the procedure and the importance of minimizing swallowing during the examination is important.

Due to excessively loud gradient noise associated with some sequences, ear plugs must always be provided to prevent hearing impairment.

Contrast usage

This is rarely indicated but may be useful to distinguish the extent or nature of a lesion.

Further reading

Castelijns J.A., van den Brekel M.W., Niekoop V.A. & Snow G.B. (1996) Imaging of the larynx. *Neuroimaging Clinics of North America*, **6**(2), 401–15.

Curtin H.D., Ishwaran H., Mancuso A.A., Dalley R.W., Caudry D.J. & McNeil B.J. (1998) Comparison of CT and MR imaging in staging of neck metastases. *Radiology*, **207**(1), 123–30.

Duda J.J. Jr., Lewin J.S. & Eliachar I. (1996) MR evaluation of epiglottic disruption. *American Journal of Neuroradiology*, **17**(3), 563–6.

Kumazawa H., Tsuta Y., Nakamura A., Yamashita T. & Kurokawa H. (1997) Magnetic resonance imaging of vocal failure in patients undergoing laryngectomy with tracheoesophageal fistula. *Annals of Otology, Rhinology & Laryngology*, **106**(9), 795–8.

Lev M.H. & Curtin H.D. (1998) Larynx. *Neuroimaging Clinics of North America*, **8**(1), 235–56.

Story B.H., Titze I.R. & Hoffman E.A. (1996) Vocal tract area functions from magnetic resonance imaging. *Journal of the Acoustic Society of America*, **100**(1), 537–54.

Tsunoda K., Ohta Y., Soda Y., Niimi S. & Hirose H. (1997) Laryngeal adjustment in whispering magnetic resonance imaging study. *Annals of Otology, Rhinology & Laryngology*, **106**(1), 41–3.

Thyroid and parathyroid glands
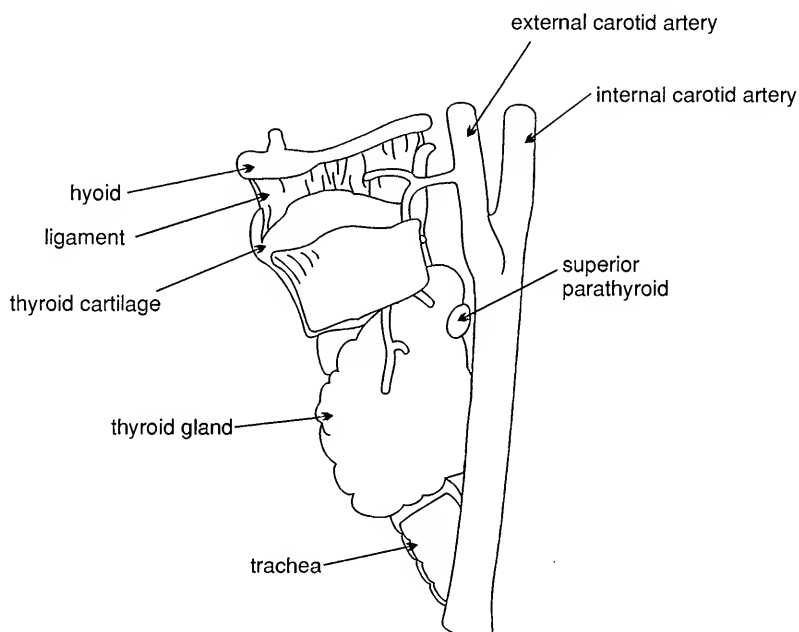
Basic anatomy (Figs 58 and 59)

Fig. 58. Sagittal view of the thyroid gland and its relationships.

Common indications

- Retrosternal goitre.
- Evaluation of recurrent thyroid carcinoma.
- Detection and characterization of parathyroid adenoma.

Equipment

- Anterior neck coil/volume neck coil.
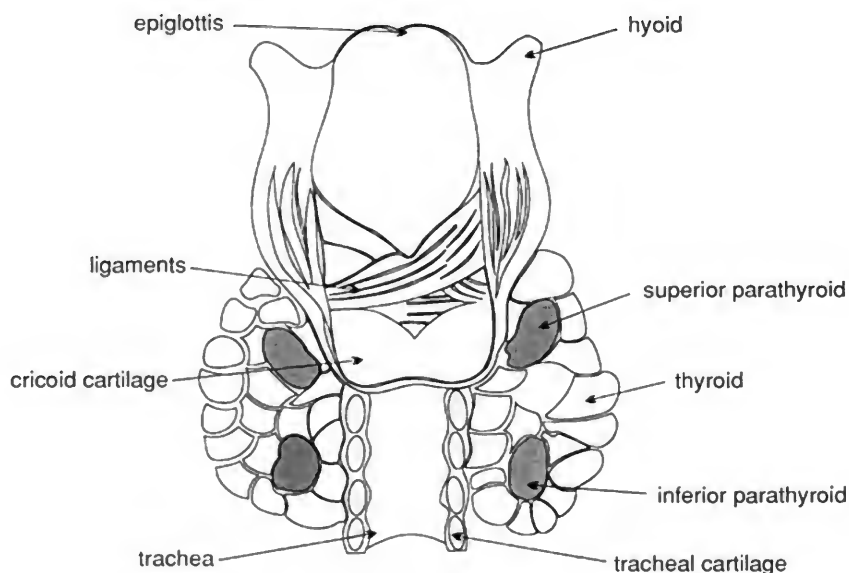- Immobilization foam pads and straps.
- Ear plugs.

Fig. 59. Anterior view of the thyroid gland and its relationships.

Patient positioning

The patient lies supine on the examination couch. The coil is placed around or anterior to the patient's neck. The patient's head is straightened as this usually straightens the neck as well. The patient is positioned so that the longitudinal alignment light lies in the midline, and the horizontal alignment light passes just inferior to the thyroid cartilage (Adam's apple). The vertical alignment light should be located midway between the posterior and anterior surfaces of the neck. A soft pad may be placed under the patient's neck to facilitate this, although many dedicated coils ensure that the neck naturally assumes the correct position. Straps and foam pads are used for immobilization.

Suggested protocol

Coronal SE/FSE T1

Thin slices/gap are prescribed through the thyroid relative to the vertical alignment light. The area from the mandible to the arch of the aorta is included in the image.

A 0 mm to A 20 mm

Axial/Coronal SE/FSE T1

Thin slices and gap are prescribed through the thyroid or ROI. Slices are displaced inferiorly for retrosternal goitre.

Axial/Coronal SE/FSE PD/T2

Slice prescription as for the Axial/Coronal T1.

Chemical/spectral pre-saturation/STIR is sometimes required for the parathyroid glands.

Image optimization

Technical issues

The anterior portion of the neck is a notoriously difficult area to examine. The SNR is often poor, especially if a substandard coil is used. An anterior neck coil moulded to the face and neck is probably the best coil for this examination. However, even with these coils, multiple NEX/NSA are often necessary to maintain SNR. Spatial resolution is also important in this area, and therefore thin slices/gap and a fairly fine matrix are required to optimize resolution. The use of these matrices and multiple NEX/NSA often leads to long scan times.

A solution to these problems is the use of FSE in conjunction with a rectangular/asymmetric FOV. FSE reduces the scan time significantly and yields higher SNR, especially on the T2 weighted sequences. A rectangular/asymmetric FOV allows the acquisition of fine matrices in shorter scan times. In coronal and axial imaging, the long axis of the rectangle is placed S to I and A to P, respectively. The parathyroid gland sometimes returns a very high signal on FSE T2 weighted sequences necessitating the use of chemical/spectral pre-saturation techniques.

Artefact problems

Artefact in this region arises from flow in the carotid, vertebral and jugular vessels, and from swallowing. Spatial pre-saturation pulses placed S and I to the FOV reduce flow artefact significantly. Bringing the spatial pre-saturation pulses into the FOV increases their effectiveness, but care must be taken that they do not obscure important anatomy. GMN further reduces artefact but, as it also increases signal in vessels and the minimum TE, it is not usually beneficial in T1 weighted sequences.

Swallowing is commonly troublesome in this area. Using multiple NEX/NSA to average out motion artefact reduces phase ghosting but leads to longer scan times. The patient should be advised to swallow as little as possible during the examination. Respiratory motion may move the anterior neck coil during the acquisition of data. If this is a problem, instruct the patient to breathe shallowly. In addition, small foam pads placed between the chest and the coil help to reduce coil movement.

Patient considerations

A careful explanation of the procedure and the importance of minimizing swallowing during the examination is important.

Due to excessively loud gradient noise associated with some sequences, ear plugs must always be provided to prevent hearing impairment.

Contrast usage

This is rarely indicated but may be useful to distinguish the extent or nature of a lesion.

Further reading

Bagley J.S., Ewen S.W., Smith F.W. & Krukowski Z.H. (1996) Magnetic resonance imaging of thyroid swellings. *British Journal of Surgery*, **83**(6), 828–9.

Giovagnorio F., Cordier A. & Romeo R. (1996) Lingual thyroid: value of integrated imaging. *European Radiology*, **6**(1), 105–107.

McDermott V.G., Fernandez R.J.M., Meakem T.J. 3rd, Stolpen A.H., Spritzer C.E. & Gefter W.B. (1996) Preoperative MR imaging in hyperparathyroidism: results and factors affecting parathyroid detection. *American Journal of Roentgenology*, **166**(3), 705–10.

Nakahara H., Noguchi S., Murakami N. *et al.* (1997) Gadolinium-enhanced MR imaging of thyroid and parathyroid masses. *Radiology*, **202**(3), 765–72.

Rutter A., Kunnecke B., Dowd S., Russell P., Delbridge L. & Mountford C.E. (1996) Proton magnetic resonance and human thyroid neoplasia III. Ex vivo chemical-shift microimaging. *Journal of Magnetic Resonance Imaging*, **110**(3), 240–48.

Sardanelli F., Giordano G.D., Melani E., Parodi R.C., Giusti M. & Garlaschi G. (1997) Magnetic resonance evaluation of autonomous thyroid nodules treated by percutaneous ethanol injection. *MAGMA*, **5**(4), 267–74.

Shah R.R. & Lewin J.S. (1998) Imaging of the infrahyoid neck. *Neuroimaging Clinics of North America*, **8**(1), 219–34.

Yousem D.M. (1996) Parathyroid and thyroid imaging. *Neuroimaging Clinics of North America*, **6**(2), 435–59.

Yousem D.M., Huang T., Loevner L.A. & Langlotz C.P. (1997) Clinical and economic impact of incidental thyroid lesions found with CT and MR. *American Journal of Neuroradiology*, **18**(8), 1423–8.

Salivary glands

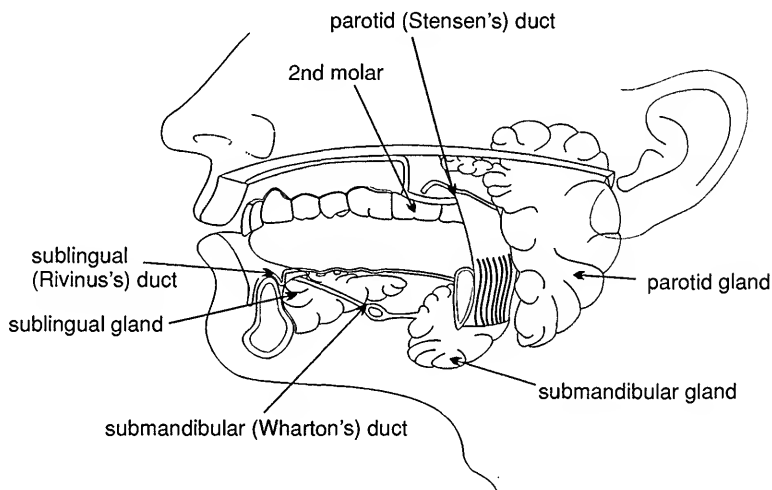## Basic anatomy (Fig. 60)

Fig. 60. The salivary glands and their ducts.

Common indications

- Detection of salivary gland masses.
- Staging of neoplasms and nodal involvement.

Equipment

- For **parotid glands:** Quadrature or phased array head coil. Foam pads and immobilization straps.
- For **submandibular glands** and **cervical nodes:** Anterior/volume neck coils. Foam pads and immobilization straps.
- Ear plugs.

Patient positioning

For parotid glands

The patient lies supine on the examination couch with their head within the head coil. The head is adjusted so that the interpupillary line is parallel to the couch and

the head is straight. The patient is positioned so that the longitudinal alignment light lies in the midline, and the horizontal alignment light passes through the level of the external auditory meatus. Straps and foam pads are used to immobilize the patient.

For submandibular glands and cervical nodes

The patient lies supine on the examination couch. The coil is placed around or anterior to the patient's neck. Care should be taken to include the floor of the mouth within the coil. The patient is positioned so that the longitudinal alignment light lies in the midline, and the horizontal alignment light passes through the angle of the jaw. The vertical alignment light should be located midway between the posterior and anterior surfaces of the neck. A soft pad may be placed under the patient's neck to facilitate this, although many dedicated coils ensure that the neck naturally assumes the correct position.

Suggested protocol

Sagittal SE T1

Thin slices/gap are prescribed on either side of the longitudinal alignment light. The area from the base of the skull to the hyoid bone is included in the image to visualize both the parotid and submandibular glands.

L 37 mm to R 37 mm

Coronal SE/FSE T1 (Fig. 61)

Mainly demonstrates the parotid glands. Thin slices/gap are prescribed from the vertebral bodies posteriorly to the superior alveolar process. The cervical lymph node chain and the skull base are included in the image.

Axial SE/FSE T1 (Fig. 62)

Thin slices/gap are prescribed from the superior aspect of the external auditory meatus to the angle of the jaw for the parotid glands, or through the submandibular glands (located just below the mandible) (Fig. 61). Coverage is extended for tumour spread.

Axial SE/FSE PD/T2

Demonstrates abnormal tissue and dilated ducts in the diagnosis of salivary gland masses. Thin slices/gap are prescribed through both glands. Coverage is extended for tumour spread. Chemical/spectral pre-saturation/STIR is sometimes necessary in imaging of the parotid gland.
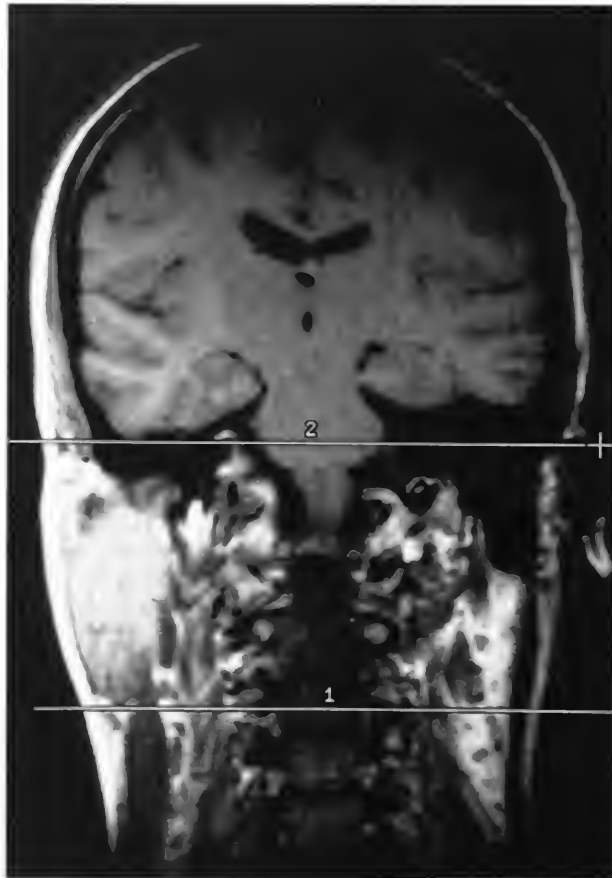
Fig. 61.   Coronal SE T1 weighted image through the neck showing slice prescription boundaries and orientation for axial imaging of the parotid salivary gland.

Additional sequences

SS-FSE/FSE T2

MR sialography may be of use in investigating ductal obstruction of the salivary system. Heavily T2 weighted images are acquired and post-processed (see *Liver and biliary system,* and *Kidneys and adrenals* and *Pancreas* later in Part 2 for the use of this technique in other areas).

Image optimization

Technical issues

The salivary glands are relatively small structures and therefore spatial resolution is important. The SNR is optimized by using the correct coil. The parotid glands are commonly examined using a quadrature or phased array head coil that yields
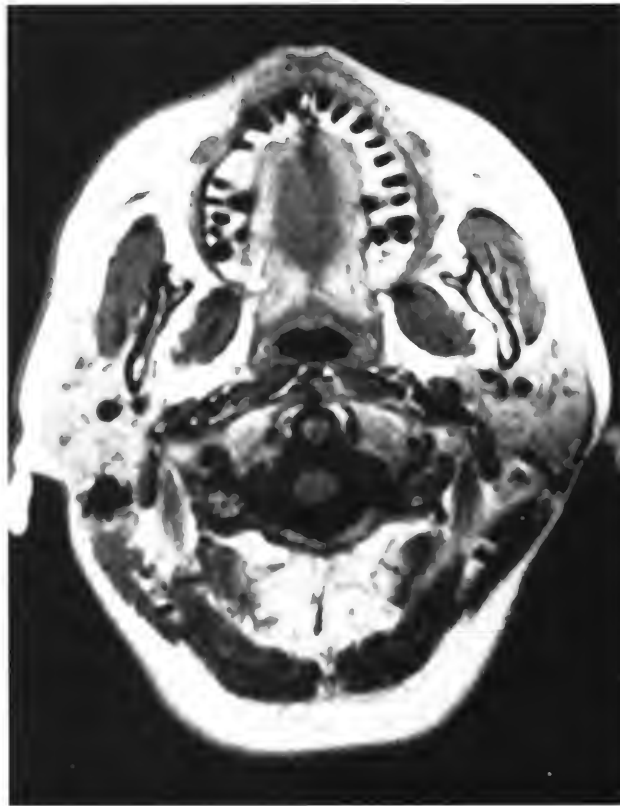
Fig. 62. Axial FSE T1 weighted image. The parotid glands are situated posterior and lateral to the mandibular condyles.

high and uniform signal. The submandibular glands can sometimes be imaged using this coil, as long as the patient is able to move well inside it; otherwise an anterior neck coil is necessary. Thin slices and fine matrices are important to maintain the necessary resolution and, as a result, multiple NEX/NSA are commonly required to maintain SNR. The use of FSE in conjunction with a rectangular/asymmetric FOV also improves SNR and facilitates the acquisition of fine matrices in relatively short scan times. Fat suppression techniques are sometimes required in FSE T2 weighted sequences as the fatty components of the parotid gland return a signal similar to pathology. The ductal salivary system may be effectively visualized using heavily T2 weighted FSE images (MR sialography). The use of long TEs (250 ms), TRs (10 s) and ETLs (16–20) produces images where the only signal returned is from fluid within the duct. As the ducts are small, good resolution is also required therefore 3D acquisitions may be superior to 2D.

Artefact problems

The main source of artefact in this area is from the carotid, jugular and vertebral vessels. Spatial pre-saturation pulses placed S and I to the FOV diminish this.

GMN further minimizes flow artefact but, as it also increases the signal in vessels and the minimum TE, it is not usually beneficial in T1 weighted sequences. Phase ghosting occurs along the R to L axis in axial and coronal imaging, and interferes with the laterally situated parotid glands. Swapping the phase axis so that it lies S to I reduces this problem, but oversampling is often necessary. Swallowing is often troublesome especially when examining the submandibular glands. Spatial pre-saturation bands placed carefully over the throat help to reduce this but may obscure the glands themselves. Instructing the patient to swallow as little as possible during the acquisition of data is advisable.

Patient considerations

Some patients with oral pathology produce copious saliva and have difficulty swallowing. This often leads to choking or major swallowing artefact. Try to calm and reassure the patient as much as possible before the examination. Give the patient plenty of tissues and, in extreme circumstances, consider examining the patient prone.

Due to excessively loud gradient noise associated with some sequences, ear plugs must always be provided to prevent hearing impairment.

Contrast usage

Contrast is not routinely given but may be helpful to distinguish pathology from normal anatomy.

Further reading

Ariyoshi Y. & Shimahara M. (1998) Determining whether a parotid tumor is in the superficial or deep lobe using magnetic resonance imaging. *Journal of Oral and Maxillofacial Surgery*, **56**(1), 23–6.

Dailiana T., Chakeres D., Schmalbrock P., Williams P. & Aletras A. (1997) High-resolution MR of the intraparotid facial nerve and parotid duct. *American Journal of Neuroradiology*, **18**(1), 165–72.

Eracleous E., Kallis S., Tziakouri C., Blease S. & Gourtsoyiannis N. (1997) Sonography, CT, CT sialography, MRI and MRI sialography in investigation of the facial nerve and the differentiation between deep and superficial parotid lesions. *Neuroradiology*, **39**(7), 506–11.

Fischbach R., Kugel H., Ernst S. *et al.* (1997) MR sialography: initial experience using a T2-weighted fast SE sequence. *Journal of Computer Assisted Tomography*, **21**(5), 826–30.

Izumi M., Eguchi K., Ohki M. *et al.* (1996) MR imaging of the parotid gland in Sjogren's syndrome: a proposal for new diagnostic criteria. *American Journal of Roentgenology*, **166**(6), 1483–7.

Lomas D.J., Carroll N.R., Johnson G., Antoun N.M. & Freer C.E. (1996) MR sialography. Work in progress. *Radiology*, **200**(1), 129–33.

Sigal R. (1996) Oral cavity, oropharynx, and salivary glands. *Neuroimaging Clinics of North America*, **6**(2), 379–400.

Soler R., Bargiela A., Requejo I., Rodriguez E., Rey J.L. & Sancristan F. (1997) Pictorial review: MR imaging of parotid tumours. *Clinical Radiology*, **52**(4), 269–75.

Takashima S., Sone S., Takayama F. *et al.* (1997) Assessment of parotid masses: which MR pulse sequences are optimal? *European Journal of Radiology*, **24**(3), 206–15.

Temporomandibular joints
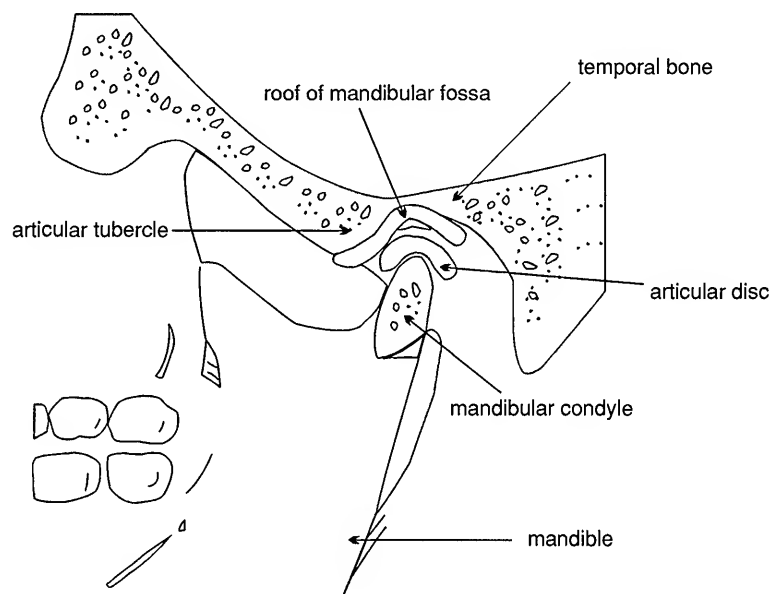
Basic anatomy (Fig. 63)

Fig. 63. Sagittal/oblique view of the components of the temporomandibular joint (TMJ).

Common indications

- Suspected internal meniscal derangement.

Equipment

- Dual three inch coils/phased array temporomandibular joint (TMJ) coils.
- Mouth opening device.
- Ear plugs.

Patient positioning

The patient lies supine on the examination couch with the coils secured over the TMJs. These can be located by placing fingers just anterior to the external auditory

meati and asking the patient to open and close their mouth. The coils are placed as close as possible, but not touching the face, with the receiving side of the coils towards the patient. Both joints are imaged together so the patient is positioned so that the longitudinal alignment light lies in the midline, and the horizontal alignment light passes through the level of the TMJs (which is the centre of the coils). Straps and foam pads are used for immobilization.

Before the examination, the function of the mouth opener is explained to the patient. The patient practises the opening of the device before the examination to minimize the risk of movement after the examination has begun. The first closed mouth acquisition should be made without the device in the patient's mouth. In some cases of anterior dislocation, it is possible that the meniscus will recapture immediately upon insertion of the device into the patient's mouth. When ready, the patient is asked to open their mouth with the opening device until they feel their jaws about to click. The operator can advise the patient when to do this over the system intercom. If a mouth opening device is not available, various size syringe barrels can be used to hold a patient's mouth open at various stages as desired.

Suggested protocol

Axial SE/FSE T1 (mouth closed) (Fig. 64)

Include the whole head so that the correct position of both coils is ascertained. Medium slices/gap are prescribed on either side of the horizontal alignment light. Both TMJs are included in the image.

I 15 mm to S 15 mm

Sagittal/oblique T1 (mouth closed) (Fig. 65)

Thin slices/gap or interleaved are prescribed through each joint. Slices are angled so that they are perpendicular to the mandibular condyles (do not over-oblique these) (Fig. 64).

Sagittal/oblique T1 (mouth open) (Fig. 65)

Slice prescription as for mouth closed.

Additional sequences

Coronal/oblique T1

As for the Sagittal/obliques,
except   slices are either prescribed perpendicular to the sagittal/obliques, or in the orthogonal coronal plane through both joints. Mouth open or closed.
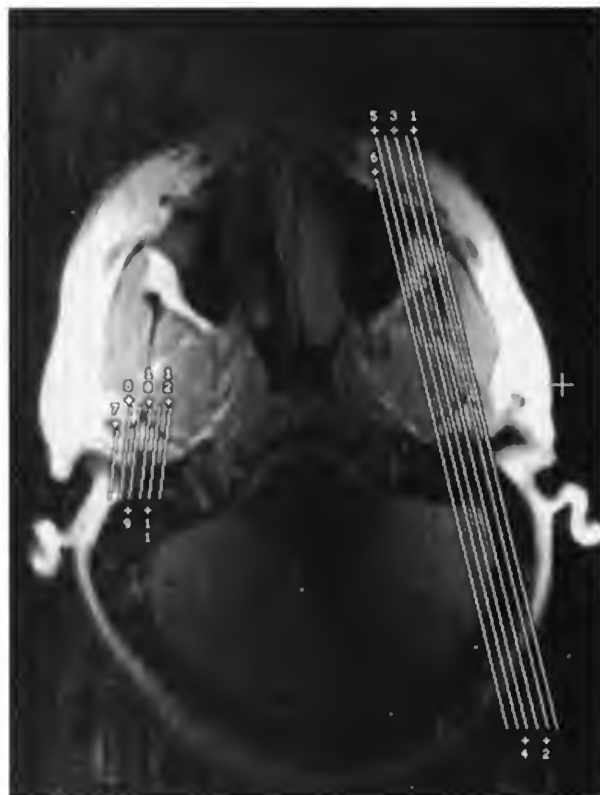
Fig. 64. Axial SE T1 weighted localizer through the temporomandibular joints (TMJs) showing correct placement of sagittal/oblique slices perpendicular to the mandibular condyles.
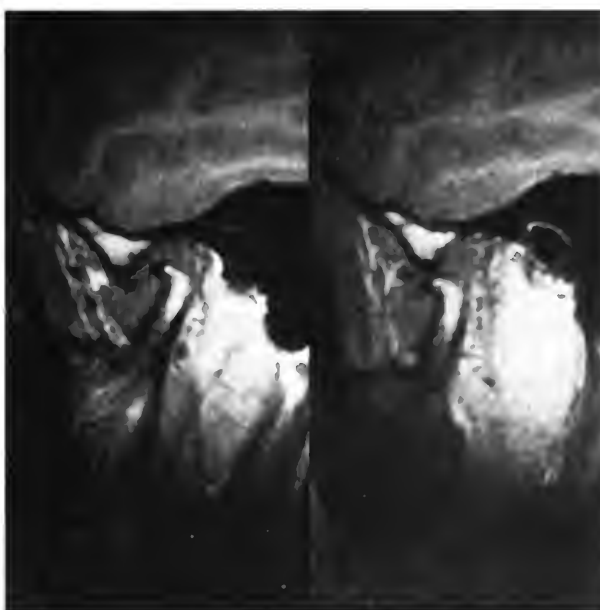

Fig. 65. Sagittal/oblique SE T1 images of the temporomandibular joint (TMJ) with mouth closed (left) and open (right).

Sagittal/oblique FSE/SS-FSE/EPI during mouth opening and closing

For dynamic imaging of the TMJ.

3D incoherent (spoiled) GRE/FSE T1

For thinner slices than 2D acquisitions and reformatting in other planes.

Image optimization

Technical issues

The SNR depends largely on the quality of the coils. Spatial resolution is important as the structures within the joint are small and therefore a small FOV, thin slices, interleaving, and relatively fine matrices are necessary. As the FOV is small, multiple NEX/NSA are often required to maintain adequate SNR and therefore scan times may be of several minutes duration. A common mistake is to over-oblique the sagittal/oblique slices. Ensure that they are perpendicular to the mandibular condyles. Dynamic imaging of the TMJs may be useful in assessing meniscal derangement. However, unless the sequence used is very rapid, temporal resolution may be insufficient and a pseudo-dynamic set of images are produced, i.e. where a single slice is acquired at each static position of mouth opening and the images are viewed sequentially in a cine mode. This type of acquisition may not show true movement of the disc during mouth opening. In order to achieve this, the temporal resolution must be high, and real-time imaging using sequences such as EPI is required (see *Dynamic imaging* under *Pulse sequences in Part 1*).

Artefact problems

Pulsation from the carotid vessels often interferes with the image. Spatial pre-saturation pulses placed S and I to the FOV are effective, but ghosting is sometimes seen. GMN also minimizes flow artefact but, as it increases signal in vessels and the minimum TE, it is not usually beneficial in T1 weighted sequences. As the images are obliqued there may be no operator control over the phase and frequency axes. If, however, the system allows for axes control, placing phase S to I is probably the best option as this largely removes the artefact from the joint. As a small FOV is used, oversampling is usually necessary.

Patient considerations

Patient cooperation is important during this examination. The patient should practise using the mouth opening device before the examination. The technologist must explain that the mouth is opened until the patient feels that the jaw is about to click, and then relaxed so that the upper and lower jaws rest against the opener.

As scan times are often lengthy, swallowing whilst the mouth is open can cause motion artefact. Obviously the patient must swallow if absolutely necessary, but it should be discouraged if possible. Another common problem is that the patient often moves from the localizer position when he opens his mouth. It is wise to obtain a second localizer with the mouth open to ensure adequate coverage of the second set of sagittal/obliques.

Due to excessively loud gradient noise associated with some sequences, ear plugs must always be provided to prevent hearing impairment.

Contrast usage

Contrast is not commonly used in this area. However, arthrography of the joints may prove useful in the future. The joint is injected with a small amount of gadolinium followed by sagittal/oblique T1 weighted imaging.

Further reading

Adame C.G., Monje F., Boffnoz M. & Martin-Granizo R. (1998) Effusion in magnetic resonance imaging of the temporomandibular joint: a study of 123 joints. *Journal of Oral and Maxillofacial Surgery*, **56**(3), 314–18.

Behr M., Fellner C., Bayreuther G. *et al.* (1996) MR-imaging of the TMJ: artefacts caused by dental alloys. *European Journal of Prosthodontic Restorative Dentistry*, **4**(3), 111–15.

Behr M., Held P., Leibrock A., Fellner C. & Handel G. (1996) Diagnostic potential of pseudo-dynamic MRI (CINE mode) for evaluation of internal derangement of the TMJ. *European Journal of Radiology*, **23**(3), 212–15.

Choi B.H. (1997) Magnetic resonance imaging of the temporomandibular joint after functional treatment of bilateral condylar fractures in adults. *International Journal of Oral and Maxillofacial Surgery*, **26**(5), 344–7.

Cholitgul W., Nishiyama H., Sasai T., Uchiyama Y., Fuchihata H. & Rohlin M. (1997) Clinical and magnetic resonance imaging findings in temporomandibular joint disc displacement. *Dentomaxillofacial Radiology*, **26**(3), 183–8.

van Dijke C.F., Kirk B.A., Peterfy C.G., Genant H.K., Brasch R.C. & Kapila S. (1997) Arthritic temporomandibular joint: correlation of macromolecular contrast-enhanced MR imaging parameters and histopathologic findings. *Radiology*, **204**(3), 825–32.

Held P., Moritz M., Fellner C., Behr M. & Gmeinwieser J. (1996) Magnetic resonance of the disk of the temporomandibular joint. MR imaging protocol. *Clinical Imaging*, **20**(3), 204–11.

Hollender L., Barclay P., Maravilla K. & Terry V. (1998) A new coronal imaging plane for magnetic resonance imaging of the temporomandibular joint disc. *Dentomaxillofacial Radiology*, **27**(1), 48–50.

Hollender L., Barclay P., Maravilla K. & Terry V. (1998) The depiction of the bilaminar zone of the temporomandibular joint by magnetic resonance imaging. *Dentomaxillofacial Radiology*, **27**(1), 45–7.

Ikeda K., Ho K.C., Nowicki B.H. & Haughton V.M. (1996) Multiplanar MR and anatomic study of the mandibular canal. *American Journal of Neuroradiology*, **17**(3), 579–84.

Janzen D.L., Connell D.G. & Munk P.L. (1998) Current imaging of temporomandibular joint abnormalities: a pictorial essay. *Canadian Association of Radiologists Journal*, **49**(1), 21–34.

Liedberg J., Panmekiate S., Petersson A. & Rohlin M. (1996) Evidence-based evaluation of three imaging methods for the temporomandibular disc. *Dentomaxillofacial Radiology*, **25**(5), 234–41.

Masui T., Isoda H., Mochizuki T. *et al.* (1996) Pseudodynamic imaging of the temporomandibular joint: SE versus GE sequences. *Journal of Computer Assisted Tomography*, **20**(3), 448–54.

Oezmen Y., Mischkowski R.A., Lenzen J. & Fischbach R. (1998) MRI examination of the TMJ and functional results after conservative and surgical treatment of mandibular condyle fractures. *International Journal of Oral and Maxillofacial Surgery*, **27**(1), 33–7.

Payne M. & Nakielny R.A. (1996) Temporomandibular joint imaging. *Clinical Radiology*, **51**(1), 1–10.

Ramos-Remus C., Perez-Rocha O., Ludwig R.N. *et al.* (1997) Magnetic resonance changes in the temporomandibular joint in ankylosing spondylitis. *Journal of Rheumatology*, **24**(1), 123–7.

Roditi G.H., Duncan K.A., Needham G. & Redpath T.W. (1997) Temporomandibular joint MRI: a 2-D gradient-echo technique. *Clinical Radiology*, **52**(6), 441–4.

Suenaga S., Hamamoto S., Kawano K., Higashida Y. & Noikura T. (1996) Dynamic MR imaging of the temporomandibular joint in patients with arthrosis: relationship between contrast enhancement of the posterior disk attachment and joint pain. *American Journal of Roentgenology*, **166**(6), 1475–81.

Suenaga S., Sonoda S., Oku T., Abeyama K. & Noikura T. (1997) MRI of the temporomandibular joint disk and posterior disk attachment before and after nonsurgical treatment. *Journal of Computer Assisted Tomography*, **21**(6), 892–6.

Takebayashi S., Takama T., Okada S., Masuda G. & Matsubara S. (1997) MRI of the TMJ disc with intravenous administration of gadopentetate dimeglumine. *Journal of Computer Assisted Tomography*, **21**(2), 209–15.

Trumpy I.G., Eriksson J. & Lyberg T. (1997) Internal derangement of the temporomandibular joint: correlation of arthrographic imaging with surgical findings. *International Journal of Oral and Maxillofacial Surgery*, **26**(5), 327–30.

Yamada I., Murata Y., Shibuya H. & Suzuki S. (1997) Internal derangements of the temporomandibular joint: comparison of assessment with three-dimensional gradient-echo and spin-echo MRI. *Neuroradiology*, **39**(9), 661–7.

Vascular imaging

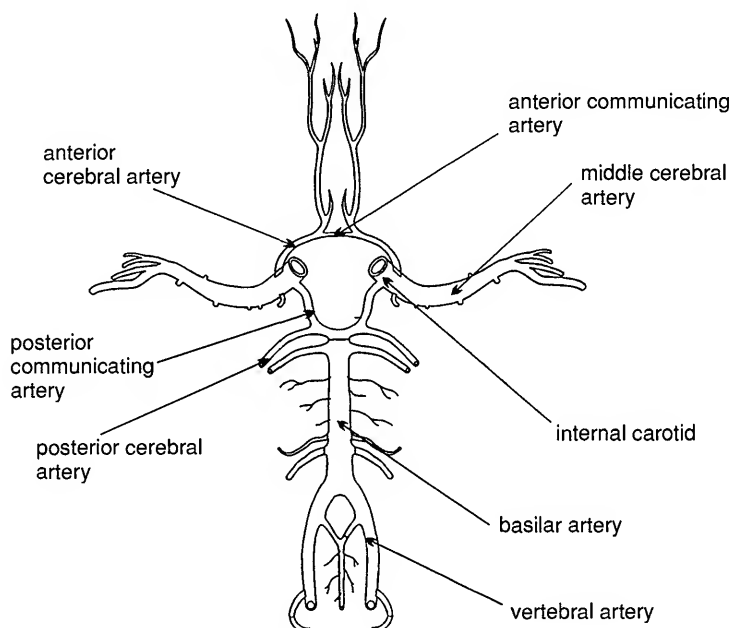## Basic anatomy (Fig. 66)

Fig. 66. The circle of Willis providing vascular supply to the brain.

Common indications

- Evaluation of the carotid arteries especially at the bifurcation.
- Intracranial vascular assessment of aneurysms and infarcts.
- Arterio-venous malformation (AVM).
- Intracranial vessel occlusion including sagittal sinus thrombosis.

Equipment

- Quadrature or phased array head coil (brain imaging).
- Anterior neck coil (neck imaging).
- Immobilization foam pads and straps.
- Ear plugs.

Patient positioning

Brain imaging

The patient lies supine on the examination couch with their head within the head coil. The head is adjusted so that the interpupillary line is parallel to the couch and the head is straight. The longitudinal alignment light lies in the midline and the horizontal alignment light passes through the nasion. Straps and foam pads are used to immobilize the patient as much as possible.

Neck imaging

The patient lies supine on the examination couch and an anterior neck coil is secured so that the base of the skull to the arch of the aorta are included within the volume of the coil. The longitudinal alignment light lies in the midline and the horizontal alignment light passes through the angle of the jaw.

Suggested protocol

Vascular imaging in the brain

A sagittal SE T1 series can be performed as a localizer. This is then followed by either 3D TOF or PC images (see later in Fig. 261). 3D acquisitions allow for increased SNR and very thin contiguous slices, so improving the spatial resolution. Depending on the coverage required, 28 to 124 thin slice locations may be selected. In PC-MRA all three axes are usually flow encoded. Due to the increased likelihood of intra-slab flow saturation with 3D TOF-MRA, PC-MRA is usually the sequence of choice for volume imaging in the head. However, intra-slab flow saturation in 3D TOF-MRA is improved by the implementation of ramped flip angles. 2D TOF-MRA is reserved for visualizing intracranial venous flow or small peripheral vessels. If MRA software is not available, cine or ultrafast coherent GRE T2* sequences in conjunction with GMN are beneficial, especially in the visualization of sagittal sinus thrombosis and post-embolization of giant aneurysms. When used in conjunction with SE sequences, spatial pre-saturation pulses produce black blood. If signal persists in a vessel it may indicate either slow flow or occlusion. When used in conjunction with GRE sequences, GMN produces bright blood. If a signal void is seen within the vessel, it may indicate either slow flow or occlusion.

Vascular imaging in the neck

A coronal coherent GRE sequence can be performed as a localizer. Axial 2D TOF-MRA using thin slices prescribed through the carotid and bifurcation are required, followed by 3D TOF-MRA for improved resolution of the bifurcation (Fig. 67). Spatial pre-saturation pulses should be placed S to the FOV to saturate venous flow entering the slice stack from above. If MRA software is not available,
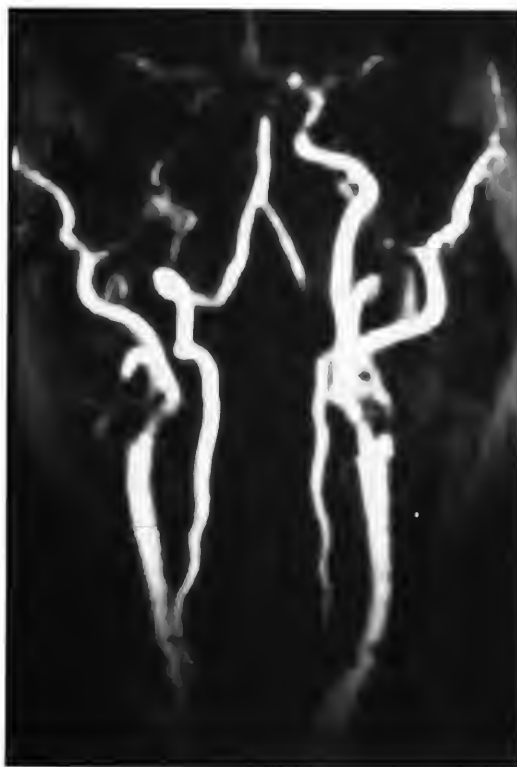
Fig. 67. Coronal triggered 2D TOF-MRA through the carotids and bifurcation.

the carotid vessels can sometimes be adequately visualized using conventional 3D coherent GRE T2* sequences in conjunction with GMN, although the resolution is not as good as in conventional MRA imaging. In addition, when used in conjunction with SE sequences, spatial pre-saturation pulses produce black blood. If signal persists in a vessel it may indicate either slow flow or occlusion. When used in conjunction with GRE sequences, GMN produces bright blood. If a signal void is seen within the vessel, it may indicate either slow flow or occlusion.

Image optimization

Technical issues

The quality of MRA images depends on a variety of factors. Firstly, the type of sequence used is important. Most examinations require both TOF and 3D PC sequences to adequately visualize all the cerebral vasculature. TOF-MRA is beneficial when imaging flow that moves perpendicular to the slice plane. Therefore it should be reserved for the circle of Willis and peripheral intracranial vessels. 3D TOF-MRA can result in a loss of signal from nuclei becoming saturated within the slice stack, and is mainly valuable on faster arterial flow unless ramped flip angles are available.

Spatial pre-saturation pulses are carefully placed so as to only saturate unwanted flow. The use of GMN and MT in TOF-MRA sequences improves image contrast by increasing the signal within vessels (GMN), and suppressing background signal (MT) (see *Pulse sequences* in Part 1). Scan times are lengthy especially in PC-MRA where the scan time is dependent (among other things) on the number of flow encoding axes implemented. Image quality also depends on the accurate setting of flow encoding axis and VENCs. Fast 2D images acquired before the 3D acquisition often help to determine the direction and speed of flow.

Artefact problems

In TOF-MRA, signal from the fatty components of the orbit and the scalp are commonly not saturated adequately and therefore interfere with the image. This is due to the short recovery times of these tissues. Chemical/spectral pre-saturation often successfully reduces this unwanted signal, but on some systems may also saturate the vessels. Alternatively, using a TE when the fat and water signals are out of phase with each other and applying MT usually adequately suppresses background signal. Motion artefact is sometimes troublesome especially on 3D PC-MRA images as their acquisition times are very long, and any motion of flowing nuclei within the vessels produces signal.

Patient considerations

Some of these patients may be incapacitated by their illness especially if this involves tumours, AVM or stroke. A careful explanation of the examination

Fig. 68. Coronal contrast enhanced MRA of the great vessels and neck.

and the approximate length of the study is required. In brain imaging, claustrophobia is sometimes troublesome due to the enclosing nature of the head coil. Ensure that the coil mirror is adjusted and that the patient is provided with an alarm bell.

Due to excessively loud gradient noise associated with some sequences, ear plugs must always be provided to prevent hearing impairment.

Contrast usage

Due to the inherent contrast between vessels and background tissue, these examinations do not usually require IV contrast. However, the use of contrast increases vessel conspicuity as it shortens the T1 of blood, increases vessel signal and improves image contrast in TOF-MRA sequences (Fig. 68).

Further reading

Kim O.H. & Suh J.H. (1997) Intracranial and extracranial MR angiography in Menkes' disease. *Pediatric Radiology*, **27**(10), 782–4.

Mascalchi M., Bianchi M.C., Mangiafico S. *et al.* (1997) MRI and MR angiography of vertebral artery dissection. *Neuroradiology*, **39**(5), 329–40.

Naganawa S., Ito T., Shimada H. *et al.* (1997) Cerebral black blood MR angiography with the interleaved multi-slab three-dimensional fast spin echo sequence. *Radiation Medicine*, **15**(6), 385–8.

Nesbit G.M. & DeMarco J.K. (1997) 2D time-of-flight MR angiography using concatenated saturation bands for determining direction of flow in the intracranial vessels. *Neuroradiology*, **39**(7), 461–8.

Okamoto K., Ito J., Furusawa T., Sakai K. & Tokiguchi S. (1997) 'Pseudoocclusion' of the internal carotid artery: a pitfall on intracranial MRA. *Journal of Computer Assisted Tomography*, **21**(5), 831–3.

Pant B., Sumida M., Kurisu K. *et al.* (1997) Usefulness of two-dimensional time-of-flight MR angiography combined with surface anatomy scanning for convexity lesions. *Neurosurgery Review*, **20**(2), 108–13.

Reichenbach J.R., Venkatesan R., Schillinger D.J., Kido D.K. & Haacke E.M. (1997) Small vessels in the human brain: MR venography with deoxyhemoglobin as an intrinsic contrast agent. *Radiology*, **204**(1), 272–7.

Rubinstein D., Sandberg E.J., Breeze R.E. *et al.* (1997) T2-weighted three-dimensional turbo spin-echo MR of intracranial aneurysms. *American Journal of Neuroradiology*, **18**(10), 1939–43.

Sengar A.R., Gupta R.K., Dhanuka A.K., Roy R. & Das K. (1997) MR imaging, MR angiography, and MR spectroscopy of the brain in eclampsia. *American Journal of Neuroradiology*, **18**(8), 1485–90.

Van Hemert R.L. (1997) MRA of cranial tumors and vascular compressive lesions. *Clinical Neuroscience*, **4**(3), 146–52.

Yamada K., Naruse S., Nakajima K. *et al.* (1997) Flow velocity of the cortical vein and its effect on functional brain MRI at 1.5T: preliminary results by cine-MR venography. *Journal of Magnetic Resonance Imaging*, **7**(2), 347–52.

Yano T., Kodama T., Suzuki Y. & Watanabe K. (1997) Gadolinium-enhanced 3D time-of-flight MR angiography. Experimental and clinical evaluation. *Acta Radiologica*, **38**(1), 47–54.

SPINE

Cervical spine
Thoracic spine
Lumbar spine
Whole spine imaging

Summary of parameters. The figures given are general and should be adjusted according to the system used.

Spin echo (SE)				Coherent GRE		
0.2 T to 0.5 T	short TE	min–30 ms			long TE	15 ms+
	long TE	70 ms+			short TR	<50 ms
	short TR	250–500 ms			low flip	5°–20°
	long TR	2000 ms+			medium flip	20°–40°
					high flip	60°+
1 T to 1.5 T	short TE	min–20 ms		**Incoherent GRE**		
	long TE	70 ms+			short TE	min–5 ms
	short TR	300–600 ms			short TR	<50 ms
	long TR	2000 ms+			medium flip	20°–40°
					high flip	60°+

Fast spin echo (FSE)				Inversion recovery (IR)		
	short TE	min–20 ms			short TE	min–20 ms
	long TE	90 ms+			long TE	60 ms+
	short TR	400–600 ms			short TR	1800 ms
	long TR	4000 ms+			long TR	6000 ms+
	short ETL	2–6			short TI	100–175 ms
	long ETL	16+			medium TI	200–600 ms
					long TI	1700–2200 ms

Slice thickness				Slice numbers		
2D	thin	2.5–4 mm		Volumes	small	<32
	medium	5–6 mm			medium	64
	thick	8 mm+			large	128+
3D	thin	<1 mm		**Matrix**		
	thick	>3 mm			coarse	256 × 128
					medium	256 × 192
					fine	256 × 256
					very fine	512 × 256

133

Summary of parameters   *Continued*

FOV			PC-MRA			
	small	<18 cm	2D and 3D		TE	min
	medium	20–26 cm			TR	25–33 ms
	large	30 cm+			flip	30°
					VENC venous	20–40 cm/s
					VENC arterial	60 cm/s
NEX/NSA			**TOF-MRA**			
	short	1 or less	2D		TE	min
	medium	2–3			TR	28–45 ms
	multiple	4+			flip	40°–60°
			3D		TE	min
					TR	25–50 ms
					flip	20°–30°

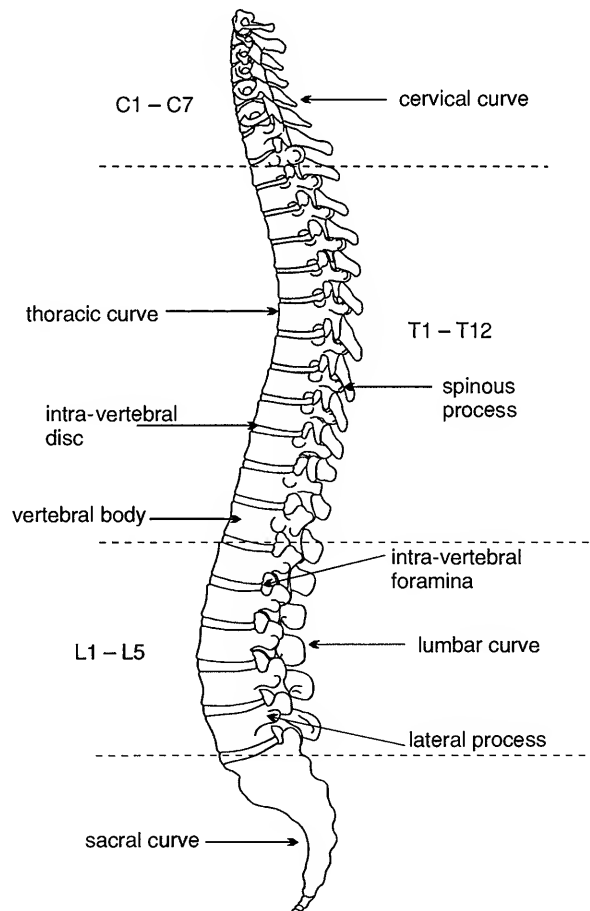# Basic anatomy (Figs 69 and 70)

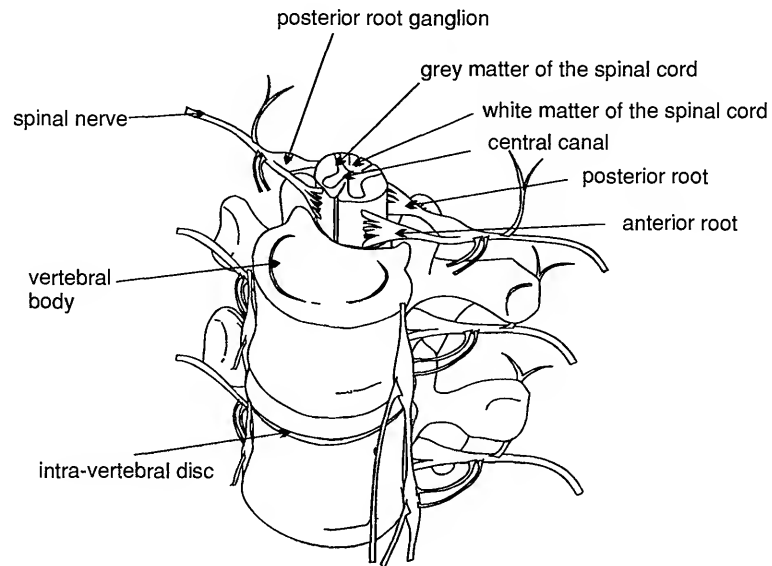**Fig. 69.** Sagittal view of the spine showing vertebral levels

Fig. 70. The components of the spine and spinal cord.

Cervical spine

Common indications

- Cervical myelopathy.
- Cervical radiculopathy.
- Cervical cord compression or trauma.
- Assessment of extent of spinal infection or tumour.
- Diagnosis of Chiari malformation and cervical syrinx. (Total extent of syrinx must be determined. Whole spine imaging may be necessary.)
- MS plaques within the cord.

Equipment

- Posterior cervical neck coil/volume neck coil/phased array spinal coil.
- Immobilization pads and straps.
- Pe gating leads if required.
- Ear plugs.

Patient positioning

The patient lies supine on the examination couch with the neck coil placed under or around the cervical region. Coils are often moulded to fit the back of the head and neck so that the patient is automatically centred to the coil. If a flat coil is used, placing supporting pads under the shoulders flattens the curve of the cervical spine so that it is in closer proximity to the coil. The coil should extend from the base of the skull to the sternoclavicular joints in order to include the whole of the cervical spine.

The patient is positioned so that the longitudinal alignment light lies in the midline, and the horizontal alignment light passes through the level of the hyoid bone (this can usually be felt above the thyroid cartilage/Adam's apple). The patient's head is immobilized with foam pads and retention straps. Pe gating leads are attached if required.

Suggested protocol

*Sagittal/coronal SE/FSE T1 or coherent GRE T2**

Acts as a localizer if three-plane localization is unavailable. The coronal or sagittal planes may be used (see *Localizers* in the section *How to use this book*).

Coronal localizer: Medium slices/gap are prescribed relative to the vertical alignment light, from the posterior aspect of the spinous processes to the anterior border of the vertebral bodies. The area from the base of the skull to the second thoracic vertebra is included in the image.

<div align="right">

P 20 mm to A 30 mm

</div>

Sagittal localizer: Medium slice thickness/gap are prescribed on either side of the longitudinal alignment light, from the left to the right lateral borders of the vertebral bodies. The area from the base of the skull to the second thoracic vertebra is included in the image.

<div align="right">

L 7 mm to R 7 mm

</div>

Sagittal SE/FSE T1 (Fig. 71)

Thin slices/gap are prescribed on either side of the longitudinal alignment light, from the left to the right lateral borders of the vertebral bodies (unless the paravertebral areas are required). The area from the base of the skull to the second thoracic vertebra is included in the image.

<div align="right">

L 22 mm to R 22 mm

</div>

*Sagittal SE/FSE T2 or coherent GRE T2** (Fig. 72)

Slice prescription as for Sagittal T1.

*Axial/oblique SE/FSE T1/T2 or coherent GRE T2** (Fig. 75)

Thin slices/gap are angled so that they are parallel to the disc space or perpendicular to the lesion under examination (Figs 73 and 74). For disc disease, three or four slices per level usually suffice. For larger lesions such as tumour or syrinx, thicker slices covering the lesion and a small area above and below may be necessary.

Additional sequences

Sagittal/axial oblique SE/FSE T1

Slice prescription as for Axial/oblique T2* with contrast enhancement for tumours.

Sagittal SE/FSE T2 or STIR

Slice prescription as for Sagittal T2*.
  An alternative to coherent GRE T2*.

Fig. 71. Sagittal SE T1 weighted midline image through the cervical spine showing an atrophied cord at the thoraco-cervical junction.

Fig. 72. Sagittal FSE T2 weighted midline image through the cervical cord. Small protruding discs are clearly seen at C4/5 and C5/6.
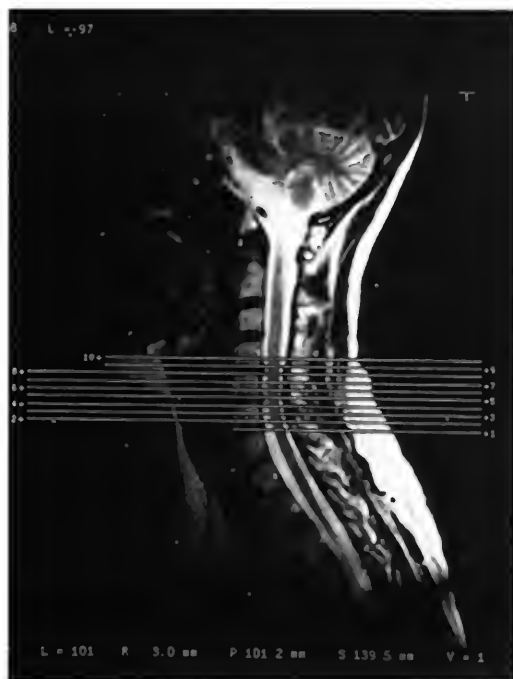

Fig. 73. Sagittal FSE T2 weighted image showing slice prescription boundaries and orientation for axial imaging of the cervical cord.
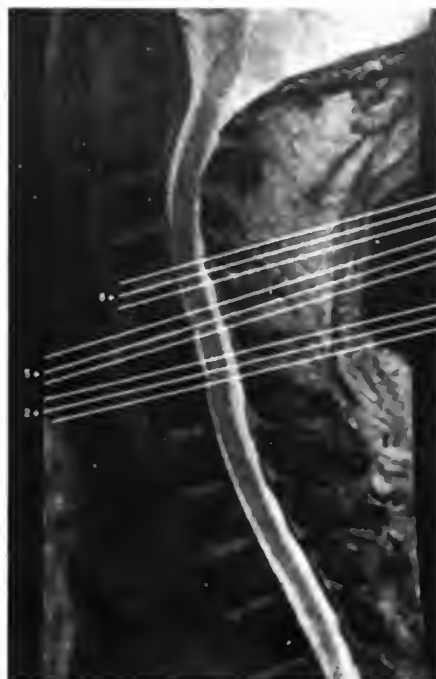

Fig. 74. Sagittal coherent GRE T2* weighted image of the cervical spine showing axial/oblique slice positions parallel to each disc space.
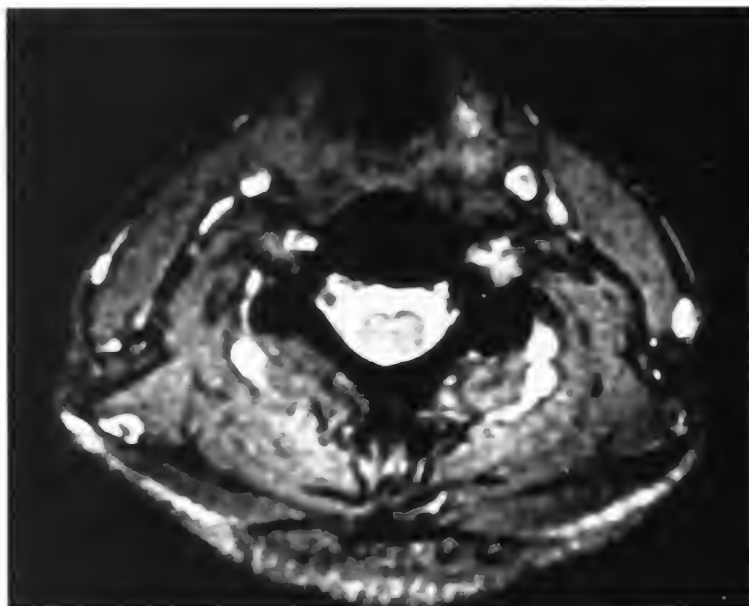
Fig. 75.   Axial/oblique coherent GRE T2* weighted image through the cervical cord.

3D coherent/incoherent (spoiled) GRE T2*/T1

Thin slices and a few or medium number of slice locations are prescribed through the ROI. If PD or T2* weighting is desired, then a coherent or steady-state sequence is utilized. If T1 weighting is required an incoherent or spoiled sequence is necessary. These sequences may be acquired in any plane but, if reformatting is required, isotropic datasets must be acquired.

Sagittal SE/FSE T1 or fast incoherent (spoiled) GRE T1/PD

Slice prescription as for Sagittal T1, T2 and T2*,
except   neck in flexion and extension to correlate the potential relevance of spondylitic changes to signs and symptoms.

Image optimization

Technical issues

The SNR in this region is mainly dependent on the quality of the coil. Posterior neck coils give adequate signal for the cervical spine and cord, but signal usually falls off at the anterior part of the neck, so they are not recommended for imaging structures such as the thyroid or larynx. In addition, flare from the posterior skin surface can be troublesome in sagittal T1 imaging, where the large fat pad situated at the back of the neck returns a high signal. Volume coils produce even distribution

of signal, but the SNR in the cord is sometimes reduced compared to a posterior neck coil. Phased array coils commonly produce optimum SNR, and may be used with a large FOV to include the thoracic spine. This strategy is important when pathology extends from the cervical to the thoracic areas of the cord, e.g. syrinx.

Spatial resolution is also important, especially in axial/oblique imaging, as the nerve roots in the cervical region are notoriously difficult to visualize. Thin slices with a small gap and relatively fine matrices are employed to maintain spatial resolution. Multiple NEX/NSA are also advisable if the inherent SNR is poor. Therefore, unless FSE is utilized, scan times are often of several minutes duration.

Fortunately, a rectangular/asymmetric FOV is used very effectively in sagittal imaging as the cervical spine fits into a rectangle with its longitudinal axis running S to I. This facilitates the acquisition of fine matrices in short scan times. With a reduced FOV in the phase direction, aliasing may be a problem. In sagittal imaging, this artefact originates from the chin and the back of the head wrapping into the FOV. Increasing the size of the overall FOV or utilizing oversampling (if available) may eliminate or reduce this artefact. In addition, spatial pre-saturation pulses brought into the FOV to nullify signal coming from these structures are effective (see *Flow phenomena and artefacts* in Part 1).

The multiple 180° RF pulses used in FSE sequences cause lengthening of the T2 decay time of fat so that the signal intensity of fat on T2 weighted FSE images is higher than in CSE. This sometimes makes the detection of marrow abnormalities difficult. Therefore, when imaging the vertebral bodies for metastatic disease, a STIR sequence should be utilized (see *Pulse sequences* in Part 1).

Artefact problems

The cervical area is often plagued with artefact. Not only does aliasing from structures outside the FOV obscure the image, but the periodic, pulsatile, motion of CSF within the spinal canal produces phase ghosting. The speed of flow is usually quite rapid in the cervical region, and therefore conventional flow-reducing measures, such as spatial pre-saturation and GMN, are less effective than in the lumbar region where CSF flow is slower. On T1 weighted images, spatial pre-saturation pulses placed S and I to the FOV are usually sufficient. However, on T2 weighted sequences flow artefact is commonly troublesome. In addition, selecting a S–I phase direction along with oversampling can also reduce CSF flow in sagittal imaging.

As FSE sometimes demonstrates more flow artefact than CSE, it is usually not utilized in the cervical spine. This is especially true on T2 weighted images where flow artefact can totally degrade the image. However, in cases where there is severe pathology such as a disc protrusion, FSE often produces images that demonstrate acceptable levels of artefact. This may be because the protruding disc locally slows down the CSF flow. In practice, it is probably worth trying FSE on the T2 images, and only if the artefact is intolerable, repeat the scan using coherent GRE. However, FSE is not commonly recommended in axial/oblique imaging because of

flow-related problems. When using coherent GRE T2* sequences, GMN should be implemented as this not only increases the signal from CSF, but also reduces artefact from CSF flowing down the canal within the slice. Pe gating minimizes artefact even further but, as the scan time is dependent on the patient's heart rate, it is sometimes rather time-consuming. The implementation of Pe gating is therefore best reserved for cases of severe flow artefact that cannot be reduced to tolerable levels by other measures.

Multiple NEX/NSA reduce artefact from signal averaging, but result in an increase in the scan time. Nevertheless their implementation is often necessary, especially where the SNR is poor, and flow artefact severe. Swallowing during data acquisition is a common source of artefact. Spatial pre-saturation pulses placed over the throat largely eliminate this, but care must be taken not to nullify signal from important anatomy. Another problem in the cervical region is truncation artefact (or Gibbs artefact) that produces a thin line of low signal in the cord and mimics a syrinx. Truncation artefact is reduced by selecting a higher phase matrix (see *Flow phenomena and artefacts* in Part 1).

Patient considerations

Some patients have difficulty placing their neck over the posterior neck coil, especially in cases of fixed deformity. It is important that the neck is as close to the coil as possible to achieve maximum SNR. Placing pads under the patient's shoulders flattens the spine, and therefore positions the back of the neck nearer to the coil. Patients with cervical cord trauma, cord compression, or tumours are often severely disabled. The magnetic safety of any stabilization devices should be established before the examination. Great care must be taken when transferring these patients onto the examination couch, and they should be moved as little as possible.

Due to excessively loud gradient noise associated with some sequences, ear plugs must always be provided to prevent hearing impairment.

Contrast usage

Contrast is not routinely given for disc disease. However, in cases of leptomeningeal spread of certain tumours such as medulloblastoma, contrast is invaluable. Other cord lesions such as ependymomas and pinealoblastomas also enhance well with contrast, as do infectious processes and active MS plaques. Bony tumours, especially those that return a low signal on T1 weighted images, enhance with contrast but this often increases their signal intensity so that they are isointense with the surrounding vertebra. Under these circumstances, chemical/spectral pre-saturation or the Dixon technique should be implemented to reduce the signal from fatty marrow in the vertebral bodies. Inversion recovery sequences that suppress fat (STIR) should not be used in conjunction with contrast, as their inverting pulses may nullify the signal from the tumour that, as a result of contrast enhancement, now has a similar T1 recovery time to fat.

Further reading

Benzel E.C., Hart B.L., Ball P.A., Baldwin N.G., Orrison W.W. & Espinosa M.C. (1996) Magnetic resonance imaging for the evaluation of patients with occult cervical spine injury. *Journal of Neurosurgery*, **85**(5), 824–9.

Gillams A.R., Soto J.A. & Carter A.P. (1997) Fast spin echo vs conventional spin echo in cervical spine imaging. *European Radiology*, **7**(8), 1211–14.

Melhem E.R., Benson M.L., Beauchamp N.J. & Lee R.R. (1996) Cervical spondylosis: three-dimensional gradient-echo MR with magnetization transfer. *American Journal of Neuroradiology*, **17**(4), 705–11.

Melhem E.R., Jara H., Shakir H. & Gagliano T.A. (1997) Fast inversion-recovery MR: the effect of hybrid RARE readout on the null points of fat and cerebrospinal fluid. *American Journal of Neuroradiology*, **18**(9), 1627–33.

Moulopoulos L.A., Kumar A.J. & Leeds N.E. (1997) A second look at unenhanced spinal magnetic resonance imaging of malignant leptomeningeal disease. *Clinical Imaging*, **21**(4), 252–9.

Quencer R.M., Nunez D. & Green B.A. (1997) Controversies in imaging acute cervical spine trauma. *American Journal of Neuroradiology*, **18**(10), 1866–8.

Swainson C.J., Hutchinson C.E. & Watson Y.A. (1997) Comparison of 2-D and 3-D FSE imaging in MR of the cervical spine. *Clinical Radiology*, **52**(3), 194–7.

Terae S., Takahashi C., Abe S., Kikuchi Y. & Miyasaka K. (1997) Gd-DTPA-enhanced MR imaging of injured spinal cord. *Clinical Imaging*, **21**(2), 82–9.

Wu W., Thuomas K.A., Hedlund R., Leszniewski W. & Vavruch L. (1996) Fast spin-echo MR assessment of patients with poor outcome following spinal cervical surgery. *Acta Radiologica*, **37**(2), 153–61.

Yoshioka H., Onaya H., Itai Y. *et al.* (1997) Comparison between magnetization transfer contrast and fast spin-echo MR imaging of degenerative disease of the cervical spine at 0.3 T. *Magnetic Resonance Imaging*, **15**(1), 37–45.

Thoracic spine

Common indications

- Thoracic disc disease.
- Thoracic cord compression.
- Visualization of a MS plaque in the thoracic cord.
- Thoracic cord tumour.
- To visualize the inferior extent of cervical syrinx.

Equipment

- Posterior spinal coil/phased array spinal coil.
- Pe gating leads if required.
- Ear plugs.

Patient positioning

The patient lies supine on the examination couch with the spinal coil extending from the top of the shoulders to the lower costal margin to ensure total coverage of the thoracic spine and conus. The patient is positioned so that the longitudinal alignment light lies in the midline, and the horizontal alignment light passes through the centre of the coil, which corresponds approximately to the level of the fourth thoracic vertebra. Pe gating leads are attached if required.

Suggested protocol

Sagittal/coronal SE/FSE T1 or coherent GRE T2*

Acts as a localizer if three-plane localization is unavailable. The coronal or sagittal planes may be used (see *Localizers* in the section *How to use this book*).

Coronal localizer: Medium slices/gap are prescribed relative to the vertical alignment light, from the posterior aspect of the spinous processes to the anterior border of the vertebral bodies. The area from the seventh cervical vertebra to the conus is included in the image.

P 40 mm to A 30 mm

143

Sagittal localizer: Medium slices/gap are prescribed on either side of the longitudinal alignment light, from the left to the right lateral borders of the vertebral bodies. The area from the seventh cervical vertebra to the conus is included in the image

L 7 mm to R 7 mm

It is often difficult to ascertain the exact level of the cervico-thoracic junction if there are no visible landmarks. This problem is overcome on sagittal localizers by offsetting the FOV S 100 mm and increasing its size to include from the base of the skull to the conus. As the first cervical vertebra is visualized, the offset enables accurate assessment of the vertebral levels and easy placement of spatial pre-saturation pulses for the following series. The body coil can be used for this localizer as long as a receive-only spinal coil is implemented, and interference from the spinal coil is usually well demonstrated so that its correct placement can be confirmed. The patient is then offset back to isocentre for the subsequent series.

Sagittal SE/FSE T1 (Fig. 76)

Thin slices/gap are prescribed on either side of the longitudinal alignment light, from the left to the right lateral borders of the vertebral bodies (unless the paravertebral areas are required). The area from the seventh cervical vertebra to the conus is included in the image.

L 22 mm to R 22 mm

Sagittal SE/FSE T2 or coherent GRE T2* (Fig. 77)

Slice prescription as for Sagittal T1.

Axial/oblique SE/FSE T1 or coherent gradient echo T2* (Fig. 79)

Thin slices/gap are angled so that they are parallel to the disc space or perpendicular to the lesion under examination (Fig. 78). For disc disease, three or four slices per level usually suffice. For larger lesions such as tumour or syrinx, thicker slices covering the lesion and a small area above and below are necessary.

Additional sequences

Sagittal/axial/oblique SE/FSE T1 +/- contrast

For evaluating the conus and other cord lesions.

Fig. 76.   Sagittal FSE T1 weighted midline slice through the thoracic spine. Note the expansion of the conus by an ependymoma.

Image optimization

Technical issues

The SNR in this region is mainly dependent on the quality of the coil. Flare from the posterior skin surface may be troublesome, especially in sagittal T1 imaging where the fatty tissues posterior to the thoracic spine return a high signal. In addition, there is signal fall-off from the anterior part of the chest due to its distance from the posteriorly situated coil. For this reason the posterior spinal coil is not utilized to image the thorax, unless the patient is a very small child. Phased array coils are useful to image the whole of the cervical and thoracic cord whilst maintaining optimum SNR and resolution.

Fig. 77. Sagittal FSE T2 weighted midline slice through the thoracic cord demonstrating the same pathology as Fig. 76.

Spatial resolution is important especially in axial/oblique images, as the nerve roots in the thoracic region are commonly difficult to visualize. Thin slices with a small gap and relatively fine matrices are implemented to maintain spatial resolution. Multiple NEX/NSA are also advisable if the inherent SNR is poor. Therefore, unless FSE is utilized, scan times are usually of several minutes duration.

Fortunately, a rectangular/asymmetric FOV is used very effectively in sagittal imaging as the thoracic spine fits into a rectangle with its longitudinal axis running S to I. This facilitates the acquisition of fine matrices in short scan times. With a reduced FOV in the phase direction, aliasing may be a problem. In sagittal imaging, this artefact originates from the anterior chest wrapping into the FOV. Increasing the size of the overall FOV or utilizing oversampling (if available) may eliminate or reduce this artefact. In addition, spatial pre-saturation pulses brought into the FOV
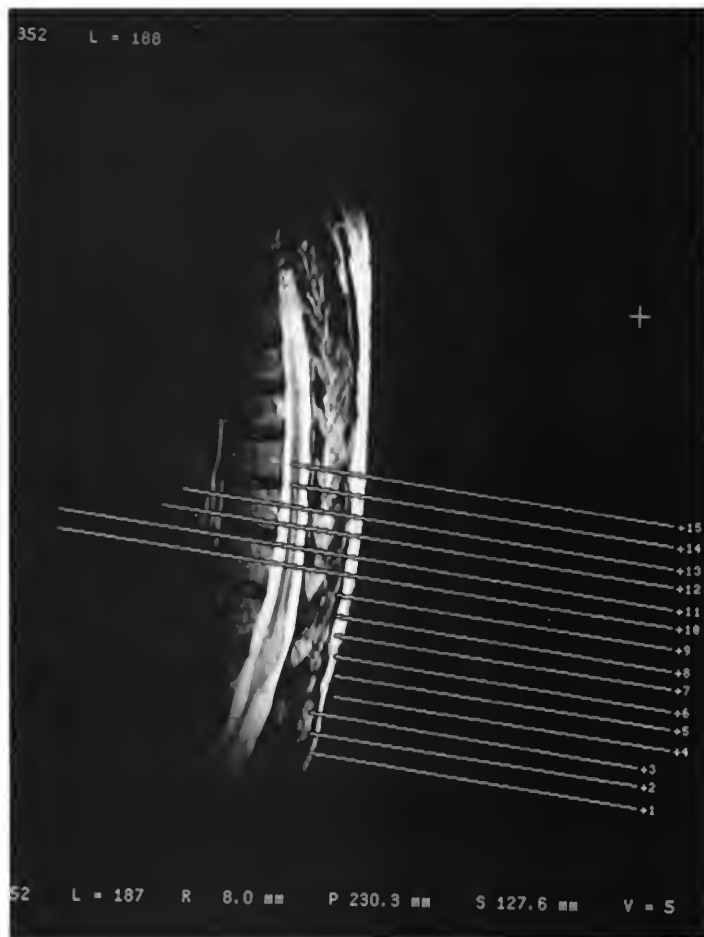
Fig. 78. Sagittal FSE T2 weighted midline slice through the thoracic spine showing slice prescription boundaries and orientation for axial imaging of the conus.

are effective (see *Flow phenomena and artefacts* in Part 1). In practice, as a fairly large FOV is used to image the thoracic spine and there is signal fall-off in the anterior part of the chest, aliasing is not usually troublesome.

The multiple 180° RF pulses used in FSE sequences cause lengthening of the T2 decay time of fat so that the signal intensity of fat on T2 weighted FSE images is higher than in CSE. This sometimes makes the detection of marrow abnormalities difficult. Therefore, when imaging the vertebral bodies for metastatic disease, a STIR sequence should be utilized.

Artefact problems

Flow from CSF pulsations commonly causes severe phase ghosting in the thoracic region, although the speed of flow is often less than in the cervical area. Spatial pre-
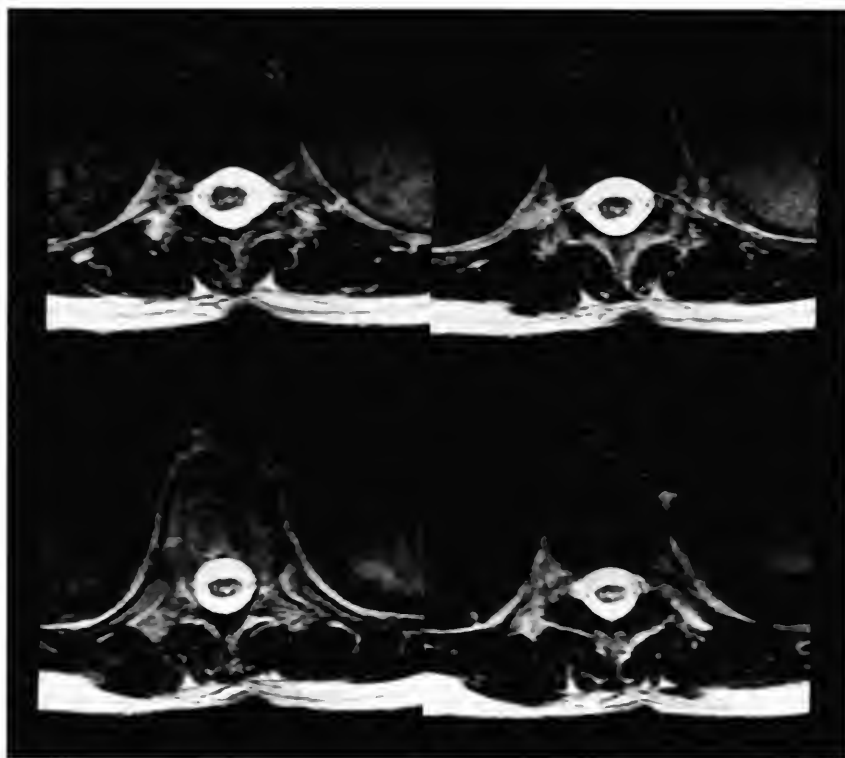
Fig. 79. Axial/oblique FSE T2 weighted images through the thoracic cord.

saturation pulses placed S and I to the FOV are necessary to reduce these flow-related problems. GMN also minimizes flow artefact but, as it increases the signal from CSF and the minimum TE available, it is usually reserved for T2 and T2* weighted sequences. FSE is commonly utilized in this area as the associated scan time reduction enables the implementation of very fine matrices. However, this sequence often demonstrates increased flow artefact compared to SE and GRE sequences. Therefore, if flow artefact is too troublesome, SE or GRE may be substituted.

Phase ghosting from cardiac and respiratory motion is the main source of artefact in the thoracic region. Spatial pre-saturation pulses brought into the FOV and placed over the heart and lung fields are very effective at reducing this. Pe gating minimizes artefact even further but, as the scan time is dependent on the patient's heart rate, it is sometimes time-consuming. The implementation of Pe gating is therefore best reserved for cases of severe flow artefact that cannot be reduced to tolerable levels by other measures.

In sagittal imaging, swapping the phase axis so that it runs from S to I instead of A to P removes the artefact from the cord. However, if there is significant kyphosis, the artefact may still obscure the cervical and lumbar regions. In addition, if a rectangular/asymmetric FOV is implemented, swapping the phase axis

places the longitudinal axis of the rectangle horizontally so that its benefits cannot be utilized. On newer systems it is possible to use curved spatial pre-saturation pulses so that accurate placement of bands over the thoracic aorta is possible.

Due to the implementation of a small FOV in axial/oblique imaging, aliasing commonly occurs and therefore oversampling is necessary. In addition, phase artefact from movement of the lateral walls of the chest during respiration, and some vessel pulsation, often interferes with the images. Careful placement of spatial pre-saturation pulses A, R, and L of the FOV is usually effective at reducing this. RC is rarely necessary in the thoracic spine because the posteriorly situated spinal coil causes signal fall-off from the anterior chest wall, and therefore respiratory artefact is usually less troublesome than when imaging the whole chest in the body coil. Movement of the diaphragm is more significant, however, and RC may be considered if this is a particular problem.

Patient considerations

Patients with cord trauma may be severely disabled and in great pain. The examination should obviously be undertaken as speedily as possible under these circumstances.

Due to excessively loud gradient noise associated with some sequences, ear plugs must always be provided to prevent hearing impairment.

Contrast usage

Contrast is not routinely given for disc disease. However, in cases of leptomeningeal spread of certain tumours such as medulloblastoma, contrast is invaluable. Other cord lesions such as ependymomas and pinealoblastomas also enhance well with contrast, as do infectious processes and active MS plaques. Bony tumours, especially those that return a low signal on T1 weighted images, enhance with contrast but this often increases their signal intensity so that they are isointense with the surrounding vertebra. Under these circumstances, chemical/spectral presaturation or the Dixon technique should be implemented to reduce the signal from fatty marrow in the vertebral bodies. STIR should not be used in conjunction with contrast, as its inverting pulse may nullify the signal from the tumour that, as a result of contrast enhancement, now has a similar T1 recovery time to fat.

Further reading

Falbo S.E., Martin D.S., Mitchell H.L. & Sundaram M. (1997) Radiologic case study. Symptomatic, calcified extruded disk of the thoracic spine. *Orthopedics*, **20**(1), 84–6.

Hirabayashi Y., Saitoh K., Fukuda H., Igarashi T., Shimizu R. & Seo N. (1997) Magnetic resonance imaging of the extradural space of the thoracic spine. *British Journal of*

SPINE

Anaesthesia, **79**(5), 563–6.

Hochstenbag M.M., Snoep G., Cobben N.A. *et al.* (1996) Detection of bone marrow metastases in small cell lung cancer. Comparison of magnetic resonance imaging with standard methods. *European Journal of Cancer*, **32A**(5), 779–82.

Jinkins J.R., Bazan C. 3rd & Xiong L. (1996) MR of disc protrusion engendered by infectious spondylitis. *Journal of Computer Assisted Tomography*, **20**(5), 715–18.

Moulopoulos L.A., Kumar A.J. & Leeds N.E. (1997) A second look at unenhanced spinal magnetic resonance imaging of malignant leptomeningeal disease. *Clinical Imaging*, **21**(4), 252–9.

Stabler A., Bellan M., Weiss M., Gartner C., Brossmann J. & Reiser M.F. (1997) MR imaging of enhancing intraosseous disk herniation (Schmorl's nodes). *American Journal of Roentgenology*, **168**(4), 933–8.

Wiltse L.L., Berger P.E. & McCulloch J.A. (1997) A system for reporting the size and location of lesions in the spine. *Spine*, **22**(13), 1534–7.

Wolfla C.E., Azzarelli B. & Shah M.V. (1997) Primary extramedullary ependymoma of the thoracic spine. Case illustration. *Journal of Neurosurgery*, **87**(4), 643.

Lumbar spine

Common indications

- Disc prolapse with cord or nerve root compression.
- Spinal dysraphism (to assess cord termination, syrinx, diastematomyelia).
- Discitis.
- Evaluation of the conus in patients with appropriate symptoms.
- Failed back syndrome.
- Arachnoiditis.

Equipment

- Posterior spinal coil/phased array spinal coil.
- Foam pads to elevate the knees.
- Ear plugs.

Patient positioning

The patient lies supine on the examination couch with their knees elevated over a foam pad, for comfort and to flatten the lumbar curve so that the spine lies nearer to the coil. The coil should extend from the xiphisternum to the bottom of the sacrum for adequate coverage of the lumbar region. The patient is positioned so that the longitudinal alignment light lies in the midline, and the horizontal alignment light passes just below the lower costal margin, which corresponds to the third lumbar vertebra.

Suggested protocol

Sagittal/coronal SE/FSE T1 or coherent GRE T2*

Acts as a localizer if three-plane localization is unavailable. The coronal or sagittal planes may be used (see *Localizers* in the section *How to use this book*).

Coronal localizer: Medium slices/gap are prescribed relative to the vertical alignment light, from the posterior aspect of the spinous processes to the anterior border of the vertebral bodies. The area from the conus to the sacrum is included in the image.

P 20 mm to A 30 mm

Sagittal localizer: Medium slices/gap are prescribed on either side of the longitudinal alignment light, from the left to the right lateral borders of the vertebral bodies. The area from the conus to the sacrum is included in the image.

L 7 mm to R 7 mm

Sagittal SE/FSE T1 (Fig. 80)

Thin slices/gap are prescribed on either side of the longitudinal alignment light, from the left to the right lateral borders of the vertebral bodies (unless the paravertebral region is required). The area from the conus to the sacrum is included in the image.

L 22 mm to R 22 mm

Fig. 80. Sagittal FSE T1 weighted midline slice through the lumbar spine showing normal appearances.

Sagittal SE/FSE T2 or coherent GRE T2* (Fig. 81)

Slice prescription as for Sagittal T1.

Axial/oblique SE/FSE T1/T2 or coherent GRE T2* (Fig. 83)

Thin slices/gap are angled so that they are parallel to each disc space and extend from the lamina below to the lamina above the disc. The lower three lumbar discs are commonly examined (Fig. 82).

Additional sequences

Axial/oblique or Sagittal SE/FSE T1

With contrast for determining disc prolapse versus scar tissue in failed back syndrome, and for some tumours. Without contrast in spinal dysraphism. Chemical/

Fig. 81. Sagittal FSE T2 weighted midline slice through the lumbar spine showing normal appearances.

Fig. 82.   Sagittal FSE T2 weighted midline slice showing slice prescription boundaries and orientation for axial/oblique imaging of lumbar discs.

spectral pre-saturation is beneficial to differentiate between fat and enhancing pathology.

Coronal SE/FSE T1

For cord tethering or alternative view of conus when sagittals are inconclusive.

Axial/oblique FSE T2

For arachnoiditis. As for Axial/obliques,

except   prescribe one slice through, and parallel to, each disc space and vertebral body from the sacrum to the conus (Fig. 84).
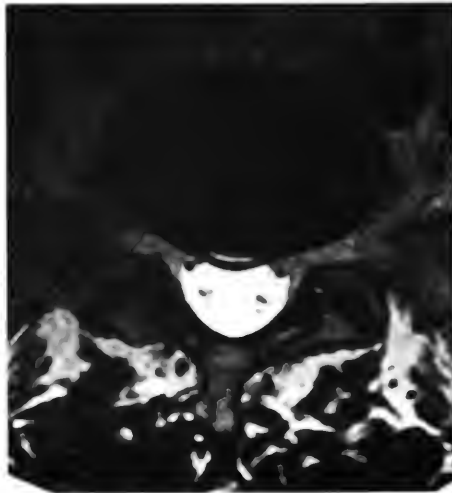
Fig. 83. Axial/oblique FSE T2 weighted high-resolution image of the lumbar spine showing a small central disc protrusion. The lumbar nerve roots are seen as small black dots surrounded by high-signal intensity CSF.

Fig. 84. Sagittal FSE T2 weighted image of the lumbar spine showing axial/oblique slice prescription for arachnoiditis.

Image optimization

Technical issues

The SNR in the lumbar region depends on the quality of the coil. Posterior spinal coils return high signal in the area of the lumbar canal and vertebral bodies, but flare from the fatty tissues in the buttocks sometimes interferes with the image. Phased array coils allow for imaging of the thoracic and lumbar spine in conjunction with good SNR and resolution. As CSF flow is reduced in this area, FSE is routinely used. This enables the implementation of very fine matrices so that spatial resolution is significantly increased. Resolution is also maintained by using rectangular/asymmetric FOV in sagittal imaging (with the long axis of the rectangle running from S to I), and a small FOV in axial/oblique imaging. Fine matrices are especially necessary in arachnoiditis to detect nerve root clumping.

Artefact problems

CSF pulsation is not usually troublesome as the speed of flow is relatively slow. However, phase artefact from the aorta and the inferior vena cava (IVC), and lateral flow from the lumbar vessels, sometimes obscures the lumbar canal. Spatial presaturation pulses brought into the FOV and placed S, I, and A in the sagittal images, and A, R, and L in the axial/oblique images, reduce phase ghosting. GMN minimizes flow artefact even further but, as it increases the signal in CSF and the

Fig. 85. Sagittal FSE T1 weighted images of the lumbar spine with phase A to P (left) and S to I (right). The definition of the spinal cord is clearly improved on the right-hand image.

minimum TE available, it is mainly reserved for the T2 and T2* weighted sequences.

Swapping the phase axis in sagittal imaging so that it runs from S to I instead of A to P is probably the best way of removing this artefact from the cord. However, a rectangular/asymmetric FOV cannot be used under these circumstances as the long axis of the rectangle is placed horizontally (Fig. 85). A compromise is to swap the phase axis and not use a rectangular/asymmetric FOV in the T1 sagittal image, and keep the phase axis AP and use a rectangular/asymmetric FOV in the T2 sagittal image.

With a reduced FOV in the phase direction, aliasing may be a problem. In sagittal imaging, this artefact originates from the buttocks and abdomen wrapping into the FOV (Fig. 86). Increasing the size of the overall FOV or utilizing oversampling (if available) may eliminate or reduce this artefact. If the phase axis is swapped, aliasing occurs as the areas superior and inferior to the coil are wrapped into the FOV and therefore oversampling is necessary to avoid this. In addition, due to the implementation of a small FOV in the axial/oblique imaging, aliasing commonly

Fig. 86. Sagittal FSE T2 weighted midline slice through the lumbar spine using rectangular/asymmetric FOV. Note phase aliasing from the buttocks (arrow).
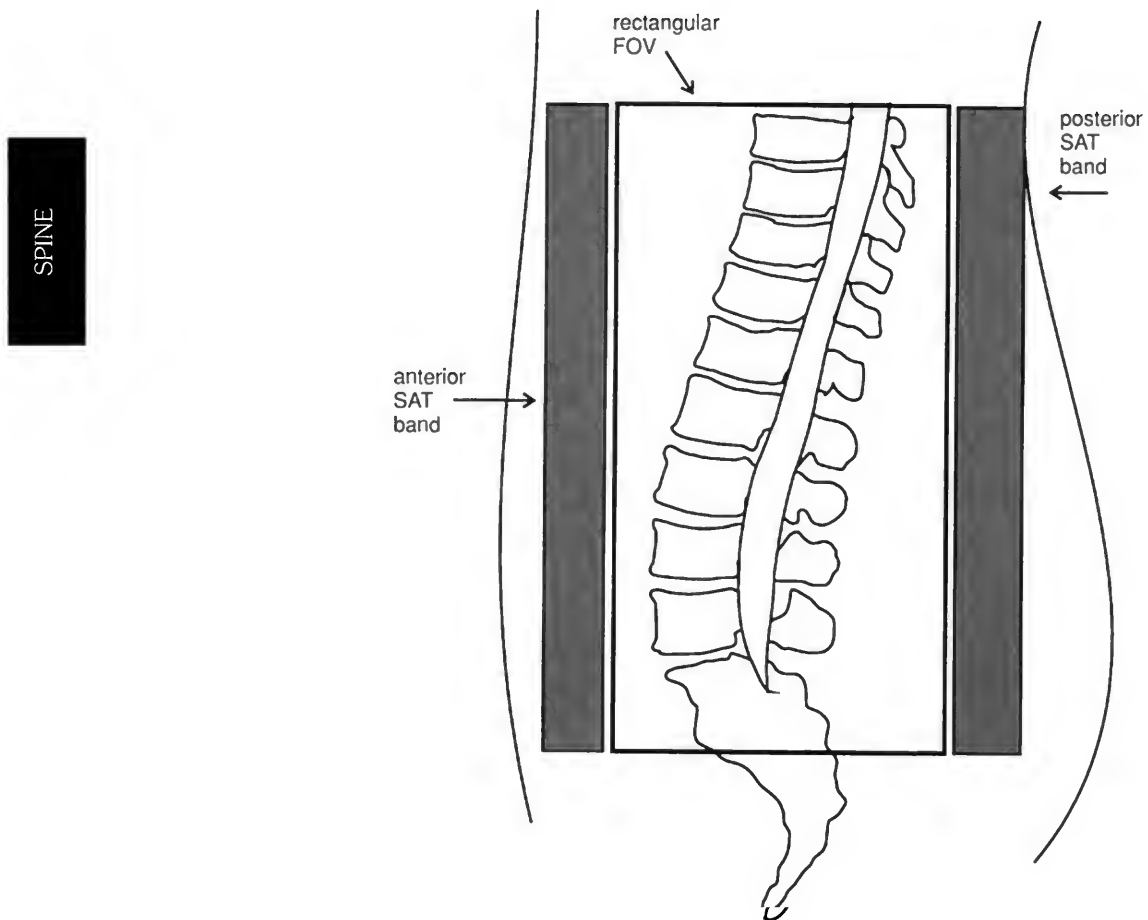
Fig. 87.   Correct placement of spatial pre-saturation bands when using rectangular/asymmetric FOV in the lumbar spine.

occurs and therefore oversampling is also required in this plane. Spatial pre-saturation pulses brought into the FOV are also effective (Fig. 87).

The multiple 180° RF pulses used in FSE sequences cause lengthening of the T2 decay time of fat so that the signal intensity of fat on T2 weighted FSE images is higher than in CSE. This sometimes makes the detection of marrow abnormalities difficult. Therefore, when imaging the vertebral bodies for metastatic disease, a STIR sequence should be utilized.

Patient considerations

Many patients are in severe pain especially if they are suffering from a prolapsed lumbar disc. Make the patient as comfortable as possible with pads supporting their

knees in a slightly flexed position. Small pads placed in the lumbar curve often help to alleviate sciatica and other types of back pain.

Due to excessively loud gradient noise associated with some sequences, ear plugs must always be provided to prevent hearing impairment.

Contrast usage

Contrast is used to distinguish disc prolapse from scar tissue post-operatively in failed back syndrome. These images are acquired with or without chemical/ spectral pre-saturation. STIR should not be used with contrast enhancement, as the contrast reduces the T1 value of damaged tissues so that it is similar to that of fat, and is therefore nullified by the inverting pulse. Scar tissue enhances immediately after the injection, but disc material does not. However, about 20–30 min after the injection, disc material also enhances and therefore scanning should not be delayed after the administration of contrast. In addition, the epidural veins and granulation tissue at the periphery of a disc and fibrosis may enhance. Contrast is also invaluable to visualize suspicious lesions in the conus.

Further reading

Eberhardt K.E., Hollenbach H.P., Tomandl B. & Huk W.J. (1997) Three-dimensional MR myelography of the lumbar spine: comparative case study to X-ray myelography. *European Radiology*, **7**(5), 737–42.

Grane P. (1998) The postoperative lumbar spine. A radiological investigation of the lumbar spine after discectomy using MR imaging and CT. *Acta Radiologica*, **414**(Supplement), 1–23.

Grane P. & Lindqvist M. (1997) Evaluation of the post-operative lumbar spine with MR imaging. The role of contrast enhancement and thickening in nerve roots. *Acta Radiologica*, **38**(6), 1035–42.

Grane P., Josephsson A., Seferlis A. & Tullberg T. (1998) Septic and aseptic post-operative discitis in the lumbar spine – evaluation by MR imaging. *Acta Radiologica*, **39**(2), 108–15.

Komori H., Okawa A., Haro H., Muneta T., Yamamoto H. & Shinomiya K. (1998) Contrast-enhanced magnetic resonance imaging in conservative management of lumbar disc herniation. *Spine*, **23**(1), 67–73.

McGregor A.H., McCarthy I.D., Dore C.J. & Hughes S.P. (1997) Quantitative assessment of the motion of the lumbar spine in the low back pain population and the effect of different spinal pathologies of this motion. *European Spine Journal*, **6**(5), 308–15.

Petersilge C.A., Lewin J.S., Duerk J.L., Yoo J.U. & Ghaneyem A.J. (1996) Optimizing imaging parameters for MR evaluation of the spine with titanium pedicle screws. *American Journal of Roentgenology*, **166**(5), 1213–18.

Rankine J.J., Hutchinson C.E. & Hughes D.G. (1997) MRI of lumbar spondylosis: a comparison of sagittal T2 weighted and three sequence examinations. *British Journal of Radiology*, **70**(839), 1112–21.

Robertson W.D., Jarvik J.G., Tsuruda J.S., Koepsell T.D. & Maravilla K.R. (1996) The comparison of a rapid screening MR protocol with a conventional MR protocol for lumbar spondylosis. *American Journal of Roentgenology*, **166**(4), 909–16.

Tyrrell P.N., Cassar-Pullicino V.N. & McCall I.W. (1998) Gadolinium-DTPA enhancement of symptomatic nerve roots in MRI of the lumbar spine. *European Radiology*, **8**(1), 116–22.

Wang J.C., Sandhu H.S., Yu W.D., Minchew J.T. & Delamarter R.B. (1997) MR parameters for imaging titanium spinal instrumentation. *Journal of Spinal Disorders*, **10**(1), 27–32.

Wilkinson L.S., Elson E., Saifuddin A. & Ransford A.O. (1997) Defining the use of gadolinium enhanced MRI in the assessment of the postoperative lumbar spine. *Clinical Radiology*, **52**(7), 530–34.

Wilmink J.T. & Hofman P.A. (1997) MRI of the postoperative lumbar spine: triple-dose gadodiamide and fat suppression. *Neuroradiology*, **39**(8), 589–92.

Whole spine imaging

Common indications

- Cord compression (level unknown), due to metastatic disease or primary cord tumour.
- Bone marrow screening.
- Congenital abnormalities of spinal curvature (scoliosis and kyphosis).
- Evaluation of the extent of a syrinx.
- Leptomeningeal disease.

Equipment

- Body coil/phased array spinal coil.
- Pe gating leads if required.
- Ear plugs.

Patient positioning

The patient lies supine on the examination couch. The patient is positioned so that the longitudinal alignment light lies in the midline, and the horizontal alignment light passes through a point midway between the sacrum and the base of the skull (which corresponds to about 2 cm below the sternal notch). Pe gating leads are attached if required.

Suggested protocol

Sagittal SE/FSE T1 (Fig. 88)

Thin slices/gap are prescribed on either side of the longitudinal alignment light, from the left to the right lateral borders of vertebral bodies (or prescribe graphically from a coronal localizer).

L 22 mm to R 22 mm

Include the entire canal from the base of the skull to below the sacrum and use the largest FOV available. Repeat the scan if an area is missed. If severe scoliosis is present, coronal images may be more beneficial than sagittals to assess the direction and extent of the curvature.

161

Sagittal SE/FSE T2 or coherent GRE T2* (Figs 89 and 90)

Slice prescription as for Sagittal T1.

Axial/oblique SE/FSE T1/T2

Thin slices/gap are prescribed through the ROI. Use a smaller local coil once the ROI has been established (not necessary with a phased array coil). In patients with severe spinal curvature, obliques may be performed to achieve orthogonal images.

Additional sequences

Sagittal SE/FSE T2 or STIR

For bone marrow screening include the sternum in the image and add coronals of the bony pelvis. Use chemical/spectral pre-saturation pulses in SE/FSE sequences.

Sagittal/oblique SE/FSE T1 (Fig. 91)

With contrast for tumour infection and leptomeningeal disease.

MR myelography/neurography

Examination of nerve roots and peripheral nerves with high-resolution imaging may prove to be useful additional techniques in the future.

Image optimization

Technical issues

These examinations are often carried out to establish the level and cause of a cord compression. Therefore, spatial resolution is not necessarily as important as a quick diagnosis. The level of the compression may be unknown, and therefore coverage of the whole spinal canal is the most important consideration. In the past this could only be achieved with the body coil, as surface coils did not cover the entire spine. However, phased array coils have now been introduced that give the benefits of maximum coverage and optimum SNR. If phased array coils are unavailable, the body coil is implemented. This results in a loss of overall SNR and poor local spatial resolution, as a large FOV is utilized to cover the whole spine. Once a level has been established, the body coil may be substituted for a surface coil and higher-quality images obtained. This strategy is unnecessary when using a phased array coil as the increase in SNR enables acquisition of images with adequate resolution. With both coil types, a rectangular/asymmetric FOV is used in the sagittal images to improve spatial resolution with the long axis of the rectangle S to I.

Fig. 88. Sagittal FSE T1 weighted image of the cervical and thoracic cord imaged using a phased array coil.

Fig. 89. Sagittal FSE T2 weighted image of the cervical and thoracic cord using a phased array coil.

Fig. 90. Sagittal FSE T2 weighted image of the thoraco-lumbar spine showing a large destructive lesion at the level of the conus.

Fig. 91. Sagittal FSE T1 weighted image with chemical/spectral pre-saturation and after contrast of the same lesion shown in Fig. 90.

Artefact problems

When imaging the entire spine with the body coil, artefacts are caused by CSF flow, heart and great vessel motion, and respiration. Spatial pre-saturation pulses placed S and I to the FOV reduce CSF artefact. They are often also placed over the heart and great vessels but can obscure some of the spine if there is spinal curvature. However, on newer systems it is possible to use curved spatial pre-saturation pulses that enable accurate placement of the bands over the aorta. Spatial pre-saturation pulses are commonly less effective over a large FOV and therefore phase ghosting may still be evident. In addition, if chemical/spectral pre-saturation is employed, it may be less effective than with a small FOV. This is because the energy of the pre-saturation pulse is now delivered to a greater volume of tissue, thereby reducing its effectiveness. Additional shimming may be required before chemical/spectral pre-saturation sequences.

GMN also minimizes flow artefact but, as it increases signal in CSF and the minimum TE available, it is usually only beneficial in T2 and T2* weighted sequences. Pe gating minimizes artefact even further but, as the scan time is dependent on the patient's heart rate, it is sometimes time-consuming. The implementation of Pe gating is therefore best reserved for cases of severe flow artefact that cannot be reduced to tolerable levels by other measures.

The multiple 180° RF pulses used in FSE sequences cause lengthening of the T2 decay time of fat so that the signal intensity of fat on T2 weighted FSE images is higher than in CSE. This sometimes makes the detection of marrow abnormalities difficult. Therefore, when imaging the vertebral bodies for metastatic disease, a STIR sequence should be utilized.

Patient considerations

Patients with cord compression are sometimes severely disabled and in extreme pain. A swift examination is often necessary to avoid patient movement. An analgesic administered prior to the examination may be beneficial. Patients with severe curvature of the spine often find it impossible to lie flat on the examination couch. Patient comfort is very important as these examinations are sometimes lengthy due to the extra sequences needed to achieve orthogonal images. It is wise to let the patient assume the most comfortable position and use foam pads to support them. The plane of the images is then adjusted to their position. Some-times the lung field area of these patients is compromised and respiration may become an effort when they lie supine. Oxygen can be administered to the patient during the examination, but reducing the scan time as much as possible is probably the best remedy for this problem.

Due to excessively loud gradient noise associated with some sequences, ear plugs must always be provided to prevent hearing impairment.

Contrast usage

Contrast is often necessary especially for leptomeningeal disease, intradural or extramedullary lesions and metastases. It may also be useful for spinal osteomyelitis.

Further reading

Demaerel P., Bosmans H., Wilms G. *et al.* (1997) Rapid lumbar spine MR myelography using rapid acquisition with relaxation enhancement. *American Journal of Roentgenology*, **168**(2), 377–8.

Gasparotti R., Ferraresi S., Pinelli L. *et al.* (1997) Three-dimensional MR myelography of traumatic injuries of the brachial plexus. *American Journal of Neuroradiology*, **18**(9), 1733–42.

Jaramillo D., Laor T. & Mulkern R.V. (1994) Comparison between fast spin-echo and conventional spin-echo imaging of normal and abnormal musculoskeletal structures in children and young adults. *Investigative Radiology*, **29**(9), 803–11.

Maravilla K.R., Aagaard B.D. & Kliot M. (1998) MR neurography. MR imaging of peripheral nerves. *Magnetic Resonance Imaging Clinics of North America*, **6**(1), 179–94.

Metha R.C., Marks M.P., Hinks R.S., Glover G.H. & Enzmann D.R. (1995) MR evaluation of vertebral metastases: T1-weighted, short-inversion-time inversion recovery, fast spin-echo, and inversion-recovery fast spin-echo sequences. *American Journal of Neuroradiology*, **16**(2), 281–8.

Pui M.H., Goh P.S., Choo H.F. & Fok E.C. (1997) Magnetic resonance imaging of musculoskeletal lesions: comparison of three fat-saturation pulse sequences. *Australasian Radiology*, **41**(2), 99–102.

Williamson D.S., Mulken R.V., Jakab P.D. & Jolesz F.A. (1996) Coherence transfer by isotropic mixing in Carr-Purcell-Meiboom-Gill imaging: implications for the bright fat phenomenon in fast spin-echo imaging. *Magnetic Resonance in Medicine*, **35**(4), 506–13.

READING LIST AND RESOURCES

Internet sites

http://www.bir.org.uk/online/index.html   (*British Journal of Radiology* online, must be a member of British Institute of Radiology)

http://www.bodley.ox.ac.uk/olig/bids   (an excellent source of on-line journals and literature search)

http://www.cis.rit.edu/htbooks/mri   (excellent physics resource)

http://www.comp.glam.ac.uk/pages/staff/ajcblyth/Research/Med-Info/uk.medicine.html   (MRI resources)

http://www.kanal.arad.upmc.edu/mrsafety.html   (*The* safety site!)

http://www.mri-efi.com   (books and educational resources)

http://www.neoforma.com/modal.html   (excellent resource for other MRI and radiology sites)

http://www.t2star.com   (protocols, book recommendations)

Journals

British Journal of Radiology. Monthly, British Institute of Radiology.

Clinics in MRI and Developments in MR. Quarterly, Clinical Press.

Journal of Computer Assisted Tomography. Bimonthly, Lippincott Raven.

Journal of Magnetic Resonance Imaging. Bimonthly, Williams and Wilkins.

Magnetic Resonance in Medicine. Monthly, Williams and Wilkins.

MRI Clinics of North America. Quarterly, Saunders.

Radiology. Monthly, Radiological Society of North America.

Topics in Magnetic Resonance Imaging. Bimonthly, Lippincott Raven.

Physics

Elster A.D. (1994) *Questions and Answers in MRI.* Mosby, St Louis.

Hendrick R.E., Russ P.D. & Simon J.H. (1993) *MRI Principles and Artefacts (Teaching File Series).* Raven, New York.

Horowitz A. (1996) *MRI Physics for Radiologists: A Visual Approach.* Springer Verlag, Berlin.

Kaut C. (1992) *MRI Workbook for Technologists.* Lippincott Raven, New York.

Kaut C. & Faulkner W. (1994) *Review Questions in MRI.* Blackwell Science, Oxford.

NessAiver M. (1997) *All You Really Need to Know about MRI Physics.* University of Maryland, Baltimore.

Shellock F.G. & Kanal E. (1996) *Magnetic Resonance Bioeffects, Safety and Patient Management*, 2nd edn. Lippincott Raven, Philadelphia.

Westbrook C. & Kaut C. (1998) *MRI in Practice*, 2nd edn. Blackwell Science, Oxford.

Anatomy

Agur, A.M.R. *et al.* (1991) *Grant's Atlas of Anatomy*, 9th edn. Williams and Wilkins, Baltimore.
Heimer L. (1995) *The Human Brain and Spinal Cord*. Springer Verlag, Berlin.
Moore K.L. (1992) *Clinically Orientated Anatomy*. Williams and Wilkins, Baltimore.
Netter F.H. (1998) *Atlas of Human Anatomy*, 2nd edn. CIBA-Geigy, Summit NJ.